NUCLEAR PHYSICS METHODOLOGY FOR RELOAD DESIGN OF TURKEY POINT & ST. LUCIE NUCLEAR PLANTS

NF-TR-95-01

JANUARY 1995

FLORIDA POWER & LIGHT COMPANY
NUCLEAR FUEL SECTION
JUNO BEACH, FLORIDA

ABSTRACT

This document describes the nuclear design methodology employed by Florida Power & Light Company (FPL) to analyze the core design characteristics necessary to support a fuel reload for Turkey Point Units 3 and 4 and St. Lucie Units 1 and 2. This methodology, including all computer programs used, was obtained from Westinghouse Electric Corporation. Calculations were performed using this methodology and the results compared to operating data from Turkey Point and St. Lucie. The quality of the comparisons demonstrates FPL's ability to perform reload core design for FPL's nuclear units.

TABLE OF CONTENTS

TABLE OF CONTENTS
(CONTINUED)

LIST OF TABLES

LIST OF TABLES
(CONTINUED)

LIST OF FIGURES

LIST OF FIGURES
(CONTINUED)

LIST OF FIGURES
(CONTINUED)

LIST OF FIGURES
(CONTINUED)

LIST OF FIGURES
(CONTINUED)

1.0 INTRODUCTION AND CONCLUSIONS

This report describes the physics methods used by Florida Power & Light Company (FPL) to analyze the core characteristics for our four Pressurized Water Reactors (PWR). It includes a summary description of the Westinghouse computer programs and methodology as applied by FPL to model the Turkey Point and St. Lucie Nuclear Power Station cores. Comparisons between predictions and operating data are provided as a demonstration of FPL's qualifications to use the Westinghouse methodology to perform reload design calculations for the Turkey Point and St. Lucie nuclear units.

1.1 OBJECTIVE

The objective of this report is to demonstrate FPL's competence to perform reload design analyses for our four nuclear power plants. To this end, extensive design calculations have been performed for Cycles 12, 13 and 14 of Turkey Point Unit 4 and the results are compared to actual plant operating data herein. Unit 4 was chosen for its wide variety of assembly and poison types, its transition to axial blanketed fuel, its large number of reinserted fuel assemblies, vessel flux reduction features (e.g., Hafnium inserts at the periphery), and its low leakage fuel management. Design calculations have also been performed for St. Lucie Unit 1, Cycles 10, 11, and 12 and a limited set of results have been compared to actual plant operating data. Unit 1 was chosen for comparison because of its use of Gadolinium burnable poisons, axial blankets and vessel flux reduction features in the core design.

1.2 BACKGROUND

FPL has determined that in-house capability to design reload cores for our units would provide the following benefits:

- Improved control over the design, yielding more control of the decision process,
- Improved optimization of the design, allowing better fuel utilization and economics, and
- A better understanding of the design, leading to more comprehensive evaluations of core safety.

Various physics methodologies were reviewed to determine which best satisfied FPL's needs. FPL decided to use the Westinghouse approach, one of our NSSS vendors and present fuel supplier for Turkey Point. The Westinghouse methodology provided four important advantages:

- A physics methodology which included extensive written procedures (METCOM) which documented in step by step fashion core design calculational practices.
- A training program which provided hands on experience by utilizing METCOM and performing actual calculations on the computer workstation to ensure that the FPL engineers understood the Westinghouse methodology.
- A physics methodology previously reviewed and generically approved by the NRC for all PWR applications, and
- An agreed upon process under which FPL engineers would perform the calculations related to the reload physics analysis process independently of Westinghouse for Turkey Point Unit 3, Cycle 14 with Westinghouse providing Quality Assurance of all calculations. The purpose of this effort was to demonstrate the ability of FPL to perform the required analysis and to use lessons learned to improve the implementation prior to operating independently from Westinghouse.

Implementation of the above decision required entering into a technology exchange agreement with Westinghouse Electric Corporation. This agreement also provides FPL the ability to upgrade codes and methods to be consistent with any revisions developed by Westinghouse. The relevant computer programs and associated methodology of Westinghouse's Commercial Nuclear Fuel Division have been transferred to FPL. A description of the applicable physics models is provided in the next chapter while the computer programs themselves are discussed in Appendix A. The computer programs and procedures (METCOM) are incorporated into the FPL Quality Assurance Program.

Training of FPL personnel in the Westinghouse methods was performed during 1993 utilizing the Nuclear Core Design Training Center approach provided by Westinghouse. FPL individuals were trained in areas ranging from Loading Pattern Scoping, Cross-Section Development, Loading Pattern Generation, Safety Analysis Models and Analysis, Nuclear Design Models and Analysis, to the development of Core Follow Analysis. In all, 14 FPL individuals were trained by Westinghouse in these areas representing well over 5500 manhours of training. Ongoing training by Westinghouse has also been provided, a recent two day training session reviewed modifications to METCOM and provided technical interactions between FPL personnel and Westinghouse designers.

1.3 SCOPE

FPL has performed in-house core design calculations and core follow analysis for Turkey Point for many cycles. Core follow results obtained during Unit 4 Cycles 12, 13, and 14 provide ample data with which to compare predicted power distributions, predicted boron letdown curves, and fuel depletion calculations. In addition, the startup physics measurements conducted during the startup of each cycle provide an

additional source of valid data for evaluating the physics model predictions of critical boron concentrations, control rod worth, and temperature coefficients. Detailed comparisons of the predictions and measurements are presented in Section 4.

FPL has also performed in-house core design calculations and core follow analysis for the St. Lucie Units. Comparisons between measurements and predictions for St. Lucie Unit 1 Cycles 10, 11, and 12 are presented in Section 5 using Westinghouse methodology.

All methods used to generate the results detailed in this report (computer programs and model development) are standard licensed methods used by the Westinghouse Commercial Nuclear Fuel Division. Therefore, the calculational uncertainties (e.g., see Reference 1) associated with the methods are unchanged and do not require re-quantification. In addition, the methods utilized to process measured data (e.g., see Reference 2) for Turkey Point are also standard to Westinghouse such that measurement uncertainties do not require re-determination by FPL.

1.4 CONCLUSIONS

This report describes the use of the Westinghouse methodology as applied by FPL to model the Turkey Point Unit 4 and St. Lucie Unit 1 cores. Calculations were performed for Cycles 12, 13, and 14 for Turkey Point Unit 4 and the results were compared to actual operating data. Assemblies from Turkey Point Unit 4, Cycles 9, 10, and 11 were also modeled to establish the appropriate axial burnup distributions. Calculations were performed for Cycles 10, 11, and 12 for St. Lucie Unit 1 as described in Section 5. The results from these comparisons demonstrate FPL's understanding of the methodology and show that FPL can apply the METCOM procedures and computer codes during the performance of future reload design analyses for FPL nuclear units.

2.0 PHYSICS METHODOLOGY

This section describes the Westinghouse codes and methodology used by FPL to perform design calculations for reload cores. The major features associated with each model are discussed, as is the interaction between models. This methodology was also used to obtain the results presented in Section 4 and Section 5. Descriptions of the individual computer codes used are provided in Appendix A.

Lattice physics parameters for unit assemblies and baffle-reflector cross sections are calculated with PHOENIX-P (Reference 3 and 11), a two-dimensional multi-group transport theory code. Fuel and clad temperatures are generated with the FIGHTH (Reference 9 and 10) code. The three-dimensional advanced nodal code ANC (Reference 8) is used to predict reactivity, power distributions, and other relevant core characteristics. In addition, APOLLO (Reference 12), a one-dimensional diffusion theory code is available to calculate differential control rod worth and axial power distributions for the heat flux hot channel factor (F_Q) synthesis to establish operational limits. The cross section library, as well as PHOENIX-P, nodal, and diffusion theory models are discussed in the following sections.

The models described here are representative of current Westinghouse practices. FPL's calculational capabilities are anticipated to evolve in parallel with Westinghouse's through planned implementation of the technology exchange agreement between the two corporations.

2.1 CROSS SECTION LIBRARY

The PHOENIX-P computer program's nuclear cross section library contains microscopic cross section data based on a 42 energy group structure derived from ENDF/B-V files. This cross section library was designed to properly capture integral properties of the multigroup data during the

group collapse in order to accurately model important resonance parameters, and to provide the overall accuracy of reactivity predictions necessary for core design. In addition, this library has been developed in a manner consistent with current Westinghouse methodologies and accumulated core design experience. The development and benchmarking of the PHOENIX-P library are described in Reference 3.

For gadolinium, the cross-sections are obtained from the Criticality Safety CSRL-V 227 group ENDF/B-V library. Resonance effects are added by the NITAWL-S code using Nordheim treatment. The 227 groups are subsequently collapsed to the PHOENIX-P 42 group structure using the XSDRN-PM transport theory cell code.

2.2 LATTICE MODELING IN PHOENIX-P

In PHOENIX-P, the fuel, discrete absorbers, and structural components within a single fuel assembly are represented in their exact lattice configuration. Discontinuity factors, pin factors, and homogenized two-group microscopic cross sections are generated as a function of burnup for input to ANC. For isotopes and materials represented explicitly in ANC, microscopic cross sections are generated, including xenon, samarium, soluble boron, water density, and burnable absorbers. To obtain constants for rodded assemblies, branch calculations are performed at selected burnups.

A three region cylindrical cell description for each cell within the lattice is allowed in PHOENIX-P. Principles of material preservation are employed to construct three region cell representations, since most lattice cells consist of more than three subregions. The outer region (third region) of each cell, defined by the fuel pin pitch, has a common composition in all cells in a given lattice configuration. Grids are modeled by smearing the grid material uniformly over this common outer region. Grids are only

smeared in the active fuel region. The sections following describe the various types of cell models.

2.2.1 FUEL CELL MODEL

The fuel pellet outer radius defines the innermost region of a fuel rod cell. The middle region is defined by the clad outer diameter and incorporates the pellet-clad gap. Appropriate number densities are specified for the uranium isotopes and oxygen for fresh fuel. Isotopic information for burned fuel, including decay chains, is obtained from previous depletion calculations of fresh fuel. For fuel pellets with integral fuel burnable absorber (IFBA) zirconium diboride coating, the coating material is smeared into the clad region rather than being explicitly installed as a coating on the surface of the pellet. PHOENIX-P corrects for the reactivity effect of modeling the absorber as smeared into the clad instead of on the pellet.

2.2.2 DISCRETE ABSORBER MODEL

A. BURNABLE ABSORBER RODS

Turkey Point has used two types of discrete burnable absorber (BA) rods: Wet Annular Burnable Absorbers (WABAs) and Pyrex glass. The cell representation for the two BA types is significantly different. The WABA contains moderator material in the central region, while the Pyrex BA is voided in the central region. The surface area of the absorber material must be preserved in addition to the quantity of material.

Since a fast neutron can pass through the absorber region of a WABA, become thermalized in the inner region, and be absorbed, both the inner and outer surfaces of the absorber are important. Region 1 of the cell is therefore defined as moderator material with an outer radius equivalent to the BA pellet inner radius. Region 2 is

defined as pure pellet material with an outer radius equal to the outer radius of the pellet. The inner WABA cladding, inner pellet-clad gap, outer pellet-clad gap, outer cladding, guide tube, and sleeve materials are all smeared into the moderator region in order to preserve material quantities.

For Pyrex absorbers, the inner gap, inner clad and pellet absorber material are smeared into the first region with a radius equivalent to the pellet outer radius. Region 2 is made up of the absorber outer clad, moderator, guide tube and sleeve volumes, and materials. The small volume of moderator between the outer clad and the guide tube is modeled as if it were outside the guide tube. This is a minor approximation, since the zircaloy guide tube material is nearly transparent to neutrons.

For gadolinium, PHOENIX-P uses 42 group microscopic cross sections for the gadolinium isotopes as a function of Gd-155 and Gd-157 depletion along with lattice and other geometry specific aspects to produce appropriately weighted two group, homogenized cross-sections for ANC.

B. CONTROL RODS

Control rod cells are modeled in a manner similar to Pyrex BA cells, except that the dimensions and material in the pellet region are different. Resonance calculations are performed by PHOENIX-P for the Ag-In-Cd control rod material. For St. Lucie, control rods are modeled as five regions consisting of B_4C absorber, clad, moderator, guide tube, and moderator.

C. HAFNIUM ABSORBERS

Hafnium absorber rod cells are modeled in a manner similar to Pyrex BA cells, except that the dimensions and material in the pellet region are different. Hafnium rods decrease the power and thereby the fast fluence in core locations close to the reactor pressure vessel weld. This reduction is required for pressurized thermal shock (PTS) considerations.

2.2.3 STRUCTURAL CELL MODELS

Certain cells, known as structural cells, contain neither a strong absorber or material that is depletable. Examples of these include guide tubes, instrument tubes, water displacer rods, and stainless steel rods. These can typically be represented with three regions or less and do not require special neutronic considerations. Sleeve volume is preserved by calculating an effective guide tube thickness that equates to the total sleeve volume.

2.3 BAFFLE-REFLECTOR MODELING

Baffle-reflector cross sections are generated by performing a one-dimensional slab calculation with PHOENIX-P. Such a model is developed by using a series of fuel cells approximating two fuel assemblies, the assembly/baffle gap, baffle, reflector, core barrel, thermal pad (on the flats), and moderator. A homogenized set of cross sections for ANC is obtained, representing the spectrum variations existing between the fuel assemblies, baffle, and reflector.

2.4 THREE-DIMENSIONAL NODAL MODEL

Homogenized cross sections, discontinuity factors, and pin factors are generated on a cycle specific basis using PHOENIX-P depletion calculations. These parameters are then used to model the three-dimensional core in ANC. A fuel assembly consists of four radial nodes.

In order to obtain an accurate pin power recovery solution, the burnup gradient within each node is represented in ANC. A burnup gradient algorithm matches nodal corner and surface average burnups.

Explicit representations of axially heterogeneous features such as axial blankets and burnable absorbers are made using the variable axial mesh capability in ANC. Typically, 24 axial mesh intervals produce accurate axial power distributions. To account for spectrum effects induced by variable length burnable absorbers and fuel burnup gradients, axial zoning of the burnup dependent cross sections is employed. Burnable absorber history effects are also taken into account by using appropriate sets of fuel cross sections.

The three-dimensional ANC calculational results can be used to predict peaking factors, critical boron concentrations, core power distributions, control rod worth, and reactivity coefficients. This model can also be collapsed to two dimensions for those calculations (e.g., determination of the highest worth stuck rod) where a three-dimensional representation is not required.

2.5 ONE-DIMENSIONAL DIFFUSION THEORY MODEL

A three-dimensional ANC model can be collapsed radially to generate a one-dimensional APOLLO model. The cross sections are flux and volume weighted, and a burnup and elevation dependent radial buckling search is performed to normalize the APOLLO model to ANC. The one-dimensional diffusion theory model is used for calculations where additional detail is desired in the axial direction. To this end, the axial mesh is redefined to comprise 40 or more axial intervals. APOLLO can be used to generate integral and differential control rod worth curves, determine control rod insertion limits, and analyze axial power distributions in order to establish limits on axial offset during power operation.

3.0 PHYSICS MODEL APPLICATIONS

The physics methodology discussed in Section 2 was developed in order to provide reliable analytical predictions in the following four major areas:

- Core power distributions at steady state conditions,
- Axial power distribution control limits,
- Core reactivity parameters, and
- Core physics parameters for transient analysis input

Often more than one model may be used to perform a specific analysis. The preferred model depends upon a number of considerations including the degree of accuracy desired and the specific applications.

3.1 CORE POWER DISTRIBUTIONS AT STEADY STATE CONDITIONS

The prediction of steady-state core power distributions is fundamental to the design, analysis, and surveillance of nuclear reactor cores. Accurate prediction of core power distributions leads to confidence in developing and optimizing core loading patterns, ensuring compliance with Technical Specification limits, and determining fuel assembly burnups and isotopic inventories.

3.1.1 POWER DISTRIBUTIONS

Global core power distributions are obtained as a function of burnup from three-dimensional ANC depletion calculations. Calculations are also performed at selected burnups for various power levels and control rod configurations. Peak rod powers and hot channel factors are generated by pin power reconstruction within ANC using rod-by-rod power distributions from single assembly two-dimensional PHOENIX-P fine mesh spectrum calculations.

3.1.2 POWER PEAKING

Local power peaking is monitored to ensure that the peak pellet power and the total energy content within each coolant channel remain within Technical Specification and/or fuel design limits. The factors used to measure local power peaking include:

- the heat flux hot channel factor, F_Q, defined as the maximum local heat flux on the surface of a fuel rod divided by the average fuel rod heat flux,

- the nuclear enthalpy rise hot channel factor, $F_{\Delta H}$, defined as the ratio of the integral of linear power along the rod with the highest integrated power to the average rod power, and

- the planar radial power peaking factor, $F_{XY}(Z)$, defined as the ratio of the peak power density to the average power density in the horizontal plane at elevation z.

For steady state conditions, these are obtained from three-dimensional ANC calculations using pin power reconstruction. For maneuvering and transient xenon conditions, a three-dimensional, one-dimensional, synthesis technique (see Section 3.2) may be used.

3.1.3 FUEL DEPLETION

Three-dimensional fuel depletion calculations are performed with ANC. Rod-by-rod burnup distributions are obtained from the ANC depletions. Specific fuel nuclide inventories are obtained from two-dimensional single assembly PHOENIX-P depletion calculations.

3.2 AXIAL POWER DISTRIBUTION CONTROL LIMITS

The axial power distribution is primarily affected by control rod position, xenon, burnup, and temperature distributions. Axial power distribution control limits are used to ensure that thermal limits are not violated during power level changes, control rod motion, and the resulting xenon redistributions. This is accomplished by maintaining the axial flux difference within acceptable boundaries. Axial flux difference, ΔI, is defined as the difference between the upper and lower excore detector signals.

Axial power distribution control limits for Turkey Point are determined using Westinghouse's Relaxed Axial Offset Control (RAOC) calculational procedure (Reference 4). The RAOC calculational procedure begins by defining "provisional" ΔI limits which are wider than the expected LOCA limits (or, alternately, the RAOC ΔI limits from the previous cycle may be used if it is desired only to verify their acceptability). Xenon transient simulations are performed with the one-dimensional APOLLO code at various burnups and for different power levels, constrained by the provisional ΔI limits and power dependent rod insertion limits. A library of axial xenon shapes is constructed at each burnup. Next, axial power shapes are generated with APOLLO for all possible combinations of xenon shapes, power levels, and rod insertions. These axial shapes are synthesized with height dependent planar radial power distributions from three-dimensional ANC calculations. Imposition of the LOCA F_Q limits for normal operation then defines the allowable ΔI limits (or verifies that the previous cycle's limits are acceptable) for the cycle. The axial power shapes corresponding to cases within the ΔI limits are checked against thermal hydraulic constraints from Loss of Flow Accident simulations and the peak power and DNB limits for accident conditions.

For normal operations, more restrictive ΔI limits are developed if either the F_Q limits or thermal hydraulic constraints are exceeded. For accident conditions, analyses are performed to verify that all design limits are met. If necessary, trip setpoints may be revised and/or the RAOC ΔI limits tightened. Therefore, the RAOC procedure provides axial power shape information which is used to verify that all design limits are met. The RAOC ΔI limits are placed in the Turkey Point Core Operating Limit Report and apply during plant operation.

3.3 CORE REACTIVITY PARAMETERS

The core reactivity is affected by changes in the reactor which occur during operation as the result of fuel depletion and abnormal or accident conditions. Reactivity coefficients quantify the rate of reactivity change to be expected in response to changes in power, moderator or fuel temperatures, and soluble boron concentration. Reactivity defects refer to the integral of the corresponding reactivity coefficient between two reactor statepoints with all other variables remaining constant. Xenon, samarium, and control rod worth are also typically required to fully define the change in reactivity between two core configurations. In addition, neutron kinetics parameters are needed to describe the time dependent behavior of the core.

Quantification of these effects are needed: (a) to provide input to safety analyses, (b) to provide guidance to the reactor operators, and (c) to ensure compliance with Technical Specifications. Therefore, the physics models described in Section 2 are used to calculate reactivity coefficients, reactivity worth, and kinetics parameters as a function of core burnup, moderator temperature, and power level.

3.3.1 MODERATOR TEMPERATURE COEFFICIENT

The moderator temperature coefficient (MTC) is defined as the change in reactivity per degree change in moderator temperature. The effect of concomitant changes in moderator and soluble boron densities are included. The MTC is sensitive to the values of the moderator density, moderator temperature, soluble boron concentration, fuel burnup, and the presence of control rods and/or burnable absorbers which reduce the required soluble boron concentration and increase the leakage of the core. The MTC may be positive or negative depending on the magnitude of change of the individual components of this coefficient.

The MTC is calculated using the ANC core model described in Section 2.4 by varying the inlet temperature around a reference temperature. The moderator temperature coefficient is analyzed for various reactor conditions, from hot zero power (HZP) to hot full power (HFP), for various boron concentrations and control rod positions, and at various cycle burnups. The moderator temperature defect is also obtained using data from the ANC core model.

3.3.2 DOPPLER COEFFICIENTS

The Doppler temperature coefficient is defined as the change in reactivity per degree change in effective fuel temperature. The effective fuel temperature accounts for the spatial variation in fuel temperature throughout the core. The Doppler power coefficient represents the corresponding change in reactivity per percent change in reactor power. These coefficients are primarily a consequence of the Doppler broadening of U-238 and Pu-240 resonance absorption peaks which increases the effective resonance absorption cross section of the fuel with increasing fuel temperature.

The Doppler power coefficient is normally calculated using the ANC core model by varying the reactor power level about a reference power (which in turn varies the fuel temperature) while holding the product of the power level and the enthalpy rise constant. The FIGHTH code provides effective fuel temperatures, which account for spatial variations in temperature within the pellet, as a function of power level and burnup. The Doppler coefficient is analyzed at different power levels and for various cycle burnups. Doppler reactivity defects can also be obtained using the ANC model by varying the reactor power at various times in life, while holding the product of the power level and the enthalpy rise constant.

At hot zero power, the Doppler temperature coefficient may be calculated by subtracting the moderator temperature coefficient from the isothermal temperature coefficient (ITC), provided ITC is explicitly calculated (see Section 3.3.4).

3.3.3 TOTAL POWER COEFFICIENT

The total power coefficient is defined as the change in reactivity per percent change in core power level. This coefficient represents the combined effect of moderator temperature and fuel temperature changes for an associated change in core power level.

The total power coefficient is calculated using the ANC core model by varying the core power level around a reference value while allowing the inlet temperature to change in accordance with the inlet program for the plant. The power coefficient is analyzed at different power levels and at various times in core life. The power defect is also obtained using the ANC model by varying the reactor power.

3.3.4 ISOTHERMAL TEMPERATURE COEFFICIENT

The isothermal temperature coefficient (ITC) is defined as the change in reactivity per uniform degree change in core temperature. The ITC is the temperature coefficient directly measured during startup physics testing. The ITC can be calculated by summing the moderator temperature coefficient and the Doppler temperature coefficient. Alternately, the ITC may be calculated explicitly using the ANC core model by varying both the moderator temperature and the fuel temperature about a uniform reference temperature.

The isothermal temperature defect (ITD) refers to the change in reactivity between hot zero power temperatures and temperatures below hot zero power. ITDs are needed as a function of temperature and burnup for various rod patterns to establish shutdown boron concentration requirements. ITDs are calculated with the ANC model using cross sections generated with PHOENIX-P at specific temperatures between hot zero power and 68°F.

3.3.5 BORON REACTIVITY COEFFICIENT

The boron reactivity coefficient, also referred to as the differential boron worth, is defined as the change in reactivity per ppm change in the soluble boron concentration. The inverse of the boron reactivity coefficient is referred to as the inverse boron worth. It provides a means of determining the change in soluble boron concentration necessary to compensate for a given reactivity change. The magnitude of the boron reactivity coefficient depends primarily on the soluble boron concentration, the moderator temperature, control rod insertion, and the presence of burnable absorbers.

The boron reactivity coefficient is calculated using the ANC core model by perturbing the boron concentration in both directions about a reference

value and computing the reactivity change. Boron worths are calculated as a function of boron concentration, power level, temperature, burnup, and control rod configuration.

3.3.6 XENON AND SAMARIUM WORTH

The fission products Xe-135 and Sm-149 possess large thermal absorption cross sections. Knowledge of the concentrations and reactivity worth of these isotopes as well as the changes which occur in response to plant maneuvers is crucial to reactor control. Since Xe-135 is also produced by iodine decay, it initially builds up and then decays following a reduction in power or shutdown. Sm-149 is a stable isotope produced by promethium decay. Following a reactor shutdown, its concentration increases. Upon restart it gradually returns to its equilibrium value.

Equilibrium xenon and samarium worth are calculated with the ANC core model at various power levels and core burnups. Changes in their worth and axial fluctuations in isotopic concentrations during transient operation are obtained using the ANC and/or APOLLO models.

3.3.7 CONTROL ROD WORTH

Control rod worth refers to the reactivity difference between two control rod configurations. The total control rod worth, trip reactivity shape (i.e., the inserted rod worth versus rod position), integral and differential worth of individual banks, and worth of individual rod cluster control assemblies (e.g., stuck, ejected, and dropped rods) are determined as required for startup physics testing, plant operations, and input to safety analyses.

Control rod worths are analyzed for all normal and many abnormal control rod configurations as a function of burnup, power level, and moderator temperature. Total rod worth and the integral worth of individual rod banks and rod clusters are calculated using the ANC core model.

Differential rod worths are obtained with the ANC and/or APOLLO models.

3.3.8 NEUTRON KINETICS PARAMETERS

Neutron kinetics parameters, which include delayed neutron fractions, decay constants, and the prompt neutron lifetime, are required as input to the plant reactivity computer and to various safety analyses. These parameters are also input to the Inhour equation to generate core reactivity as a function of startup rate and period. The kinetics parameters are evaluated at hot full power and hot zero power conditions for various cycle burnups and control rod configurations.

The PHOENIX-P cross section library contains delayed neutron fractions and decay constants for fissionable nuclides for each of the six delayed neutron energy groups. The core averaged delayed neutron fractions are obtained by weighting the delayed neutron fractions for each group by the regionwise fraction of fissions in each isotope and the regionwise power and volume weighting in the core. The core average decay constants are calculated in a similar manner. The fraction of fissions in each isotope are obtained from single assembly PHOENIX-P calculations. Regionwise power sharings for various core conditions are obtained using the ANC core model. A delayed neutron importance factor (to account for spectrum differences between delayed and prompt neutrons) is used to calculate an effective core average delayed neutron fraction.

The prompt neutron lifetime also depends upon the core composition (fuel enrichment, burnup, absorbers, etc.). Single assembly PHOENIX-P calculations provide the neutron lifetime for the fuel in each core region. The core average value is determined through a power and volume weighting process.

3.4 CORE PHYSICS PARAMETERS FOR TRANSIENT ANALYSIS INPUT

The physics models described in Section 2 are used to generate key input parameters for various safety analyses. These key safety parameters include reactivity coefficients, control rod worth, and limiting power distributions during both normal operations and accidental transients. Reference 5 provides a detailed description of how these parameters are calculated for Turkey Point.

4.0 PHYSICS MODEL VERIFICATION TURKEY POINT UNITS

Core physics model verification typically includes comparisons of predictions to plant startup and operating data. Turkey Point Units 3 & 4 are currently in their fourteenth and fifteenth cycles of operation, respectively. In this section, predictions made using the physics methodology described in Section 2 are compared to zero power physics test measurements and at power operating data for Turkey Point. For St. Lucie, this data is presented in Section 5.

As stated in Section 1, the methods employed to generate the predictions reported in this section are standard licensed and NRC approved methods used by Westinghouse's Commercial Nuclear Fuel Division. The comparisons reported herein provide additional verification of the predictive capabilities of this methodology; however, their primary purpose is to demonstrate FPL's ability to perform design calculations for the Turkey Point Units 3 & 4.

Turkey Point Units 3 & 4 are similar in design. Each reactor is a closed cycle pressurized light water moderated and cooled system, which uses slightly enriched uranium dioxide fuel. Each unit is currently designed to produce 2200 MWt core power. The reactor core consists of 157 fuel assemblies. Turkey Point Units 3 and 4 core and fuel assembly designs are essentially identical, both utilizing a low leakage core design. Each fuel assembly consists of a 15x15 array of 204 fuel rods, 20 guide thimbles, and one instrument thimble. The Turkey Point Unit 4 Cycles 12, 13, and 14 were selected for core physics model verification, since each of these cycles has different design attributes which provide an opportunity to model different design features.

4.1 CYCLE DESCRIPTIONS

Turkey Point Unit 4 Cycle 12 began operation on June 11, 1989, and shutdown on November 24, 1990 after 406 effective full power days (EFPD), corresponding to a cycle burnup of 12441 megawatt days per metric ton

(MWD/MTU). Turkey Point Unit 4 Cycle 12 was fueled with two different fuel designs. The burned fuel of Regions 9B, 11B, 12C, 13A, 13B, and 13C are the familiar Low Parasitic Fuel (LOPAR) design. Regions 12A, 12B, 13D, and 13E and the fresh regions 14A, 14B, 14C, and 14D are of the Westinghouse Optimized Fuel Assembly (OFA) design. The core loading pattern for Cycle 12, including the assembly locations, the number of Integral Fuel Burnable Absorbers (IFBAs), the number of Wet Annular Burnable Absorbers (WABAs), and the locations of control banks are shown in Figure 4.1-1. The core also contains part-length hafnium rods. These rods decrease the power and thereby the fast fluence in core locations close to the reactor pressure vessel weld. This reduction is required for pressurized thermal shock (PTS) considerations. There are 240 hafnium rods in the core. They are 36 inches long and positioned slightly below the core midplane. Figure 4.1-1 gives the core locations for the hafnium rods. A quarter core representation is used since the core is symmetric.

Turkey Point Unit 4 Cycle 13 began operation on October 27, 1991 and shutdown on April 10, 1993 after 441 EFPD, corresponding to a cycle burnup of 13433 MWD/MTU. Turkey Point Unit 4 Cycle 13 was also fueled with both LOPAR and OFA fuel assembly designs. In Cycle 13, sixteen assemblies from earlier cycles were re-inserted. Special modeling of these re-inserted assemblies was necessary to account for their loss in reactivity due to the excessive time that the re-inserted assemblies resided in the spent fuel pool. The core loading pattern for Cycle 13, including the assembly locations, the number of IFBAs, the number of WABAs, and the locations of control banks are shown in Figure 4.1-2. The Cycle 13 core also contains the part-length hafnium rods as in Cycle 12.

Turkey Point Unit 4 Cycle 14 began operation on May 26, 1993 and was shutdown on October 2, 1994 after 454 EFPD, corresponding to a cycle

burnup of 13793 MWD/MTU. Turkey Point Unit 4 Cycle 14 was fueled entirely with assemblies of OFA design, and the fresh fuel of Region 16 introduced axial blankets into Unit 4. Axial blankets consist of a nominal six inches of natural UO_2 pellets at the top and bottom of the fuel pellet stack to reduce neutron leakage and to improve uranium utilization. The core loading pattern for Cycle 14, including the assembly locations, the number of IFBAs, the number of WABAs, and the locations of control banks are shown in Figure 4.1-3. The Cycle 14 core also contains the part-length hafnium rods as in Cycles 12 and 13. Fuel batch characteristics for Cycles 12, 13, and 14 are summarized in Table 4.1-1.

4.2 ZERO POWER PHYSICS TESTS

After each refueling at the Turkey Point units, startup physics tests are conducted to verify that the nuclear characteristics of the core are consistent with design predictions. While the reactor is maintained at hot zero power (HZP) conditions, the following physics parameters are measured:

- Critical boron concentrations,
- Isothermal temperature coefficient,
- Control rod worth, and
- Differential boron worth

Table 4.2-1 contains the zero power physics test review criteria, which represent the maximum expected deviation between predicted and measured values for each parameter.

The following sections briefly describe the measurement and calculational techniques and summarize the results of the zero power physics tests for Turkey Point Unit 4, Cycles 12, 13, and 14. Small changes in core reactivity were measured by feeding the signal from a power range neutron

detector into a reactivity computer which solves the point kinetics equation. The computer output was plotted on a strip chart recorder. All predictions were made with the three-dimensional ANC model described in Section 2.4.

4.2.1 CRITICAL BORON CONCENTRATIONS

Critical boron concentrations were measured by acid-based titration of reactor coolant samples taken under equilibrium conditions. Samples were taken with all rods essentially out and with the reference bank (see Section 4.2.3) inserted. Critical boron searches were performed with the three-dimensional ANC model for these core configurations to obtain the predicted concentrations. The measured and predicted critical boron concentrations are compared in Table 4.2-2. All differences are within the ±50 ppm review criteria.

4.2.2 TEMPERATURE COEFFICIENTS

Isothermal temperature coefficients (ITCs) were measured by making small changes in the reactor coolant system temperature and determining the corresponding change in reactivity with the reactivity computer. ITCs were predicted by uniformly varying the core temperature by ±5°F about the HZP temperature in the ANC model. The moderator temperature is varied directly; Doppler effects on reactivity are determined using fitting coefficients obtained from FIGHTH calculations. The measured and predicted ITCs and Moderator Temperature Coefficients (MTCs) are compared in Table 4.2-3. All differences are well within the review criteria of ±2 pcm/°F. The measured Moderator Temperature Coefficient is obtained by subtracting the Doppler Coefficient from the measured ITC.

4.2.3 CONTROL ROD WORTH

Control rod worths were measured by the Rod Swap Technique. First, the worth of the reference bank (the bank of highest worth) was measured by

boron dilution. Stepwise bank insertion was used to maintain criticality and differential worth were obtained from the reactivity computer response. The differential worths were summed to provide the integral worth of the reference bank. Then, maintaining the boron concentration at a constant value, critical configurations were established with each remaining bank fully inserted and the reference bank partially withdrawn. The integral worth of each inserted bank was determined from the critical position of the reference bank after the exchange by applying analytical corrections to account for the effect of the inserted bank on the partial integral worth of the reference bank. This procedure is described in Reference 6.

The ANC model was used to predict the individual control rod bank worth as well as to generate the corrections used to infer the measured worth. The measured and predicted worth are compared in Table 4.2-4; all differences are within the review criteria listed in Table 4.2-1. Measured and predicted reference bank integral rod worth shapes are compared in Figures 4.2-1 through 4.2-3.

4.2.4 DIFFERENTIAL BORON WORTH

Measured differential boron worths were obtained by dividing the measured reference bank worth (see Section 4.2.3) by the difference between the critical boron concentrations measured with all rods out and with the reference bank inserted. The differential boron worth does not change significantly over this range of boron concentration. Boron worths were predicted by varying the boron concentration by ±25 ppm about the HZP all rods out critical boron concentration in the ANC model. The measured and predicted boron worth are compared in Table 4.2-5. All differences are well within the ±15% review criteria.

4.3 POWER OPERATION

In support of the Turkey Point Technical Specification requirements, the core power distribution is measured at least once every 31 EFPD using the in-core instrumentation system. Neutron flux measurements made by movable in-core fission chambers are combined with analytically determined power to reaction rate ratios using the computer program INCORE (Reference 2) to infer (i.e., "measure"), a three-dimensional power distribution. The power to reaction rate ratios are generated with the three-dimensional ANC model using cross sections derived from PHOENIX. INCORE is a data analysis code written to process information obtained by in-core instrumentation. INCORE synthesizes measured axial flux shapes and theoretical elevation dependent X-Y power distributions to obtain a power distribution throughout the core.

In this section, measured data obtained from INCORE is compared to predictions made with the three-dimensional ANC Model. Included are:

- Power peaking factors, F_Q and $F_{\Delta H}$,
- Average assembly radial power distributions,
- Core average axial power distributions, and
- Axial offset

Also, measured and predicted boron letdown curves are compared. Boron letdown refers to the reduction of the all rods out (ARO), hot full power (HFP) critical boron concentration as a function of core burnup.

4.3.1 BORON LETDOWN CURVES

Reactor coolant system boron concentrations are measured daily regardless of power level or control rod bank insertion. Critical boron concentrations measured at or very close to hot full power all rods out equilibrium xenon and samarium conditions are compared to the predicted

boron letdown curves for Cycles 12, 13, and 14 in Figures 4.3-1 through 4.3.3. The predicted curves were obtained from design depletions with the three-dimensional ANC model.

Table 4.3-1 compares measured and predicted critical boron concentrations at the time of INCORE power distribution measurements. The measured concentrations were corrected to hot full power all rods out equilibrium xenon and samarium conditions in accordance with the Turkey Point units surveillance procedures. The predicted concentrations were obtained by performing critical boron searches with the ANC model at the specified burnups of the measurements. The mean difference between measured and predicted critical boron concentrations for all three cycles is 9 ppm with a standard deviation of 13 ppm.

4.3.2 POWER PEAKING FACTORS

The nuclear enthalpy rise hot channel factor ($F_{\Delta H}$) and the heat flux hot channel factor (F_Q) were measured using the INCORE code, as discussed above. Predicted peaking factors were obtained from three-dimensional ANC calculations performed for core conditions similar to those at the time of the measurements. Power peaking factors measured during Cycles 12, 13, and 14 are compared to predicted values in Figures 4.3-4 through 4.3-9 and in Tables 4.3-2 and 4.3-3. For $F_{\Delta H}$, the mean difference between the measured and predicted values for the three cycles is 2.02% with a standard deviation of 1.27%; for F_Q the mean difference is 3.33% with a standard deviation of 1.86%. Regarding the F_Q comparisons, it is noted that spacer grid effects are inherent in the measured values but the grids are not explicitly modeled in ANC. The magnitude of this effect can be seen from Figures 4.3-19 through 4.3-27.

4.3.3 RADIAL POWER DISTRIBUTIONS

Core power distributions were measured with the INCORE code, as discussed above. The measured power distributions are typically referred to as flux maps. INCORE also produces predicted power distributions at the burnup of the flux map by interpolating between power distributions generated using the three-dimensional ANC model at specific burnups during a depletion calculation. Since the core is loaded symmetrically, ANC depletion calculations are performed assuming quarter-core reflective symmetry for Cycles 12 and 13, and rotational symmetry for Cycle 14. The predicted power distributions are expanded to full core for comparison to the measured distributions.

Figures 4.3-10 through 4.3-18 compare measured and predicted assembly relative power distributions at selected burnups for Cycles 12, 13, and 14. All comparisons are for the hot full power all rods out condition since this is the normal mode of operation for the Turkey Point units. The mean absolute difference between measured and predicted assembly relative powers is less than .021 and the standard deviation is less than .023 for these comparisons.

4.3.4 AXIAL POWER DISTRIBUTIONS AND AXIAL OFFSETS

Measured core average axial power distributions from each of the flux maps discussed in the previous section are compared to predicted axial distributions in Figures 4.3-19 through 4.3-27. The predicted distributions were obtained from three-dimensional ANC calculations performed for core conditions similar to those at the time of the flux maps. Note that since the grid straps are not modeled explicitly in the ANC model, no depressions are seen at the grid locations in the predicted distributions. This difference coupled with the normalization of both measured and predicted axial power distributions to unity causes the measured relative power to appear slightly higher between grid locations.

Axial offset refers to the percent difference between the relative power in the top half of the core and that in the bottom half of the core divided by the sum of these two relative powers. Axial offsets measured using the INCORE code are compared to predicted values from ANC calculations for core conditions similar to those at the time of the measurements in Table 4.3-4. The mean difference between measured and predicted values for Cycles 12, 13, and 14 is 0.66% with a standard deviation of 1.54%.

4.4 SUMMARY

In this section, predictions made using Westinghouse's reload core design methodology are compared to zero power physics test measurements and at-power operating data from Turkey Point Unit 4, Cycles 12, 13, and 14. In all cases, the predictions agree well with the measurements. All startup test predictions are within the review criteria listed in Table 4.2-1. Predicted critical boron concentrations at power are within 50 ppm of the measured values, and the predicted power distributions are close to the measured values, as evidenced by Figures 4.3-10 through 4.3-27. The excellent agreement between the predictions and the measurements reported here demonstrates FPL's capability to apply the Westinghouse licensed methodology to reload core design for Turkey Point Units 3 and 4.

TABLE 4.1-1

TURKEY POINT UNIT 4 CYCLE 12,13 AND 14 FUEL SPECIFICATION

CYCLE	BATCH	NUMBER OF ASSEMBLIES	INITIAL ENRICHMENT w/o U-235	BOC BURNUP MWD/MTU
12	9B	1	3.40	16080
	11B	8	3.40	29279
	12A	8	2.60	22862
	12B	12	3.45	28354
	12C	8	3.00	24975
	13A	4	3.00	18285
	13B	4	3.10	17489
	13C	4	3.10	17592
	13D	24	3.20	18769
	13E	32	3.40	15354
	14A	28	3.40	0
	14B	4	3.40	0
	14C	8	3.80	0
	14D	12	3.80	0
13	9	8	3.30	27419
	9B	1	3.40	29845
	11A	8	3.10	26325
	13B	4	3.10	28073
	13C	4	3.10	31944
	13D	8	3.20	32654
	13E	24	3.40	27752
	14A	28	3.40	16549
	14B	4	3.40	16232
	14C	8	3.80	13179
	14D	12	3.80	13952
	15A	16	3.60	0
	15B	12	3.60	0
	15C	16	4.00	0
	15D	4	4.00	0
14	13E	8	3.40	32717
	14A	25	3.40	31222
	14B	4	3.40	31768
	14C	8	3.80	24027
	14D	12	3.80	30454
	15A	16	3.60	17883
	15B	12	3.60	17489
	15C	16	4.00	15004
	15D	4	4.00	15055
	16A	16	3.60	0
	16B	16	3.60	0
	16C	4	3.60	0
	16D	8	4.00	0
	16E	8	4.00	0

TABLE 4.2-1

TURKEY POINT UNIT 4 CYCLE 12,13 AND 14
HZP PHYSICS TEST REVIEW CRITERIA

PARAMETER	REVIEW CRITERIA
Critical Boron Concentration	±50 ppm
Temperature Coefficients: Moderator Temperature Coefficient Isothermal Temperature Coefficient	±2.0 pcm/°F
Control Rod Bank Worths:	
Reference Bank Worth	±10%
"Swap" Worths	±15% or 100 pcm whichever is greater
Differential Boron Worth	±15%

TABLE 4.2-2

TURKEY POINT UNIT 4 CYCLE 12,13 AND 14 CRITICAL BORON CONCENTRATION COMPARISON BETWEEN MEASUREMENT AND PREDICTION

CYCLE	BANK CONFIGURATION	CRITICAL BORON CONCENTRATION (PPM)		
		MEASURED M	PREDICTED P	DIFFERENCE (M-P)
12	ARO	1538	1584	-46
12	BANK C in	1399	1428	-29
13	ARO	1554	1560	-6
13	BANK A in	1401	1408	-7
14	ARO	1698	1691	7
14	BANK SB in	1552	1544	8

Acceptance Criteria is ±50 ppm

TABLE 4.2-3

TURKEY POINT UNIT 4 CYCLE 12,13 AND 14
MODERATOR AND ISOTHERMAL TEMPERATURE COEFFICIENT
COMPARISON BETWEEN MEASUREMENT AND PREDICTION

CYCLE	BANK CONFIGURATION	MODERATOR TEMPERATURE COEFFICIENT (PCM/°F)		
		MEASURED M	PREDICTED P	DIFFERENCE (M-P)
12	ARO	0.92	0.58	0.34
13	ARO	0.24	0.06	0.18
14	ARO	0.26	1.13	-0.87

CYCLE	BANK CONFIGURATION	ISOTHERMAL TEMPERATURE COEFFICIENT (PCM/°F)		
		MEASURED M	PREDICTED P	DIFFERENCE (M-P)
12	ARO	-0.88	-0.63	-0.25
13	ARO	-1.66	-1.65	-0.01
14	ARO	-1.44	-0.57	-0.88

Acceptance Criteria is ±2 pcm/°F

TABLE 4.2-4

TURKEY POINT UNIT 4 CYCLE 12,13 AND 14 CONTROL ROD WORTH COMPARISON BETWEEN MEASUREMENT AND PREDICTION

CYCLE	BANK CONFIGURATION	CONTROL ROD WORTH (PCM)		
		MEASURED M	PREDICTED P	DIFFERENCE(%) ((M-P)/P)*100
12	BANK D	691	718	-3.76
	BANK C(1)	1314	1365	-3.74
	BANK B	375	380	-1.31
	BANK A	1177	1204	-2.24
	BANK SB	1180	1202	-1.83
	BANK SA	1000	1017	-1.67
	TOTAL(2)	5737	5886	-2.53
13	BANK D	641	682	-6.09
	BANK C	1022	992	2.97
	BANK B	435	457	-4.88
	BANK A(1)	1232	1275	-3.41
	BANK SB	1183	1233	-4.03
	BANK SA	826	836	-1.17
	TOTAL(2)	5338	5475	-2.51
14	BANK D	636	661	-3.78
	BANK C	1093	1172	-6.74
	BANK B	435	480	-9.37
	BANK A	1086	1102	-1.45
	BANK SB(1)	1173	1195	-1.84
	BANK SA	1052	1094	-3.84
	TOTAL(2)	5475	5704	-4.01

Acceptance Criteria is ±15% or 100 pcm which ever is greater
(1) Reference Bank - Acceptance Criteria is ±10%
(2) Sum of all measured banks within ±7%

TABLE 4.2-5

TURKEY POINT UNIT 4 CYCLE 12,13 AND 14 HZP DIFFERENTIAL BORON WORTH COMPARISON BETWEEN MEASUREMENT AND PREDICTION

CYCLE	BANK CONFIGURATION	DIFFERENTIAL BORON WORTH (PCM/PPM)		
		MEASURED M	PREDICTED P	DIFFERENCE(%) ((M-P)/P)*100
12	Average Over Bank C insertion	9.45	8.78	7.63
13	Average Over Bank A insertion	8.05	8.34	-3.47
14	Average Over Bank SB insertion	8.56	8.13	5.29

TABLE 4.3-1

TURKEY POINT UNIT 4 CYCLE 12,13 AND 14 BORON LETDOWN COMPARISON BETWEEN MEASUREMENT AND PREDICTION

CYCLE	CYCLE BURNUP MWD/MTU	CRITICAL BORON CONCENTRATION (PPM)		
		MEASURED M	PREDICTED P	DIFFERENCE (M-P)
12	0	1437	1426	11
	150	1111	1124	-13
	2000	1020	1006	14
	2320	986	989	-3
	3000	954	950	4
	4020	867	882	-15
	4940	815	812	3
	5890	744	733	11
	6975	657	637	20
	8000	567	546	21
	10000	379	361	18
	11184	277	250	27
	12000	200	174	26
	12441	161	133	28
13	150	1082	1104	-22
	1000	1014	1027	-13
	2000	938	953	-15
	2440	924	926	-2
	3224	862	869	-7
	4888	750	739	11
	6678	610	591	19
	8265	473	458	15
	8754	436	418	18
	10608	276	258	18
	12316	121	109	12
14	150	1213	1212	1
	600	1189	1166	23
	1000	1135	1142	-7
	1830	1103	1098	5
	2521	1056	1043	13
	3428	991	980	11
	5000	869	858	11
	5986	792	775	17
	8148	601	587	14
	8995	520	510	10
	9871	453	428	25
	10704	362	349	13
	12000	218	226	-8

TABLE 4.3-2

TURKEY POINT UNIT 4 CYCLE 12,13 AND 14 POWER PEAKING FACTOR ($F_{\Delta H}$) COMPARISON BETWEEN MEASUREMENT AND PREDICTION

CYCLE	CYCLE BURNUP MWD/MTU	$F_{\Delta H}$(MAX) MEASURED M	PREDICTED P	DIFFERENCE ((M-P)/P)*100
12	150	1.475	1.416	4.17
	4945	1.492	1.456	2.47
	5860	1.499	1.459	2.74
	6890	1.498	1.456	2.88
	7620	1.493	1.471	1.51
	8363	1.502	1.481	1.41
	9082	1.511	1.486	1.70
	9458	1.509	1.489	1.35
	10323	1.511	1.487	1.60
	11121	1.504	1.484	1.35
	11812	1.508	1.479	2.01
13	150	1.557	1.486	4.77
	2440	1.438	1.440	-0.14
	3224	1.442	1.437	0.35
	4888	1.447	1.435	0.84
	6678	1.519	1.455	4.39
	8265	1.509	1.477	2.16
	8754	1.511	1.491	1.34
	10608	1.541	1.507	2.26
	12316	1.545	1.508	2.45
14	600	1.468	1.420	3.38
	1830	1.462	1.421	2.89
	2521	1.485	1.427	4.06
	3428	1.465	1.427	2.66
	5986	1.471	1.440	2.15
	6836	1.472	1.452	1.38
	7659	1.478	1.460	1.23
	8143	1.476	1.464	0.82
	8995	1.482	1.464	1.23
	9871	1.494	1.461	2.26
	10704	1.496	1.462	2.33

TABLE 4.3-3

TURKEY POINT UNIT 4 CYCLE 12,13 AND 14 POWER PEAKING FACTOR (F_Q) COMPARISON BETWEEN MEASUREMENT AND PREDICTION

CYCLE	CYCLE BURNUP MWD/MTU	F_Q (MAX) MEASURED M	F_Q (MAX) PREDICTED P	DIFFERENCE ((M-P)/P)*100
12	150	1.920	1.874	2.39
	4945	1.692	1.632	3.67
	5860	1.709	1.649	3.63
	6890	1.718	1.644	4.50
	7620	1.722	1.657	3.92
	8363	1.709	1.672	2.21
	9082	1.699	1.672	1.61
	9458	1.724	1.671	3.17
	10323	1.713	1.661	3.13
	11121	1.692	1.652	2.42
	11812	1.688	1.644	2.67
13	150	1.773	1.756	0.97
	2440	1.642	1.634	0.49
	3224	1.614	1.621	-0.43
	4888	1.664	1.596	4.26
	6678	1.719	1.617	6.31
	8265	1.726	1.650	4.60
	8754	1.732	1.669	3.77
	10608	1.762	1.681	4.82
	12316	1.755	1.671	5.02
14	600	1.815	1.682	7.91
	1830	1.745	1.677	4.06
	2521	1.825	1.686	8.24
	3428	1.730	1.672	3.42
	5986	1.725	1.681	2.62
	6836	1.742	1.688	3.20
	7659	1.741	1.699	2.47
	8143	1.741	1.702	2.29
	8995	1.735	1.701	2.00
	9871	1.729	1.701	1.65
	10704	1.732	1.696	2.12

TABLE 4.3-4

TURKEY POINT UNIT 4 CYCLE 12,13 AND 14
AXIAL OFFSET COMPARISON
BETWEEN MEASUREMENT AND PREDICTION

CYCLE	CYCLE BURNUP MWD/MTU	AXIAL OFFSET (%)		
		MEASURED M	PREDICTED P	DIFFERENCE M-P
12	150	-2.46	-2.57	-0.11
	4945	-2.55	-1.85	-0.70
	5860	-2.99	-1.96	-1.03
	6890	-3.05	-2.13	-0.92
	7620	-1.60	-2.28	0.68
	8363	-1.42	-2.24	0.82
	9082	-0.87	-2.11	1.24
	9458	-1.66	-2.06	0.40
	10323	-3.09	-1.96	-1.13
	11121	-2.04	-1.93	-0.11
	11812	-2.23	-1.93	-0.30
13	150	7.00	0.34	6.66
	2440	2.34	-1.42	3.76
	3224	0.93	-1.79	2.72
	4888	-0.41	-2.25	1.84
	6678	-0.66	-2.45	1.79
	8265	-1.51	-2.59	1.08
	8754	-1.99	-2.50	0.51
	10608	-1.99	-2.23	0.24
	12316	-1.61	-1.86	0.25
14	600	3.62	1.85	1.77
	1830	1.19	0.56	0.63
	2521	-1.30	0.17	-1.47
	3428	-0.13	-0.60	0.47
	5986	-1.36	-1.88	0.52
	6836	-1.64	-2.08	0.44
	7659	-1.93	-2.20	0.27
	8143	-2.08	-2.17	0.09
	8995	-2.10	-2.09	-0.01
	9871	-1.70	-1.93	0.23
	10704	-2.12	-1.82	-0.30

FIGURE 4.1-1
TURKEY POINT
UNIT 4, CYCLE 12
LOADING PATTERN
52 ASSEMBLY FEED

	8	7	6	5	4	3	2	1
H	9B D	13A	13E SB	13E	12B D	14A	13B	12B 20 HF
G	13A	14B 4 WABA	13E	13D A	14A 8 WABA	13D SA	14C	12A 20 HF
F	13E SB	13E	12B	14A 8 WABA	13D C	14A	13E B	
E	13E	13D A	14A 8 WABA	13C SB	13E	14D	11B	
D	12B D	14A 8 WABA	13D C	13E	14D	12C		
C	14A	13D SA	14A	14D	12C			
B	13B	14C	13E B	11B				
A	12B 20 HF	12A 20 HF						

LEGEND

Batch ID

RCCA Bank or Removable BP

HF = PTS Hafnium Absorber

14A - 3.4 w/o 60 IFBA
14B - 3.4 w/o 116 IFBA
14C - 3.8 w/o No IFBA
14D - 3.8 w/o 60 IFBA

32 Assemblies @ 3.4 Wt.%
20 Assemblies @ 3.8 Wt.%

FIGURE 4.1-2

TURKEY POINT

UNIT 4, CYCLE 13
LOADING PATTERN

48 ASSEMBLY FEED

	8	7	6	5	4	3	2	1
H	9B D	15B 8 WABA	13E SB	15A 20 WABA	13B D	15A 8 WABA	14A	13C 20 HF
G	15B 8 WABA	13E	14D	14A A	15A 16 WABA	R 9 SA	15C	13D 20 HF
F	13E SB	14D	14B	14A	R 11A C	15B 4 WABA	14C B	
E	15A 20 WABA	14A A	14A	14D SB	14A	15C 8 WABA	13E	
D	13B D	15A 16 WABA	R 11A C	14A	15D	13E		
C	15A 8 WABA	R 9 SA	15B 4 WABA	15C 8 WABA	13E			
B	14A	15C	14C B	13E				
A	13C 20 HF	13D 20 HF						

LEGEND

Batch ID

RCCA Bank or Removable BP

HF = PTS Hafnium Absorber
R = Re-Inserted Assembly

15A - 3.6 w/o No IFBA
15B - 3.6 w/o 32 IFBA
15C - 4.0 w/o No IFBA
15D - 4.0 w/o 88 IFBA

28 Assemblies @ 3.6 Wt.%
20 Assemblies @ 4.0 Wt.%

FIGURE 4.1-3
TURKEY POINT
UNIT 4, CYCLE 14
LOADING PATTERN
52 ASSEMBLY FEED

	8	7	6	5	4	3	2	1
H	14A D	15A	15B SB	16B 8 WABA	14A D	16B 4 WABA	14D	14B 20 HF
G	15A	16C 8 WABA	15A	14C A	16A 16 WABA	15B SA	16D	14A 20 HF
F	15B SB	15A	14A	16A 16 WABA	14D C	16B 4 WABA	15C B	
E	16B 8 WABA	14C A	16A 16 WABA	15A SB	15C	16E	13E	
D	14A D	16A 16 WABA	14D C	15C	15D	14A		
C	16B 4 WABA	15B SA	16B 4 WABA	16E	14A			
B	14D	16D	15C B	13E				
A	14B 20 HF	14A 20 HF						

LEGEND

Batch ID

RCCA Bank or Removable BP

HF = PTS Hafnium Absorber

16A - 3.6 w/o No IFBA
16B - 3.6 w/o 32 IFBA
16C - 3.6 w/o 64 IFBA
16D - 4.0 w/o 16 IFBA
16E - 4.0 w/o 48 IFBA

36 Assemblies @ 3.6 Wt.%
16 Assemblies @ 4.0 Wt.%

FIGURE 4.2-1
TURKEY POINT UNIT 4 CYCLE 12
MEASURED VERSUS PREDICTED
BANK C INTEGRAL ROD WORTH

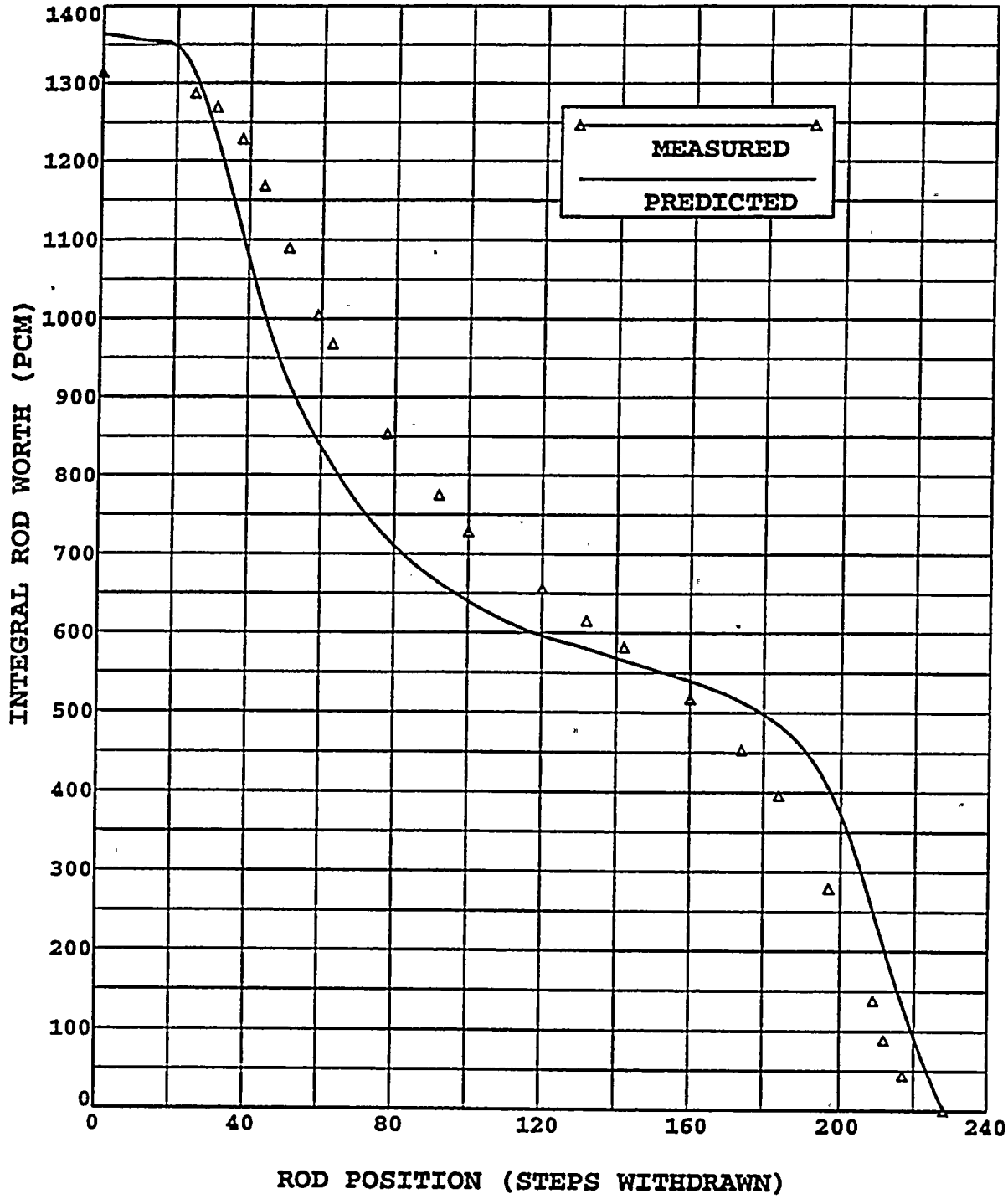

FIGURE 4.2-2
TURKEY POINT UNIT 4 CYCLE 13
MEASURED VERSUS PREDICTED
BANK A INTEGRAL ROD WORTH

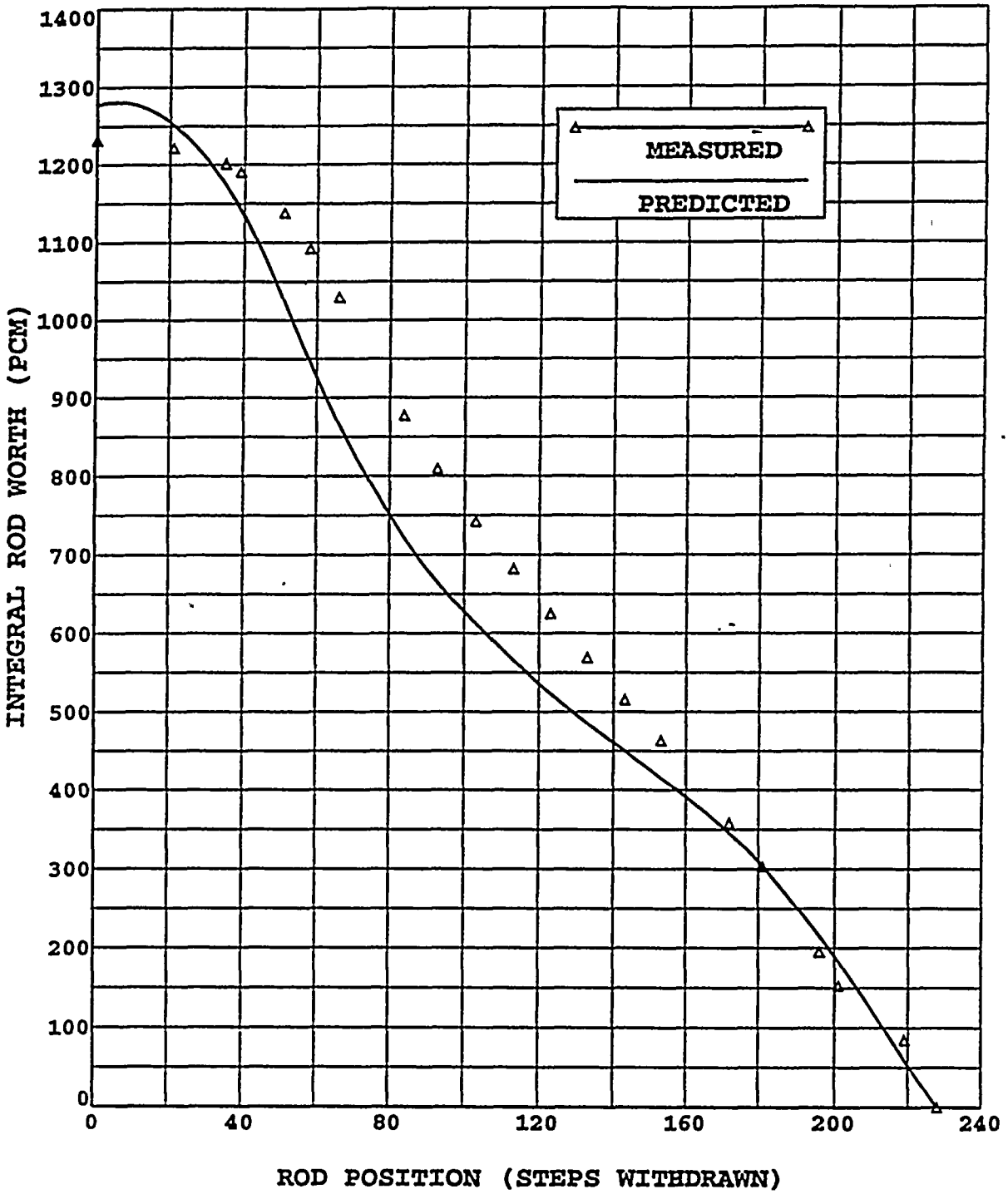

FIGURE 4.2-3
TURKEY POINT UNIT 4 CYCLE 14
MEASURED VERSUS PREDICTED
BANK SB INTEGRAL ROD WORTH

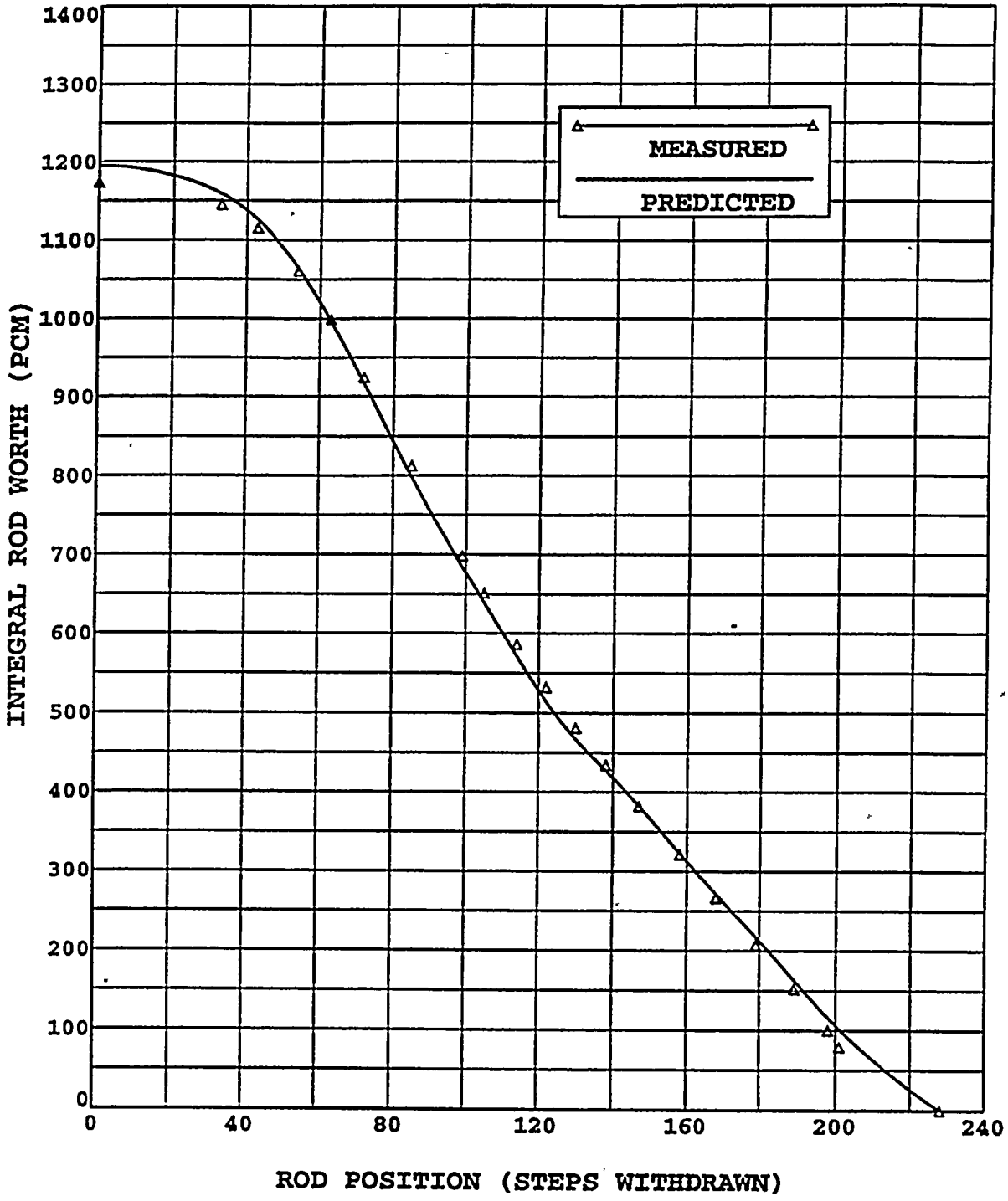

FIGURE 4.3-1
TURKEY POINT UNIT 4 CYCLE 12
BORON LETDOWN COMPARISON
BETWEEN MEASUREMENT AND PREDICTION

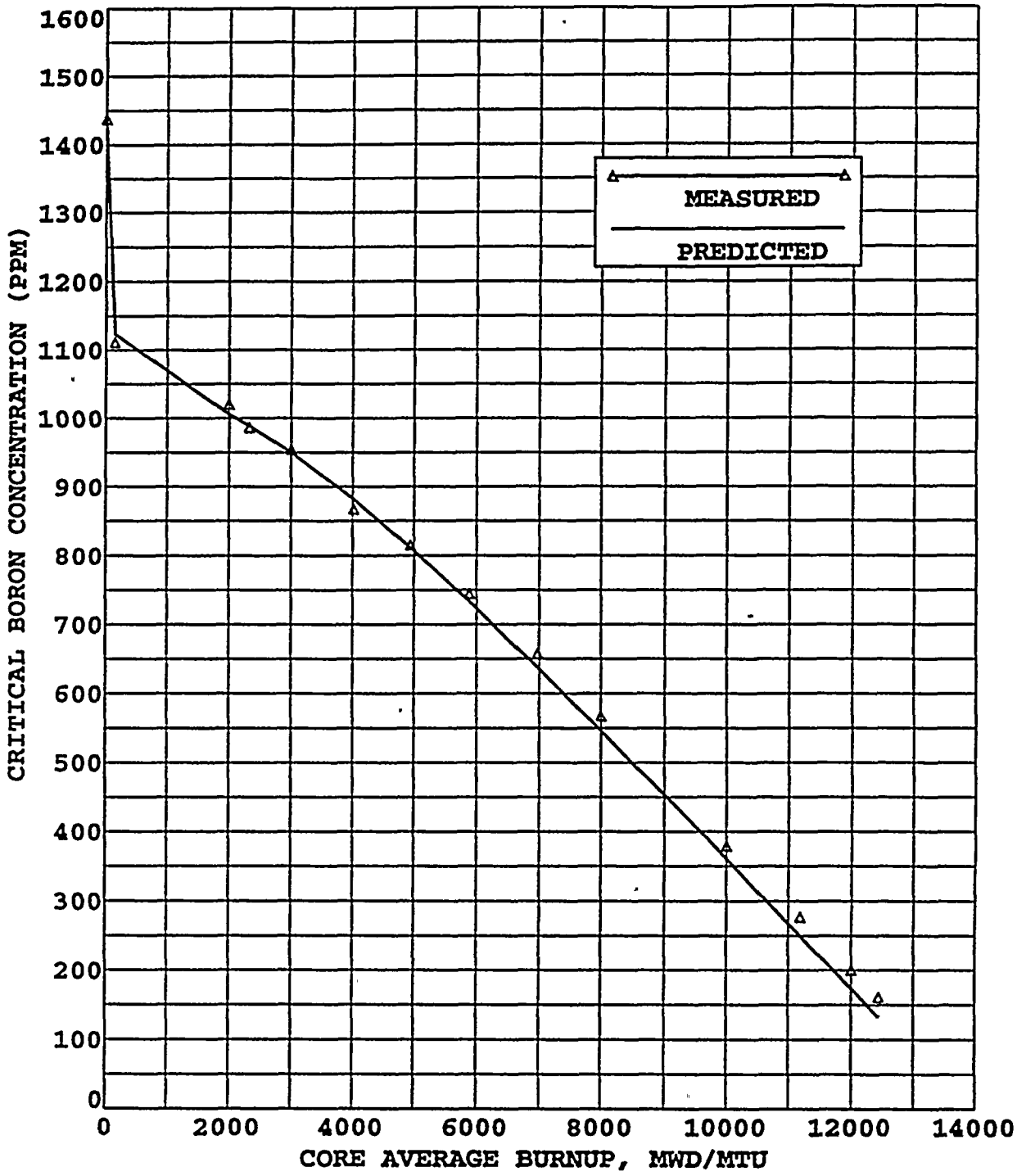

FIGURE 4.3-2
TURKEY POINT UNIT 4 CYCLE 13
BORON LETDOWN COMPARISON
BETWEEN MEASUREMENT AND PREDICTION

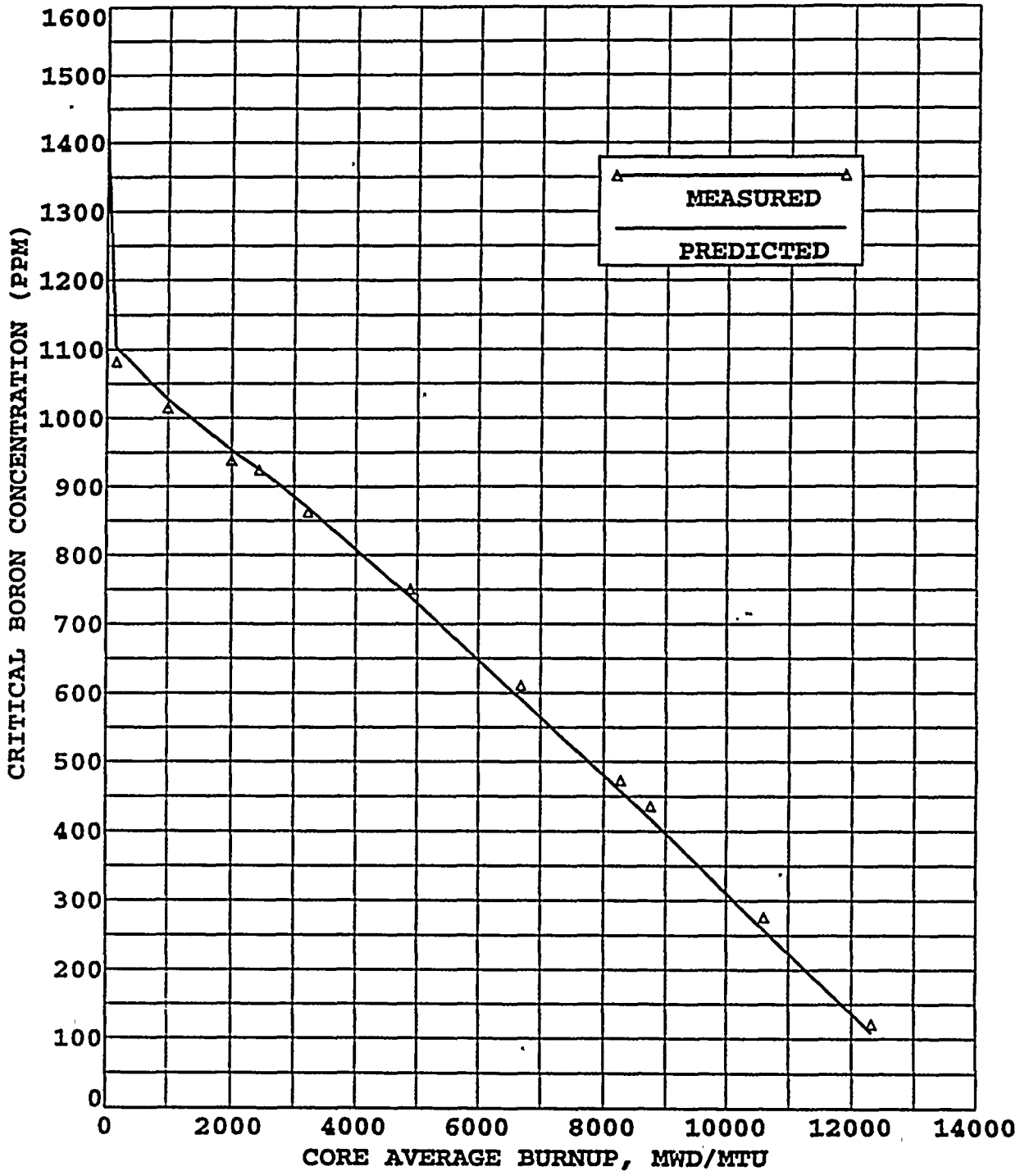

FIGURE 4.3-3
TURKEY POINT UNIT 4 CYCLE 14
BORON LETDOWN COMPARISON
BETWEEN MEASUREMENT AND PREDICTION

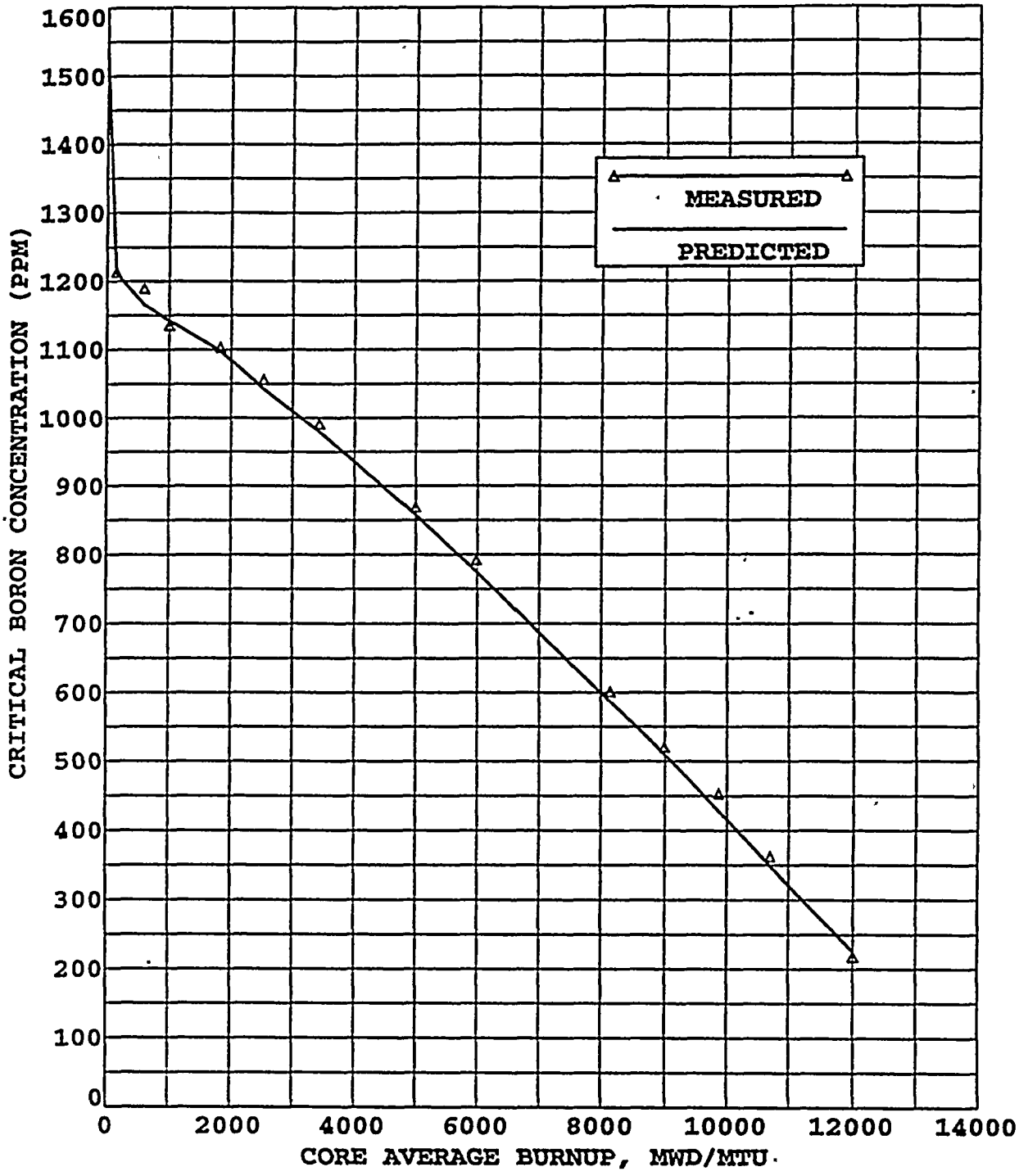

FIGURE 4.3-4
TURKEY POINT UNIT 4 CYCLE 12
F DELTA H COMPARISON
BETWEEN INCORE AND ANC

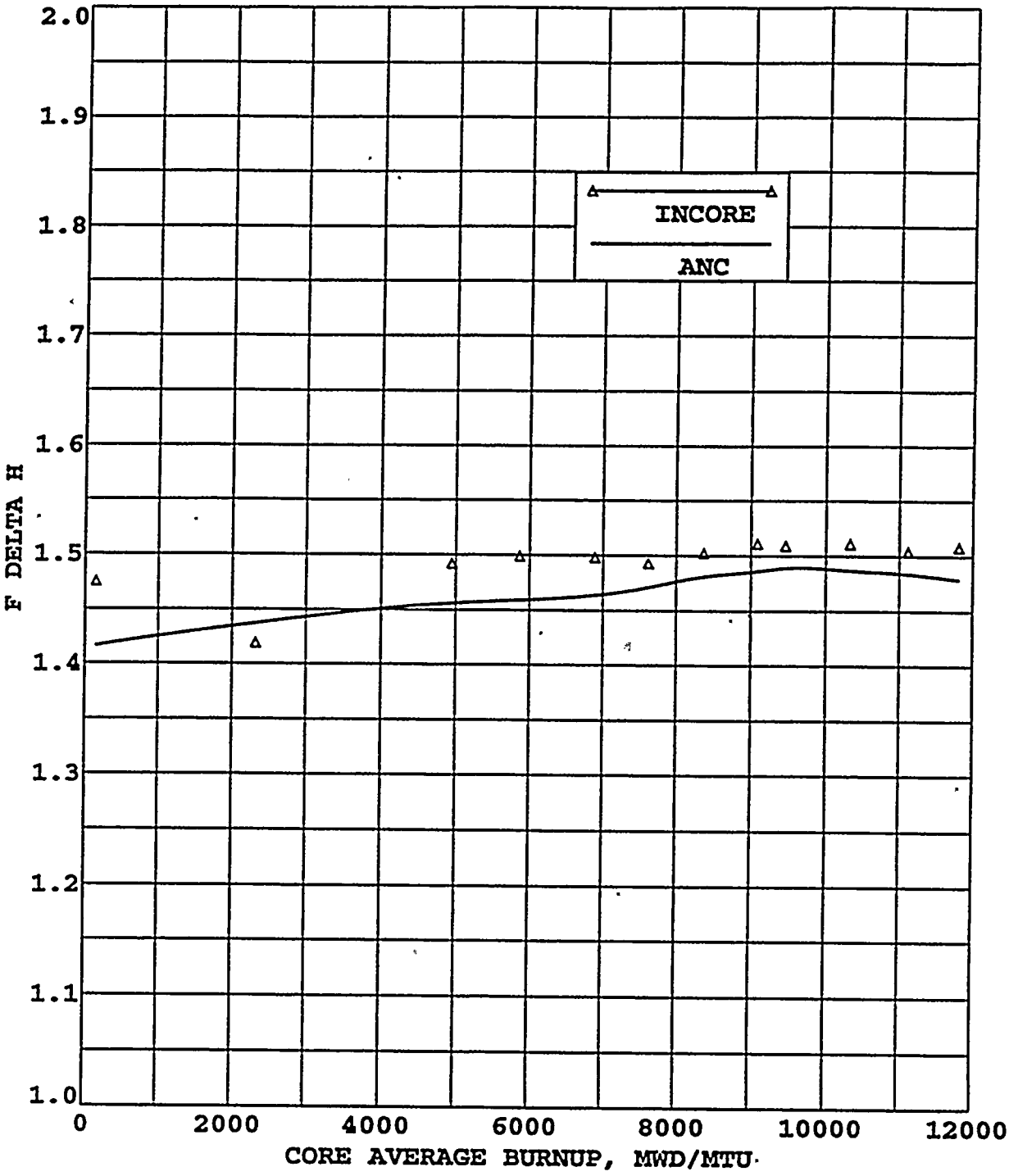

FIGURE 4.3-5
TURKEY POINT UNIT 4 CYCLE 13
F DELTA H COMPARISON
BETWEEN INCORE AND ANC

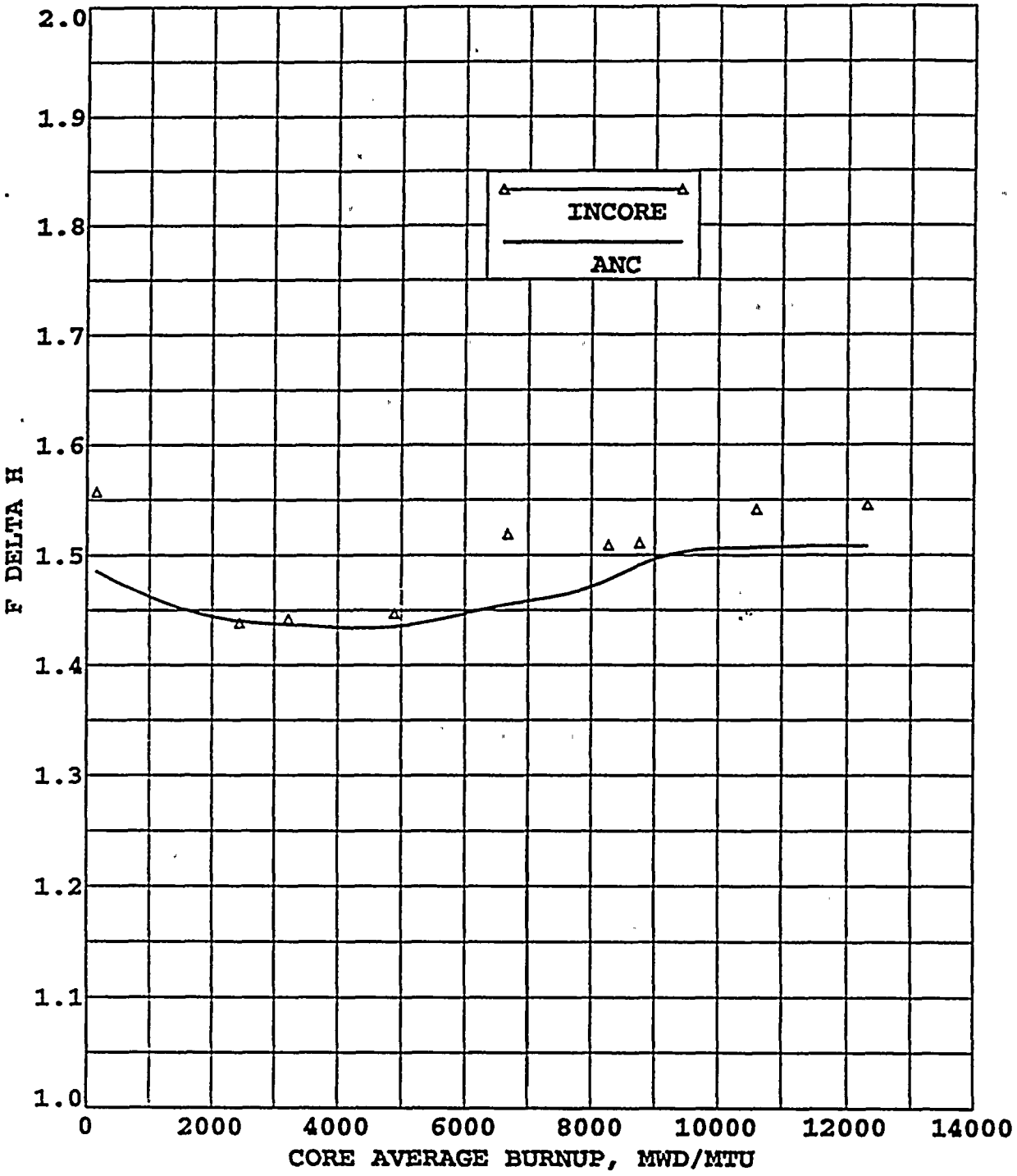

FIGURE 4.3-6
TURKEY POINT UNIT 4 CYCLE 14
F DELTA H COMPARISON
BETWEEN INCORE AND ANC

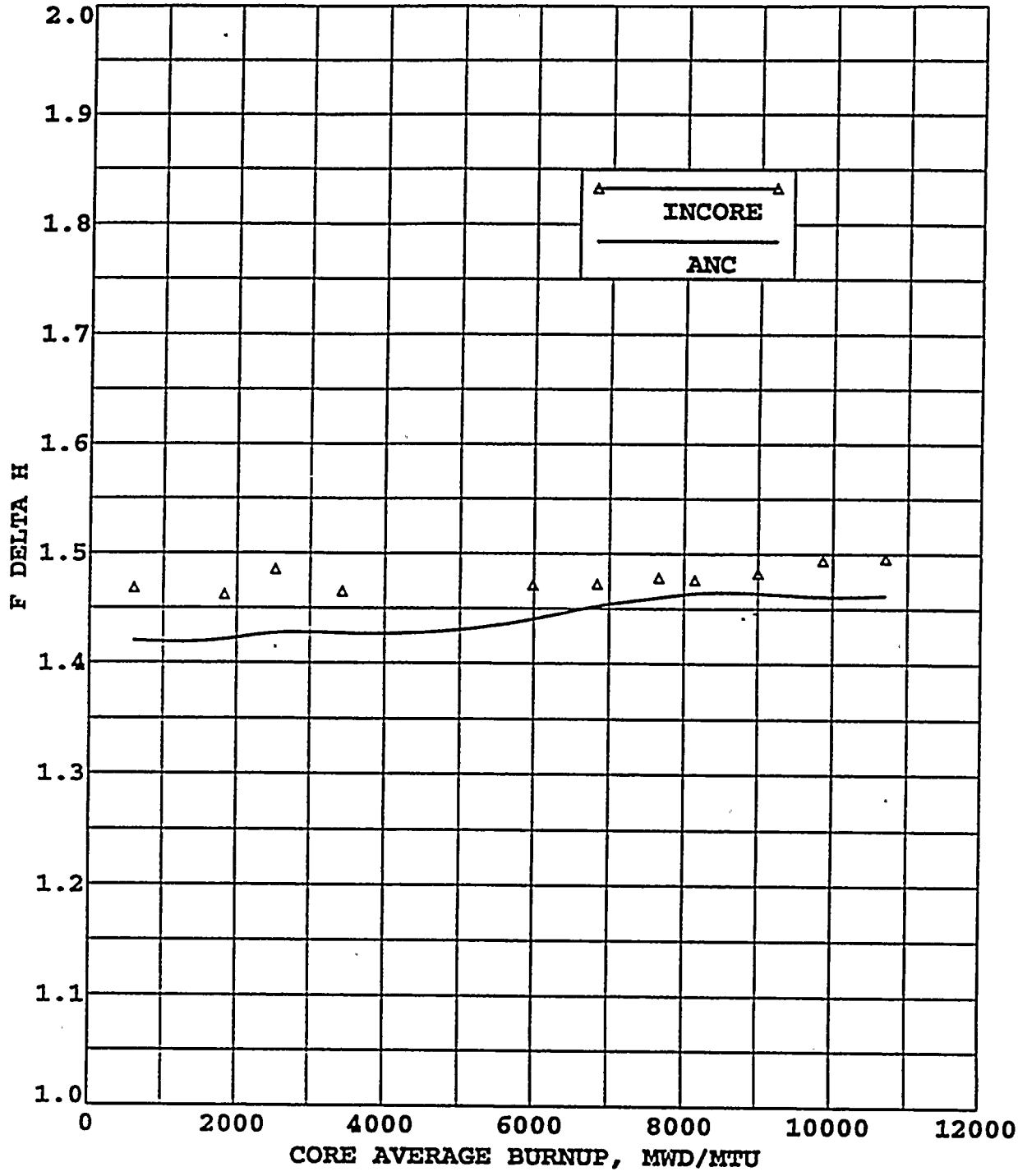

FIGURE 4.3-7
TURKEY POINT UNIT 4 CYCLE 12
FQ COMPARISON
BETWEEN INCORE AND ANC

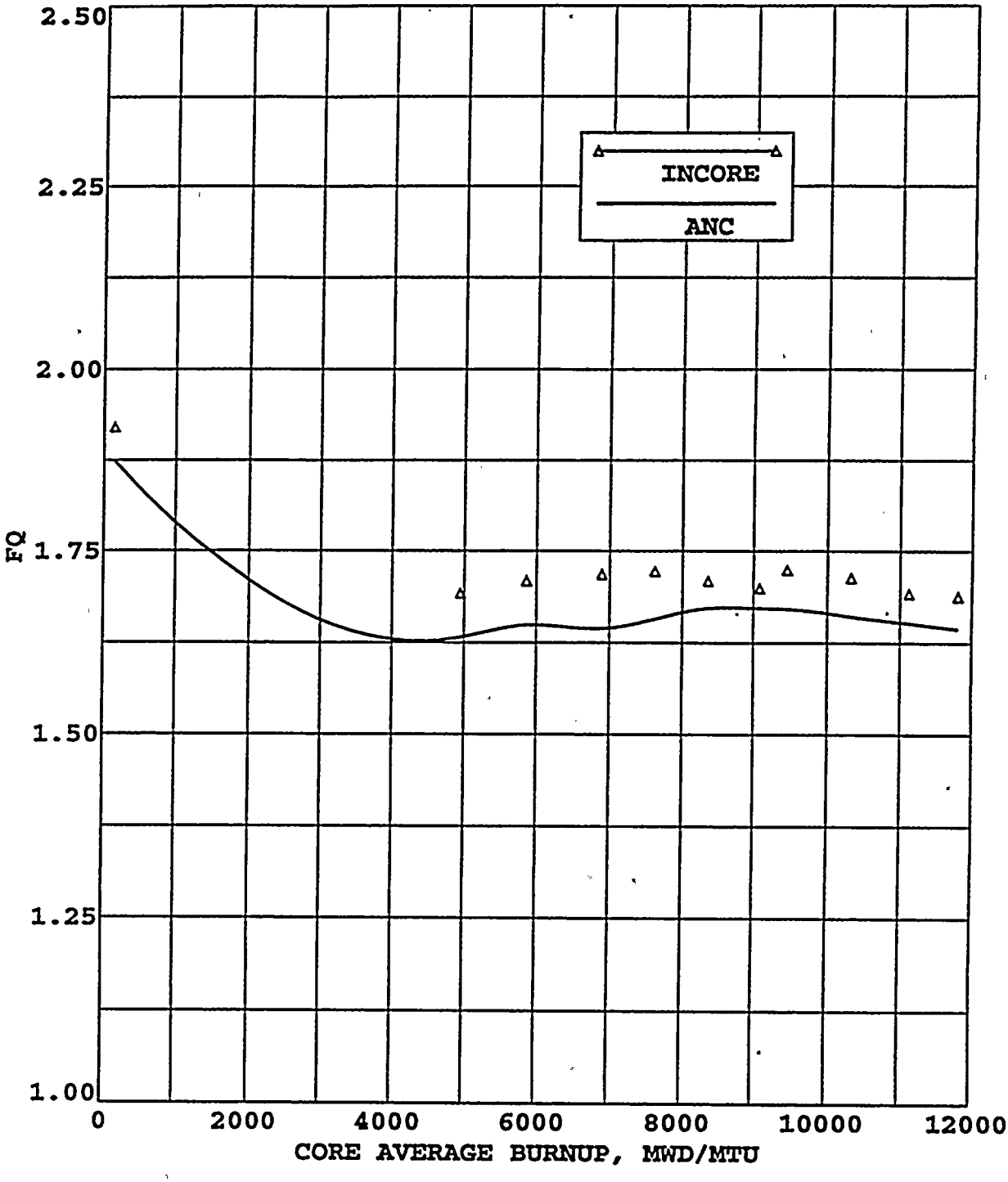

FIGURE 4.3-8
TURKEY POINT UNIT 4 CYCLE 13
FQ COMPARISON
BETWEEN INCORE AND ANC

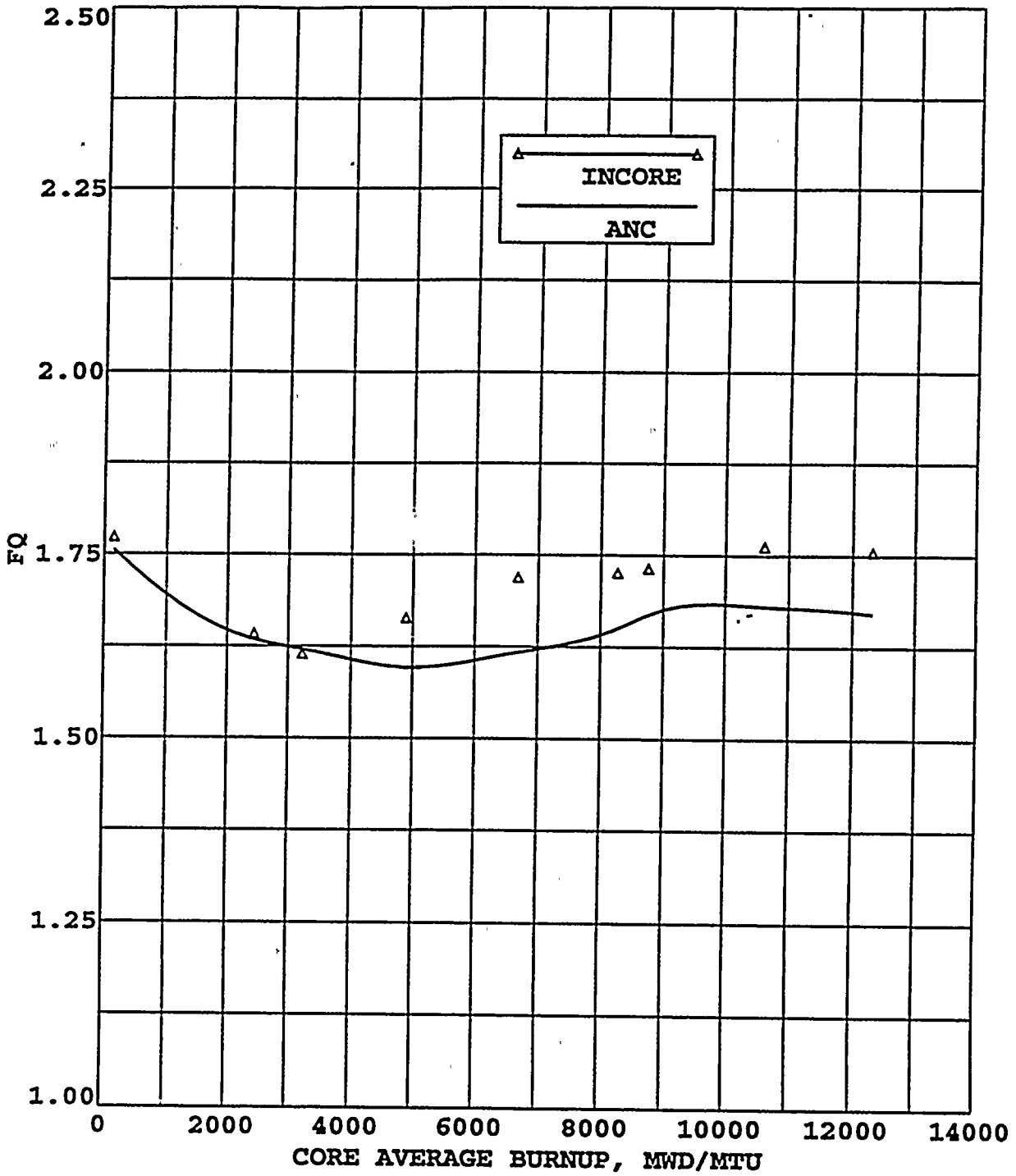

FIGURE 4.3-9
TURKEY POINT UNIT 4 CYCLE 14
FQ COMPARISON
BETWEEN INCORE AND ANC

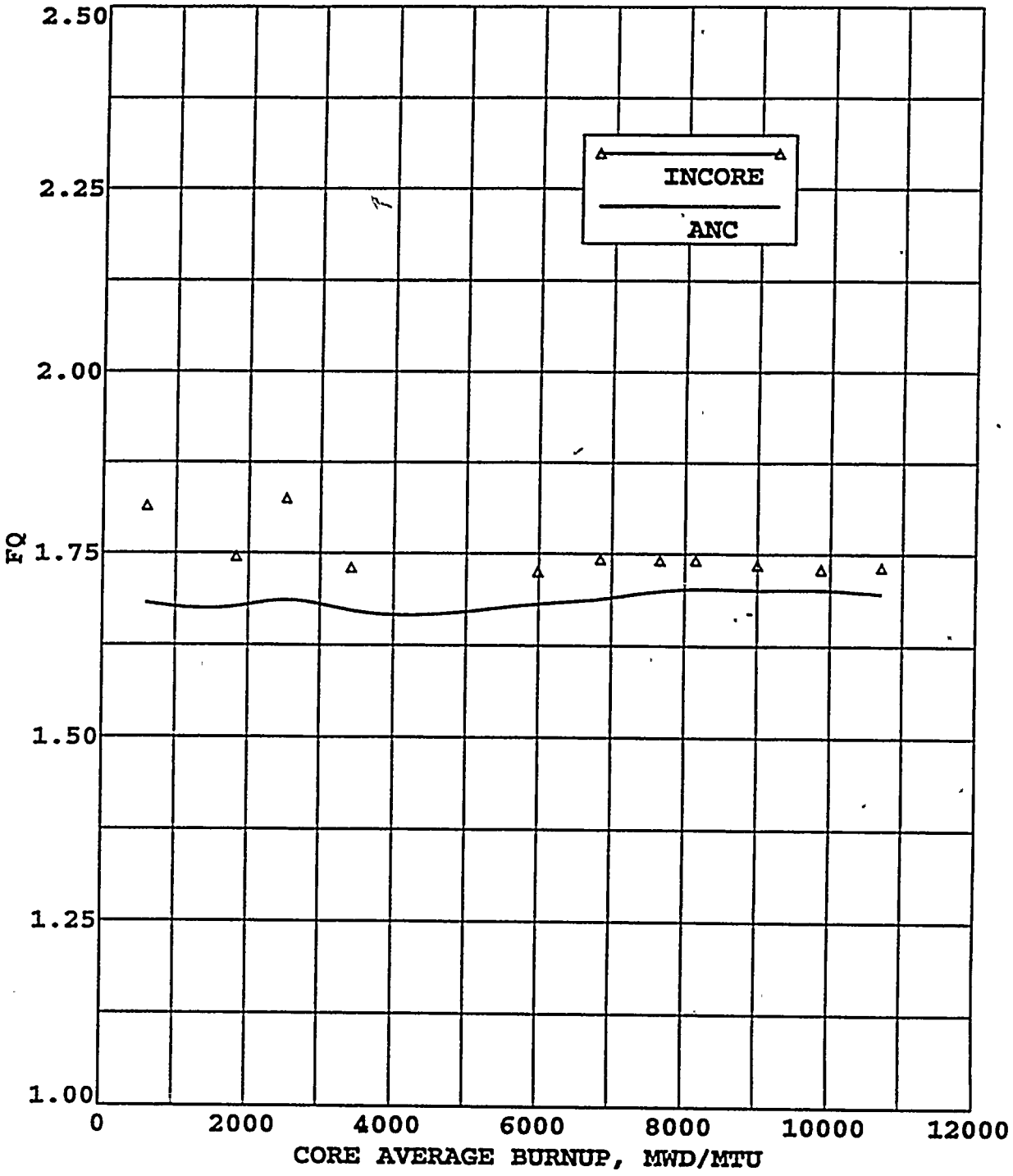

FIGURE 4.3-10

TURKEY POINT UNIT 4, CYCLE 12

RADIAL POWER DISTRIBUTION COMPARISON BETWEEN INCORE AND ANC

15	14	13	12	11	10	9	8	7	6	5	4	3	2	1	
						0.240 0.241 -0.41%	0.283 0.286 -1.05%	0.240 0.241 -0.41%							R
				0.380 0.364 4.40%	0.704 0.673 4.61%	1.102 1.088 1.29%	0.858 0.859 -0.12%	1.083 1.088 -0.46%	0.685 0.673 1.78%	0.387 0.364 6.32%					P
			0.448 0.445 0.67%	1.101 1.097 0.36%	1.315 1.290 1.94%	1.146 1.130 1.42%	1.341 1.362 -1.54%	1.117 1.130 -1.15%	1.280 1.290 -0.78%	1.122 1.097 2.28%	0.456 0.445 2.47%				N
		0.440 0.444 -0.90%	1.112 1.122 -0.89%	1.207 1.205 0.17%	1.170 1.174 -0.34%	1.313 1.337 -1.80%	1.060 1.066 -0.56%	1.311 1.337 -1.94%	1.175 1.174 0.09%	1.231 1.205 2.16%	1.130 1.122 0.71%	0.454 0.444 2.25%			M
	0.358 0.364 -1.65%	1.039 1.096 -5.20%	1.204 1.204 0.00%	1.156 1.164 -0.69%	1.288 1.330 -3.16%	1.139 1.147 -0.70%	1.207 1.207 0.00%	1.165 1.147 1.57%	1.324 1.330 -0.45%	1.181 1.164 1.46%	1.206 1.204 0.17%	1.092 1.096 -0.36%	0.367 0.364 0.82%		L
	0.648 0.672 -3.57%	1.261 1.288 -2.10%	1.174 1.172 0.17%	1.305 1.327 -1.66%	1.062 1.060 0.19%	1.184 1.177 0.59%	1.209 1.193 1.34%	1.207 1.177 2.55%	1.087 1.060 2.55%	1.318 1.327 -0.68%	1.164 1.172 -0.68%	1.277 1.288 -0.85%	0.670 0.672 -0.30%		K
0.232 0.241 -3.73%	1.094 1.086 0.74%	1.137 1.127 0.89%	1.317 1.334 -1.27%	1.156 1.144 1.05%	1.193 1.174 1.62%	1.257 1.249 0.64%	1.086 1.047 3.72%	1.264 1.249 1.20%	1.196 1.174 1.87%	1.114 1.144 -2.62%	1.270 1.334 -4.80%	1.100 1.127 -2.40%	1.083 1.086 -0.28%	0.240 0.241 -0.41%	J
0.290 0.285 1.75%	0.867 0.858 1.05%	1.359 1.358 0.07%	1.075 1.063 1.13%	1.226 1.207 1.57%	1.224 1.191 2.77%	1.087 1.046 3.92%	1.146 1.087 5.43%	1.081 1.046 3.35%	1.220 1.191 2.43%	1.182 1.206 -1.99%	1.037 1.063 -2.45%	1.318 1.358 -2.95%	0.859 0.858 0.12%	0.291 0.285 2.11%	H
0.245 0.241 1.66%	1.094 1.086 0.74%	1.125 1.127 -0.18%	1.326 1.334 -0.60%	1.171 1.144 2.36%	1.212 1.174 3.24%	1.274 1.249 2.00%	1.087 1.047 3.82%	1.259 1.249 0.80%	1.191 1.174 1.45%	1.122 1.144 -1.92%	1.273 1.334 -4.57%	1.103 1.127 -2.13%	1.099 1.086 1.20%	0.246 0.241 2.07%	G
	0.686 0.672 2.08%	1.336 1.288 3.73%	1.179 1.172 0.60%	1.312 1.327 -1.13%	1.086 1.060 2.45%	1.209 1.177 2.72%	1.228 1.193 2.93%	1.196 1.177 1.61%	1.066 1.060 0.57%	1.278 1.327 -3.69%	1.141 1.172 -2.65%	1.259 1.288 -2.25%	0.674 0.672 0.30%		F
	0.384 0.364 5.49%	1.115 1.096 1.73%	1.222 1.204 1.50%	1.172 1.164 0.69%	1.316 1.330 -1.05%	1.160 1.147 1.13%	1.224 1.207 1.41%	1.149 1.147 0.17%	1.292 1.330 -2.86%	1.148 1.164 -1.37%	1.191 1.204 -1.08%	1.080 1.096 -1.46%	0.372 0.364 2.20%		E
		0.464 0.444 4.50%	1.127 1.122 0.45%	1.206 1.205 0.08%	1.145 1.174 -2.47%	1.313 1.337 -1.80%	1.073 1.066 0.66%	1.313 1.337 -1.80%	1.160 1.174 -1.19%	1.196 1.205 -0.75%	1.115 1.122 -0.62%	0.457 0.444 2.93%			D
			0.465 0.445 4.49%	1.090 1.097 -0.64%	1.239 1.290 -3.95%	1.102 1.130 -2.48%	1.342 1.362 -1.47%	1.121 1.130 -0.80%	1.263 1.290 -2.09%	1.059 1.097 -3.46%	0.441 0.445 -0.90%				C
				0.367 0.364 0.82%	0.670 0.673 -0.45%	1.072 1.087 -1.38%	0.857 0.859 -0.23%	1.084 1.087 -0.28%	0.662 0.673 -1.63%	0.351 0.364 -3.57%					B
						0.238 0.241 -1.24%	0.285 0.286 -0.35%	0.241 0.241 0.00%							A

INCORE
ANC
% DIFFERENCE

Mean Absolute Difference = 0.016
Standard Deviation = 0.014

BURNUP = 2320 MWD/MTU POWER LEVEL = 100% D BANK AT 228 STEPS

FIGURE 4.3-11

TURKEY POINT UNIT 4, CYCLE 12

RADIAL POWER DISTRIBUTION COMPARISON BETWEEN INCORE AND ANC

15	14	13	12	11	10	9	8	7	6	5	4	3	2	1	
						0.245 0.244 0.41%	0.290 0.290 0.00%	0.245 0.244 0.41%							R
				0.393 0.383 2.61%	0.686 0.675 1.63%	1.049 1.045 0.38%	0.824 0.832 -0.96%	1.035 1.045 -0.96%	0.669 0.675 -0.89%	0.389 0.383 1.57%					P
			0.465 0.467 -0.43%	1.118 1.127 -0.80%	1.294 1.293 0.08%	1.087 1.093 -0.55%	1.302 1.341 -2.91%	1.059 1.093 -3.11%	1.260 1.293 -2.55%	1.107 1.128 -1.86%	0.462 0.467 -1.07%				N
		0.458 0.467 -1.93%	1.117 1.147 -2.62%	1.153 1.171 -1.54%	1.133 1.150 -1.48%	1.362 1.381 -1.38%	1.039 1.044 -0.48%	1.363 1.381 -1.30%	1.133 1.150 -1.48%	1.172 1.171 0.09%	1.133 1.147 -1.22%	0.469 0.467 0.43%			M
	0.376 0.384 -2.08%	1.068 1.127 -5.24%	1.194 1.171 1.96%	1.119 1.142 -2.01%	1.346 1.385 -2.82%	1.111 1.124 -1.16%	1.156 1.161 -0.43%	1.128 1.124 0.36%	1.368 1.385 -1.23%	1.131 1.142 -0.96%	1.152 1.171 -1.62%	1.109 1.128 -1.68%	0.384 0.384 0.00%		L
	0.666 0.675 -1.33%	1.267 1.293 -2.01%	1.160 1.150 0.87%	1.384 1.383 0.07%	1.043 1.058 -1.42%	1.149 1.161 -1.03%	1.171 1.159 1.04%	1.179 1.161 1.55%	1.071 1.059 1.13%	1.360 1.383 -1.66%	1.134 1.150 -1.39%	1.283 1.293 -0.77%	0.660 0.675 -2.22%		K
0.246 0.243 1.23%	1.052 1.044 0.77%	1.096 1.092 0.37%	1.368 1.380 -0.87%	1.118 1.122 -0.36%	1.143 1.158 -1.30%	1.310 1.344 -2.53%	1.111 1.066 4.22%	1.377 1.344 2.46%	1.174 1.158 1.38%	1.122 1.122 0.00%	1.378 1.380 -0.14%	1.115 1.092 2.11%	1.069 1.045 2.30%	0.247 0.243 1.65%	J
.292 .290 0.69%	0.837 0.833 0.48%	1.345 1.339 0.45%	1.050 1.043 0.67%	1.162 1.161 0.09%	1.182 1.159 1.98%	1.119 1.066 4.97%	1.169 1.104 5.89%	1.101 1.066 3.28%	1.186 1.159 2.33%	1.169 1.162 0.60%	1.059 1.043 1.53%	1.370 1.339 2.32%	0.850 0.833 2.04%	0.293 0.290 1.03%	H
0.246 0.243 1.23%	1.061 1.044 1.63%	1.098 1.092 0.55%	1.372 1.380 -0.58%	1.117 1.122 -0.45%	1.175 1.158 1.47%	1.386 1.344 3.12%	1.107 1.066 3.85%	1.363 1.344 1.41%	1.174 1.158 1.38%	1.116 1.122 -0.53%	1.371 1.380 -0.65%	1.084 1.092 -0.73%	1.052 1.045 0.67%	0.244 0.243 0.41%	G
	0.701 0.675 3.85%	1.320 1.293 2.09%	1.151 1.150 0.09%	1.366 1.383 -1.23%	1.081 1.059 2.08%	1.197 1.161 3.10%	1.204 1.159 3.88%	1.178 1.161 1.46%	1.082 1.059 2.17%	1.356 1.383 -1.95%	1.129 1.150 -1.83%	1.270 1.293 -1.78%	0.668 0.675 -1.04%		F
	0.408 0.384 6.25%	1.149 1.128 1.86%	1.181 1.171 0.85%	1.130 1.142 -1.05%	1.370 1.385 -1.08%	1.121 1.124 -0.27%	1.185 1.161 2.07%	1.125 1.124 0.09%	1.368 1.385 -1.23%	1.125 1.142 -1.49%	1.149 1.171 -1.88%	1.108 1.128 -1.77%	0.386 0.384 0.52%		E
		0.481 0.467 3.00%	1.152 1.147 0.44%	1.165 1.171 -0.51%	1.127 1.150 -2.00%	1.364 1.381 -1.23%	1.068 1.044 2.30%	1.390 1.381 0.65%	1.145 1.150 -0.43%	1.156 1.171 -1.28%	1.125 1.147 -1.92%	0.462 0.467 -1.07%			D
			0.482 0.467 3.21%	1.121 1.128 -0.62%	1.267 1.294 -2.09%	1.081 1.093 -1.10%	1.355 1.341 1.04%	1.102 1.093 0.82%	1.280 1.294 -1.08%	1.100 1.128 -2.48%	0.464 0.467 -0.64%				C
				0.389 0.383 1.57%	0.679 0.675 0.59%	1.050 1.045 0.48%	0.842 0.833 1.08%	1.058 1.045 1.24%	0.668 0.675 -1.04%	0.380 0.383 -0.78%					B
						0.245 0.244 0.41%	0.293 0.290 1.03%	0.246 0.244 0.82%							A

INCORE
ANC
% DIFFERENCE

Mean Absolute Difference = 0.015
Standard Deviation = 0.012

BURNUP = 6975 MWD/MTU POWER LEVEL = 100% D BANK AT 228 STEPS

FIGURE 4.3-12

TURKEY POINT UNIT 4, CYCLE 12

RADIAL POWER DISTRIBUTION COMPARISON BETWEEN INCORE AND ANC

15	14	13	12	11	10	9	8	7	6	5	4	3	2	1	
						0.267 0.266 0.38%	0.325 0.319 1.88%	0.267 0.266 0.38%							R
				0.410 0.410 0.00%	0.704 0.697 1.00%	1.058 1.049 0.86%	0.847 0.849 -0.24%	1.038 1.049 -1.05%	0.687 0.697 -1.43%	0.393 0.410 -4.15%					P
			0.492 0.495 -0.61%	1.158 1.139 1.67%	1.301 1.275 2.04%	1.084 1.075 0.84%	1.296 1.316 -1.52%	1.075 1.075 0.00%	1.263 1.275 -0.94%	1.111 1.139 -2.46%	0.474 0.495 -4.24%				N
		0.492 0.495 -0.61%	1.175 1.158 1.47%	1.170 1.150 1.74%	1.140 1.126 1.24%	1.370 1.377 -0.51%	1.048 1.033 1.45%	1.369 1.377 -0.58%	1.138 1.126 1.07%	1.165 1.150 1.30%	1.135 1.158 -1.99%	0.475 0.495 -4.04%			M
	0.397 0.411 -3.41%	1.140 1.139 0.09%	1.162 1.150 1.04%	1.108 1.123 -1.34%	1.383 1.385 -0.14%	1.115 1.109 0.54%	1.147 1.142 0.44%	1.112 1.108 0.36%	1.374 1.384 -0.72%	1.107 1.123 -1.42%	1.151 1.150 0.09%	1.128 1.139 -0.97%	0.398 0.410 -2.93%		L
	0.683 0.697 -2.01%	1.261 1.275 -1.10%	1.117 1.126 -0.80%	1.366 1.383 -1.23%	1.073 1.056 1.61%	1.163 1.153 0.87%	1.159 1.145 1.22%	1.152 1.152 0.00%	1.058 1.056 0.19%	1.347 1.383 -2.60%	1.126 1.126 0.00%	1.277 1.275 0.16%	0.691 0.697 -0.86%		K
0.265 0.266 -0.38%	1.038 1.049 -1.05%	1.079 1.075 0.37%	1.373 1.377 -0.29%	1.120 1.108 1.08%	1.158 1.151 0.61%	1.383 1.361 1.62%	1.079 1.071 0.75%	1.347 1.361 -1.03%	1.143 1.151 -0.70%	1.092 1.107 -1.36%	1.361 1.377 -1.16%	1.085 1.075 0.93%	1.046 1.049 -0.29%	0.267 0.266 0.38%	J
0.327 0.319 2.51%	0.879 0.850 3.41%	1.324 1.315 0.68%	1.060 1.033 2.61%	1.156 1.143 1.14%	1.155 1.145 0.87%	1.089 1.071 1.68%	1.147 1.109 3.43%	1.098 1.071 2.52%	1.153 1.145 0.70%	1.146 1.143 0.26%	1.043 1.032 1.07%	1.325 1.315 0.76%	0.846 0.849 -0.35%	0.324 0.319 1.57%	H
0.273 0.266 2.63%	1.077 1.049 2.67%	1.101 1.075 2.42%	1.378 1.377 0.07%	1.117 1.107 0.90%	1.168 1.151 1.48%	1.397 1.361 2.65%	1.091 1.071 1.87%	1.390 1.361 2.13%	1.168 1.151 1.48%	1.118 1.107 0.99%	1.362 1.377 -1.09%	1.054 1.075 -1.95%	1.036 1.049 -1.24%	0.267 0.266 0.38%	G
	0.695 0.697 -0.29%	1.281 1.275 0.47%	1.129 1.126 0.27%	1.365 1.383 -1.30%	1.065 1.056 0.85%	1.167 1.152 1.30%	1.158 1.145 1.14%	1.174 1.152 1.91%	1.075 1.056 1.80%	1.388 1.383 0.36%	1.130 1.126 0.36%	1.270 1.275 -0.39%	0.687 0.697 -1.43%		F
	0.392 0.411 -4.62%	1.120 1.139 -1.67%	1.155 1.150 0.43%	1.105 1.123 -1.60%	1.353 1.384 -2.24%	1.107 1.108 -0.09%	1.160 1.141 1.67%	1.122 1.108 1.26%	1.359 1.384 -1.81%	1.104 1.123 -1.69%	1.161 1.150 0.96%	1.156 1.139 1.49%	0.409 0.410 -0.24%		E
		0.475 0.495 -4.04%	1.137 1.158 -1.81%	1.142 1.150 -0.70%	1.114 1.126 -1.07%	1.365 1.377 -0.87%	1.073 1.032 3.97%	1.361 1.376 -1.09%	1.113 1.126 -1.15%	1.145 1.150 -0.43%	1.146 1.157 -0.95%	0.484 0.495 -2.22%			D
			0.471 0.495 -4.85%	1.113 1.139 -2.28%	1.254 1.274 -1.57%	1.083 1.075 0.74%	1.342 1.315 2.05%	1.055 1.075 -1.86%	1.252 1.274 -1.73%	1.119 1.138 -1.67%	0.475 0.495 -4.04%				C
				0.391 0.410 -4.63%	0.679 0.697 -2.58%	1.061 1.048 1.24%	0.853 0.849 0.47%	1.044 1.048 -0.38%	0.674 0.697 -3.30%	0.394 0.410 -3.90%					B
						0.269 0.266 1.13%	0.327 0.319 2.51%	0.269 0.266 1.13%							A

INCORE
ANC
% DIFFERENCE

Mean Absolute Difference = 0.013
Standard Deviation = 0.009

BURNUP = 11812 MWD/MTU POWER LEVEL = 100% D BANK AT 228 STEPS

FIGURE 4.3-13

TURKEY POINT UNIT 4, CYCLE 13

RADIAL POWER DISTRIBUTION COMPARISON BETWEEN INCORE AND ANC

15	14	13	12	11	10	9	8	7	6	5	4	3	2	1	
						0.251 0.244 2.87%	0.273 0.272 0.37%	0.251 0.244 2.87%							R
				0.424 0.416 1.92%	0.823 0.814 1.11%	1.119 1.146 -2.36%	0.907 0.928 -2.26%	1.100 1.146 -4.01%	0.806 0.814 -0.98%	0.431 0.416 3.61%					P
			0.457 0.447 2.24%	1.089 1.106 -1.54%	1.277 1.292 -1.16%	1.015 1.010 0.50%	1.326 1.342 -1.19%	0.971 1.010 -3.86%	1.252 1.292 -3.10%	1.109 1.106 0.27%	0.463 0.447 3.58%				N
		0.452 0.448 0.89%	1.070 1.080 -0.93%	1.104 1.105 -0.09%	1.014 0.989 2.53%	1.282 1.288 -0.47%	0.991 0.998 -0.70%	1.265 1.288 -1.79%	1.003 0.989 1.42%	1.115 1.105 0.90%	1.086 1.080 0.56%	0.455 0.448 1.56%			M
	0.409 0.417 -1.92%	1.051 1.107 -5.06%	1.139 1.106 2.98%	1.270 1.258 0.95%	1.205 1.187 1.52%	1.223 1.214 0.74%	1.310 1.292 1.39%	1.233 1.214 1.57%	1.197 1.187 0.84%	1.275 1.258 1.35%	1.106 1.106 0.00%	1.082 1.107 -2.26%	0.418 0.417 0.24%		L
	0.799 0.815 -1.96%	1.263 1.293 -2.32%	1.034 0.992 4.23%	1.216 1.188 2.36%	1.235 1.222 1.06%	1.315 1.300 1.15%	1.072 1.051 2.00%	1.304 1.300 0.31%	1.231 1.222 0.74%	1.203 1.188 1.26%	1.008 0.992 1.61%	1.257 1.293 -2.78%	0.804 0.815 -1.35%		K
0.257 0.244 5.33%	1.133 1.147 -1.22%	1.031 1.011 1.98%	1.300 1.290 0.78%	1.237 1.215 1.81%	1.301 1.298 0.23%	1.065 1.051 1.33%	1.316 1.369 -3.87%	1.044 1.051 -0.67%	1.294 1.298 -0.31%	1.228 1.215 1.07%	1.261 1.290 -2.25%	0.994 1.011 -1.68%	1.117 1.147 -2.62%	0.250 0.244 2.46%	J
0.280 0.272 2.94%	0.932 0.929 0.32%	1.338 1.343 -0.37%	1.011 0.999 1.20%	1.303 1.292 0.85%	1.067 1.048 1.81%	1.324 1.363 -2.86%	1.040 1.053 -1.23%	1.319 1.363 -3.23%	1.062 1.048 1.34%	1.266 1.292 -2.01%	0.966 0.999 -3.30%	1.343 1.343 0.00%	0.919 0.929 -1.08%	0.272 0.272 0.00%	H
0.257 0.244 5.33%	1.153 1.147 0.52%	1.026 1.011 1.48%	1.288 1.290 -0.16%	1.238 1.215 1.89%	1.309 1.298 0.85%	1.046 1.051 -0.48%	1.335 1.369 -2.48%	1.048 1.051 -0.29%	1.291 1.297 -0.46%	1.202 1.215 -1.07%	1.254 1.290 -2.79%	1.007 1.011 -0.40%	1.125 1.147 -1.92%	0.255 0.244 4.51%	G
	0.833 0.815 2.21%	1.292 1.293 -0.08%	1.024 0.992 3.23%	1.214 1.188 2.19%	1.240 1.222 1.47%	1.322 1.300 1.69%	1.070 1.051 1.81%	1.295 1.300 -0.38%	1.229 1.222 0.57%	1.198 1.188 0.84%	0.989 0.992 -0.30%	1.262 1.293 -2.40%	0.821 0.815 0.74%		F
	0.433 0.417 3.84%	1.112 1.107 0.45%	1.128 1.106 1.99%	1.284 1.258 2.07%	1.203 1.187 1.35%	1.214 1.214 0.00%	1.291 1.292 -0.08%	1.226 1.214 0.99%	1.207 1.187 1.68%	1.286 1.258 2.23%	1.105 1.106 -0.09%	1.085 1.107 -1.99%	0.424 0.417 1.68%		E
		0.472 0.448 5.36%	1.103 1.080 2.13%	1.111 1.105 0.54%	0.977 0.989 -1.21%	1.251 1.288 -2.87%	1.005 0.998 0.70%	1.297 1.288 0.70%	1.018 0.989 2.93%	1.103 1.105 -0.18%	1.087 1.079 0.74%	0.459 0.448 2.46%			D
			0.471 0.447 5.37%	1.084 1.106 -1.99%	1.243 1.292 -3.79%	1.001 1.010 -0.89%	1.332 1.342 -0.75%	1.020 1.010 0.99%	1.272 1.291 -1.47%	1.077 1.106 -2.62%	0.458 0.447 2.46%				C
				0.420 0.416 0.96%	0.807 0.814 -0.86%	1.116 1.146 -2.62%	0.921 0.928 -0.75%	1.149 1.146 0.26%	0.814 0.814 0.00%	0.415 0.416 -0.24%					B
						0.252 0.244 3.28%	0.281 0.272 3.31%	0.261 0.244 6.97%							A

INCORE
ANC
% DIFFERENCE

Mean Absolute Difference = 0.015
Standard Deviation = 0.012

BURNUP = 2440 MWD/MTU POWER LEVEL = 99.4% D BANK AT 215 STEPS

FIGURE 4.3-14

TURKEY POINT UNIT 4, CYCLE 13

RADIAL POWER DISTRIBUTION COMPARISON BETWEEN INCORE AND ANC

15	14	13	12	11	10	9	8	7	6	5	4	3	2	1	
						0.254 0.250 1.60%	0.277 0.280 -1.07%	0.254 0.250 1.60%							R
				0.450 0.438 2.74%	0.828 0.813 1.85%	1.108 1.115 -0.63%	0.901 0.911 -1.05%	1.102 1.115 -1.17%	0.819 0.813 0.74%	0.445 0.438 1.60%					P
			0.497 0.480 3.54%	1.149 1.145 0.35%	1.305 1.310 -0.38%	1.005 1.005 0.00%	1.355 1.352 0.22%	1.009 1.005 0.40%	1.292 1.310 -1.37%	1.138 1.145 -0.61%	0.491 0.480 2.29%				N
		0.530 0.480 10.42%	1.157 1.155 0.17%	1.098 1.100 -0.18%	0.987 0.986 0.10%	1.358 1.358 0.00%	1.035 1.026 0.88%	1.364 1.358 0.44%	0.984 0.986 -0.20%	1.087 1.100 -1.18%	1.143 1.155 -1.04%	0.486 0.480 1.25%			M
	0.481 0.438 9.82%	1.229 1.146 7.24%	1.173 1.101 6.54%	1.193 1.210 -1.40%	1.127 1.141 -1.23%	1.178 1.196 -1.51%	1.409 1.377 2.32%	1.205 1.196 0.75%	1.131 1.141 -0.88%	1.194 1.210 -1.32%	1.074 1.101 -2.45%	1.125 1.146 -1.83%	0.440 0.438 0.46%		L
	0.852 0.813 4.80%	1.396 1.311 6.48%	0.984 0.988 -0.40%	1.128 1.142 -1.23%	1.141 1.154 -1.13%	1.240 1.237 0.24%	1.038 1.019 1.86%	1.236 1.237 -0.08%	1.136 1.154 -1.56%	1.122 1.142 -1.75%	0.976 0.988 -1.21%	1.278 1.311 -2.52%	0.811 0.813 -0.25%		K
0.261 0.250 4.40%	1.117 1.116 0.09%	1.006 1.005 0.10%	1.364 1.359 0.37%	1.191 1.197 -0.50%	1.221 1.235 -1.13%	1.012 1.002 1.00%	1.328 1.360 -2.35%	0.998 1.002 -0.40%	1.211 1.235 -1.94%	1.168 1.197 -2.42%	1.324 1.359 -2.58%	1.010 1.005 0.50%	1.132 1.116 1.43%	0.269 0.250 7.60%	J
0.286 0.281 1.78%	0.914 0.912 0.22%	1.348 1.352 -0.30%	1.030 1.026 0.39%	1.380 1.377 0.22%	1.028 1.017 1.08%	1.333 1.355 -1.62%	1.027 1.022 0.49%	1.335 1.355 -1.48%	1.022 1.017 0.49%	1.333 1.377 -3.20%	0.981 1.026 -4.39%	1.352 1.352 0.00%	0.926 0.912 1.54%	0.295 0.281 4.98%	H
0.261 0.250 4.40%	1.118 1.116 0.18%	1.001 1.005 -0.40%	1.348 1.359 -0.81%	1.193 1.197 -0.33%	1.228 1.235 -0.57%	0.999 1.002 -0.30%	1.347 1.360 -0.96%	1.014 1.002 1.20%	1.226 1.235 -0.73%	1.171 1.197 -2.17%	1.323 1.359 -2.65%	0.984 1.005 -2.09%	1.115 1.116 -0.09%	0.261 0.250 4.40%	G
	0.825 0.813 1.48%	1.300 1.311 -0.84%	0.990 0.988 0.20%	1.131 1.142 -0.96%	1.146 1.154 -0.69%	1.238 1.237 0.08%	1.029 1.019 0.98%	1.230 1.237 -0.57%	1.157 1.154 0.26%	1.138 1.142 -0.35%	0.987 0.988 -0.10%	1.278 1.311 -2.52%	0.811 0.813 -0.25%		F
	0.448 0.438 2.28%	1.143 1.146 -0.26%	1.096 1.101 -0.45%	1.212 1.210 0.17%	1.139 1.141 -0.18%	1.187 1.196 -0.75%	1.372 1.377 -0.36%	1.197 1.196 0.08%	1.142 1.141 0.09%	1.198 1.209 -0.91%	1.088 1.101 -1.18%	1.123 1.146 -2.01%	0.440 0.438 0.46%		E
		0.493 0.480 2.71%	1.149 1.155 -0.52%	1.098 1.100 -0.18%	0.999 0.986 1.32%	1.367 1.358 0.66%	1.043 1.025 1.76%	1.378 1.358 1.47%	0.997 0.986 1.12%	1.097 1.100 -0.27%	1.147 1.155 -0.69%	0.484 0.480 0.83%			D
			0.493 0.480 2.71%	1.132 1.145 -1.14%	1.275 1.310 -2.67%	0.994 1.004 -1.00%	1.365 1.352 0.96%	1.020 1.004 1.59%	1.309 1.310 -0.08%	1.116 1.145 -2.53%	0.483 0.480 0.63%				C
				0.439 0.438 0.23%	0.808 0.813 -0.62%	1.113 1.115 -0.18%	0.905 0.911 -0.66%	1.173 1.115 5.20%	0.823 0.813 1.23%	0.424 0.438 -3.20%					B
						0.260 0.250 4.00%	0.297 0.280 6.07%	0.271 0.250 8.40%							A

INCORE

ANC

% DIFFERENCE

Mean Absolute Difference = 0.013
Standard Deviation = 0.014

BURNUP = 6678 MWD/MTU POWER LEVEL = 100% D BANK AT 228 STEPS

FIGURE 4.3-15

TURKEY POINT UNIT 4, CYCLE 13

RADIAL POWER DISTRIBUTION COMPARISON BETWEEN INCORE AND ANC

15	14	13	12	11	10	9	8	7	6	5	4	3	2	1	
						0.286 0.268 6.72%	0.318 0.305 4.26%	0.278 0.268 3.73%							R
				0.477 0.467 2.14%	0.844 0.821 2.80%	1.117 1.103 1.27%	0.915 0.915 0.00%	1.102 1.103 -0.09%	0.822 0.821 0.12%	0.469 0.467 0.43%					P
			0.524 0.513 2.14%	1.177 1.176 0.09%	1.312 1.035 26.76%	1.009 1.001 0.80%	1.355 1.346 0.67%	0.981 1.001 -2.00%	1.277 1.305 -2.15%	1.158 1.177 -1.61%	0.521 0.513 1.56%					N
		0.520 0.513 1.36%	1.174 1.188 -1.18%	1.086 1.092 -0.55%	0.989 0.988 0.10%	1.394 1.388 0.43%	1.040 1.036 0.39%	1.386 1.388 -0.14%	0.981 0.988 -0.71%	1.079 1.092 -1.19%	1.173 1.188 -1.26%	0.521 0.514 1.36%			M
	0.465 0.467 -0.43%	1.145 1.177 -2.72%	1.115 1.093 2.01%	1.157 1.175 -1.53%	1.095 1.112 -1.53%	1.156 1.171 -1.28%	1.450 1.414 2.55%	1.182 1.171 0.94%	1.101 1.112 -0.99%	1.164 1.175 -0.94%	1.066 1.093 -2.47%	1.156 1.177 -1.78%	0.469 0.467 0.43%		L
	0.813 0.821 -0.97%	1.299 1.306 -0.54%	1.014 0.989 2.53%	1.114 1.112 0.18%	1.096 1.110 -1.26%	1.196 1.192 0.34%	1.025 1.002 2.30%	1.195 1.192 0.25%	1.095 1.110 -1.35%	1.094 1.112 -1.62%	0.975 0.989 -1.42%	1.273 1.306 -2.53%	0.818 0.821 -0.37%		K
0.276 0.268 2.99%	1.120 1.103 1.54%	1.017 1.002 1.50%	1.412 1.389 1.66%	1.182 1.172 0.85%	1.180 1.190 -0.84%	0.992 0.976 1.64%	1.320 1.335 -1.12%	0.983 0.976 0.72%	1.172 1.190 -1.51%	1.152 1.172 -1.71%	1.359 1.388 -2.09%	0.975 1.002 -2.69%	1.097 1.103 -0.54%	0.278 0.268 3.73%	J
0.319 0.305 4.59%	0.929 0.915 1.53%	1.353 1.346 0.52%	1.056 1.036 1.93%	1.443 1.415 1.98%	1.021 1.000 2.10%	1.322 1.333 -0.83%	1.006 0.995 1.11%	1.318 1.333 -1.13%	1.005 1.000 0.50%	1.376 1.415 -2.76%	1.001 1.036 -3.38%	1.355 1.346 0.67%	0.910 0.915 -0.55%	0.308 0.305 0.98%	H
0.286 0.268 6.72%	1.117 1.103 1.27%	1.009 1.002 0.70%	1.399 1.389 0.72%	1.196 1.172 2.05%	1.194 1.191 0.25%	0.983 0.976 0.72%	1.333 1.335 -0.15%	0.985 0.976 0.92%	1.181 1.190 -0.76%	1.147 1.172 -2.13%	1.362 1.389 -1.94%	0.992 1.002 -1.00%	1.109 1.103 0.54%	0.282 0.268 5.22%	G
	0.845 0.821 2.92%	1.313 1.306 0.54%	0.994 0.989 0.51%	1.105 1.112 -0.63%	1.100 1.110 -0.90%	1.197 1.192 0.42%	1.023 1.002 2.10%	1.185 1.192 -0.59%	1.105 1.110 -0.45%	1.099 1.112 -1.17%	0.975 0.990 -1.52%	1.296 1.306 -0.77%	0.843 0.821 2.68%		F
	0.483 0.467 3.43%	1.186 1.177 0.76%	1.093 1.093 0.00%	1.167 1.175 -0.68%	1.096 1.112 -1.44%	1.157 1.171 -1.20%	1.426 1.415 0.78%	1.181 1.171 0.85%	1.110 1.112 -0.18%	1.164 1.175 -0.94%	1.079 1.093 -1.28%	1.175 1.177 -0.17%	0.479 0.467 2.57%		E
		0.533 0.514 3.70%	1.193 1.188 0.42%	1.079 1.092 -1.19%	0.961 0.988 -2.73%	1.340 1.388 -3.46%	1.075 1.036 3.76%	1.431 1.388 3.10%	0.996 0.988 0.81%	1.071 1.092 -1.92%	1.182 1.188 -0.51%	0.529 0.514 2.92%			D
			0.532 0.513 3.70%	1.168 1.177 -0.76%	1.280 1.305 -1.92%	0.988 1.002 -1.40%	1.338 1.346 -0.59%	1.016 1.002 1.40%	1.302 1.305 -0.23%	1.152 1.177 -2.12%	0.522 0.514 1.56%				C
				0.476 0.467 1.93%	0.833 0.821 1.46%	1.098 1.103 -0.45%	0.916 0.915 0.11%	1.119 1.103 1.45%	0.829 0.821 0.97%	0.463 0.467 -0.86%					B
						0.278 0.268 3.73%	0.313 0.305 2.62%	0.285 0.268 6.34%							A

INCORE	
ANC	
% DIFFERENCE	

Mean Absolute Difference = 0.015
Standard Deviation = 0.023

BURNUP = 12316 MWD/MTU POWER LEVEL = 100% D BANK AT 228 STEPS

FIGURE 4.3-16

TURKEY POINT UNIT 4, CYCLE 14

RADIAL POWER DISTRIBUTION COMPARISON BETWEEN INCORE AND ANC

15	14	13	12	11	10	9	8	7	6	5	4	3	2	1	
						0.227 0.236 -3.81%	0.242 0.251 -3.59%	0.228 0.237 -3.80%							R
				0.349 0.352 -0.85%	0.798 0.801 -0.37%	1.085 1.080 0.46%	0.789 0.795 -0.75%	1.085 1.086 -0.09%	0.797 0.803 -0.75%	0.351 0.353 -0.57%					P
			0.390 0.391 -0.26%	1.050 1.057 -0.66%	1.252 1.259 -0.56%	1.279 1.230 3.98%	1.373 1.315 4.41%	1.214 1.234 -1.62%	1.254 1.262 -0.63%	1.059 1.059 0.00%	0.401 0.392 2.30%				N
		0.390 0.392 -0.51%	0.947 0.945 0.21%	1.242 1.240 0.16%	1.090 1.081 0.83%	1.290 1.270 1.57%	1.011 1.004 0.70%	1.283 1.273 0.79%	1.072 1.084 -1.11%	1.207 1.241 -2.74%	0.936 0.945 -0.95%	0.411 0.391 5.12%			M
	0.338 0.353 -4.25%	1.077 1.059 1.70%	1.255 1.241 1.13%	1.261 1.246 1.20%	1.286 1.267 1.50%	1.178 1.166 1.03%	1.297 1.310 -0.99%	1.154 1.169 -1.28%	1.274 1.271 0.24%	1.238 1.246 -0.64%	1.154 1.240 -6.94%	1.050 1.057 -0.66%	0.368 0.352 4.55%		L
	0.773 0.803 -3.74%	1.313 1.262 4.04%	1.110 1.084 2.40%	1.295 1.271 1.89%	1.026 1.018 0.79%	1.218 1.225 -0.57%	1.257 1.263 -0.48%	1.219 1.227 -0.65%	1.019 1.018 0.10%	1.243 1.266 -1.82%	1.040 1.081 -3.79%	1.181 1.259 -6.20%	0.750 0.801 -6.37%		K
0.229 0.237 3.38%	1.067 1.086 -1.75%	1.254 1.234 1.62%	1.329 1.273 4.40%	1.191 1.169 1.88%	1.219 1.228 -0.73%	1.282 1.285 -0.23%	1.236 1.233 0.24%	1.293 1.285 0.62%	1.225 1.225 0.00%	1.168 1.166 0.17%	1.220 1.270 -3.94%	1.152 1.230 -6.34%	1.045 1.080 -3.24%	0.234 0.236 -0.85%	J
0.253 0.251 0.80%	0.793 0.795 -0.25%	1.313 1.315 -0.15%	1.023 1.004 1.89%	1.368 1.310 4.43%	1.285 1.263 1.74%	1.261 1.233 2.27%	0.987 0.961 2.71%	1.238 1.233 0.41%	1.265 1.263 0.16%	1.288 1.310 -1.68%	0.941 1.004 -6.27%	1.236 1.315 -6.01%	0.764 0.795 -3.90%	0.249 0.251 -0.80%	H
0.248 0.236 5.08%	1.132 1.080 4.81%	1.256 1.230 2.11%	1.287 1.270 1.34%	1.172 1.166 0.51%	1.248 1.225 1.88%	1.353 1.285 5.29%	1.267 1.233 2.76%	1.321 1.285 2.80%	1.270 1.227 3.50%	1.181 1.169 1.03%	1.252 1.273 -1.65%	1.205 1.234 -2.35%	1.069 1.086 -1.57%	0.233 0.237 -1.69%	G
	0.828 0.801 3.37%	1.294 1.259 2.78%	1.091 1.081 0.93%	1.273 1.267 0.47%	1.038 1.018 1.96%	1.237 1.227 0.81%	1.290 1.263 2.14%	1.279 1.225 4.41%	1.086 1.018 6.68%	1.324 1.271 4.17%	1.105 1.084 1.94%	1.261 1.262 -0.08%	0.780 0.803 -2.86%		F
	0.360 0.352 2.27%	1.085 1.057 2.65%	1.249 1.240 0.73%	1.239 1.246 -0.56%	1.260 1.271 -0.87%	1.170 1.169 0.09%	1.323 1.310 0.99%	1.197 1.166 2.66%	1.304 1.266 3.00%	1.278 1.246 2.57%	1.239 1.241 -0.16%	1.041 1.059 -1.70%	0.338 0.353 -4.25%		E
		0.402 0.391 2.81%	0.902 0.945 -4.55%	1.183 1.241 -4.67%	1.035 1.084 -4.52%	1.279 1.273 0.47%	1.021 1.004 1.69%	1.254 1.270 -1.26%	1.083 1.081 0.19%	1.272 1.240 2.58%	0.933 0.945 -1.27%	0.374 0.392 -4.59%			D
			0.386 0.392 -1.53%	1.031 1.059 -2.64%	1.230 1.262 -2.54%	1.216 1.234 -1.46%	1.374 1.314 4.57%	1.221 1.230 -0.73%	1.231 1.259 -2.22%	1.025 1.057 -3.03%	0.377 0.391 -3.58%				C
				0.346 0.353 -1.98%	0.792 0.803 -1.37%	1.082 1.086 -0.37%	0.753 0.794 -5.16%	1.032 1.080 -4.44%	0.777 0.801 -3.00%	0.340 0.352 -3.41%					B
						0.235 0.237 -0.84%	0.241 0.251 -3.98%	0.226 0.236 -4.24%							A

INCORE
ANC
% DIFFERENCE

Mean Absolute Difference = 0.021
Standard Deviation = 0.019

BURNUP = 600 MWD/MTU POWER LEVEL = 100% D BANK AT 228 STEPS

FIGURE 4.3-17

TURKEY POINT UNIT 4, CYCLE 14

RADIAL POWER DISTRIBUTION COMPARISON BETWEEN INCORE AND ANC

15	14	13	12	11	10	9	8	7	6	5	4	3	2	1	
						0.248 0.245 1.22%	0.268 0.265 1.13%	0.249 0.246 1.22%							R
				0.371 0.370 0.27%	0.797 0.790 0.89%	1.069 1.055 1.33%	0.784 0.781 0.38%	1.067 1.058 0.85%	0.792 0.791 0.13%	0.370 0.370 0.00%					P
			0.409 0.403 1.49%	1.092 1.084 0.74%	1.290 1.281 0.70%	1.196 1.188 0.67%	1.355 1.336 1.42%	1.179 1.189 -0.84%	1.282 1.282 0.00%	1.091 1.084 0.65%	0.403 0.403 0.00%					N
		0.404 0.403 0.25%	0.918 0.910 0.88%	1.177 1.170 0.60%	1.069 1.067 0.19%	1.370 1.359 0.81%	1.021 1.011 0.99%	1.371 1.360 0.81%	1.066 1.069 -0.28%	1.168 1.170 -0.17%	0.901 0.910 -0.99%	0.398 0.403 -1.24%			M
	0.362 0.370 -2.16%	1.067 1.084 -1.57%	1.172 1.170 0.17%	1.188 1.188 0.00%	1.346 1.339 0.52%	1.158 1.152 0.52%	1.384 1.375 0.65%	1.167 1.154 1.13%	1.369 1.342 2.01%	1.177 1.188 -0.93%	1.148 1.170 -1.88%	1.066 1.084 -1.66%	0.361 0.370 -2.43%		L
	0.790 0.791 -0.13%	1.275 1.282 -0.55%	1.067 1.069 -0.19%	1.356 1.342 1.04%	0.999 1.010 -1.09%	1.176 1.183 -0.59%	1.209 1.204 0.42%	1.197 1.184 1.10%	1.020 1.010 0.99%	1.339 1.339 0.00%	1.054 1.067 -1.22%	1.269 1.281 -0.94%	0.787 0.790 -0.38%		K
0.249 0.246 1.22%	1.068 1.058 0.95%	1.188 1.189 -0.08%	1.368 1.360 0.59%	1.153 1.154 -0.09%	1.166 1.184 -1.52%	1.346 1.363 -1.25%	1.199 1.187 1.01%	1.377 1.363 1.03%	1.180 1.183 -0.25%	1.155 1.152 0.26%	1.357 1.359 -0.15%	1.178 1.187 -0.76%	1.067 1.055 1.14%	0.248 0.245 1.22%	J
0.268 0.265 1.13%	0.783 0.781 0.26%	1.336 1.336 0.00%	1.022 1.011 1.09%	1.393 1.375 1.31%	1.201 1.204 -0.25%	1.183 1.187 -0.34%	0.949 0.937 1.28%	1.185 1.187 -0.17%	1.182 1.204 -1.83%	1.361 1.375 -1.02%	0.996 1.011 -1.48%	1.363 1.336 2.02%	0.786 0.780 0.77%	0.268 0.265 1.13%	H
0.247 0.245 0.82%	1.063 1.055 0.76%	1.185 1.188 -0.25%	1.367 1.359 0.59%	1.165 1.152 1.13%	1.189 1.183 0.51%	1.373 1.363 0.73%	1.183 1.187 -0.34%	1.363 1.363 0.00%	1.178 1.184 -0.51%	1.138 1.154 -1.39%	1.351 1.360 -0.66%	1.180 1.189 -0.76%	1.070 1.058 1.13%	0.248 0.246 0.81%	G
	0.792 0.790 0.25%	1.280 1.281 -0.08%	1.063 1.067 -0.37%	1.357 1.339 1.34%	1.016 1.010 0.59%	1.182 1.184 -0.17%	1.178 1.204 -2.16%	1.175 1.183 -0.68%	1.017 1.010 0.69%	1.329 1.342 -0.97%	1.043 1.068 -2.34%	1.269 1.282 -1.01%	0.788 0.791 -0.38%		F
	0.367 0.370 -0.81%	1.084 1.084 0.00%	1.170 1.170 0.00%	1.178 1.188 -0.84%	1.345 1.342 0.22%	1.142 1.154 -1.04%	1.377 1.375 0.15%	1.153 1.152 0.09%	1.339 1.339 0.00%	1.168 1.188 -1.68%	1.153 1.170 -1.45%	1.074 1.084 -0.92%	0.366 0.370 -1.08%		E
		0.404 0.403 0.25%	0.906 0.910 -0.44%	1.162 1.170 -0.68%	1.058 1.068 -0.94%	1.382 1.360 1.62%	1.034 1.011 2.27%	1.387 1.359 2.06%	1.060 1.067 -0.66%	1.158 1.170 -1.03%	0.901 0.910 -0.99%	0.402 0.403 -0.25%			D
			0.392 0.403 -2.73%	1.052 1.084 -2.95%	1.243 1.282 -3.04%	1.178 1.189 -0.93%	1.360 1.336 1.80%	1.206 1.187 1.60%	1.293 1.281 0.94%	1.089 1.084 0.46%	0.405 0.403 0.50%				C
				0.356 0.370 -3.78%	0.767 0.791 -3.03%	1.054 1.058 -0.38%	0.792 0.780 1.54%	1.076 1.055 1.99%	0.805 0.790 1.90%	0.374 0.370 1.08%					B
						0.239 0.246 -2.85%	0.271 0.265 2.26%	0.251 0.245 2.45%							A

INCORE

ANC

% DIFFERENCE

Mean Absolute Difference = 0.009
Standard Deviation = 0.007

BURNUP = 6836 MWD/MTU POWER LEVEL = 100% D BANK AT 228 STEPS

FIGURE 4.3-18

TURKEY POINT UNIT 4, CYCLE 14

RADIAL POWER DISTRIBUTION COMPARISON BETWEEN INCORE AND ANC

15	14	13	12	11	10	9	8	7	6	5	4	3	2	1	
						0.265 0.260 1.92%	0.291 0.285 2.11%	0.266 0.261 1.92%							R
				0.391 0.388 0.77%	0.800 0.797 0.38%	1.057 1.050 0.67%	0.793 0.794 -0.13%	1.060 1.052 0.76%	0.800 0.797 0.38%	0.387 0.388 -0.26%					P
			0.437 0.424 3.07%	1.104 1.090 1.28%	1.274 1.272 0.16%	1.159 1.169 -0.86%	1.310 1.320 -0.76%	1.167 1.170 -0.26%	1.275 1.272 0.24%	1.094 1.090 0.37%	0.423 0.424 -0.24%				N
		0.428 0.424 0.94%	0.944 0.921 2.50%	1.172 1.159 1.12%	1.060 1.068 -0.75%	1.369 1.372 -0.22%	1.015 1.008 0.69%	1.379 1.373 0.44%	1.071 1.069 0.19%	1.170 1.159 0.95%	0.923 0.921 0.22%	0.423 0.424 -0.24%			M
	0.379 0.388 -2.32%	1.073 1.090 -1.56%	1.167 1.159 0.69%	1.184 1.179 0.42%	1.361 1.359 0.15%	1.143 1.143 0.00%	1.375 1.369 0.44%	1.156 1.144 1.05%	1.391 1.361 2.20%	1.184 1.179 0.42%	1.161 1.159 0.17%	1.087 1.090 -0.28%	0.383 0.388 -1.29%		L
	0.805 0.797 1.00%	1.269 1.272 -0.24%	1.069 1.069 0.00%	1.369 1.361 0.59%	1.021 1.012 0.89%	1.166 1.165 0.09%	1.176 1.177 -0.08%	1.176 1.166 0.86%	1.028 1.012 1.58%	1.371 1.358 0.96%	1.064 1.068 -0.37%	1.280 1.272 0.63%	0.805 0.797 1.00%		K
0.270 0.261 3.45%	1.069 1.052 1.62%	1.165 1.170 -0.43%	1.387 1.373 1.02%	1.146 1.144 0.17%	1.167 1.166 0.09%	1.361 1.354 0.52%	1.166 1.162 0.34%	1.362 1.354 0.59%	1.163 1.165 -0.17%	1.141 1.143 -0.17%	1.378 1.372 0.44%	1.173 1.169 0.34%	1.072 1.050 2.10%	0.269 0.260 3.46%	J
0.289 0.285 1.40%	0.793 0.794 -0.13%	1.310 1.320 -0.76%	1.017 1.008 0.89%	1.374 1.369 0.37%	1.173 1.177 -0.34%	1.161 1.162 -0.09%	0.937 0.929 0.86%	1.159 1.162 -0.26%	1.166 1.177 -0.93%	1.369 1.369 0.00%	1.015 1.008 0.69%	1.339 1.320 1.44%	0.804 0.793 1.39%	0.295 0.285 3.51%	H
0.258 0.260 -0.77%	1.041 1.050 -0.86%	1.147 1.169 -1.88%	1.369 1.372 -0.22%	1.155 1.143 1.05%	1.165 1.165 0.00%	1.354 1.354 0.00%	1.146 1.162 -1.38%	1.351 1.354 -0.22%	1.161 1.166 -0.43%	1.136 1.144 -0.70%	1.372 1.373 -0.07%	1.163 1.170 -0.60%	1.068 1.052 1.52%	0.265 0.261 1.53%	G
	0.785 0.797 -1.51%	1.243 1.272 -2.28%	1.052 1.068 -1.50%	1.388 1.359 2.13%	1.016 1.012 0.40%	1.149 1.166 -1.46%	1.134 1.177 -3.65%	1.148 1.165 -1.46%	1.018 1.012 0.59%	1.352 1.361 -0.66%	1.048 1.069 -1.96%	1.260 1.272 -0.94%	0.791 0.797 -0.75%		F
	0.377 0.388 -2.84%	1.066 1.090 -2.20%	1.149 1.159 -0.86%	1.151 1.179 -2.37%	1.355 1.361 -0.44%	1.115 1.144 -2.53%	1.363 1.369 -0.44%	1.138 1.143 -0.44%	1.359 1.358 0.07%	1.171 1.179 -0.68%	1.151 1.159 -0.69%	1.087 1.090 -0.28%	0.386 0.388 -0.52%		E
		0.416 0.424 -1.89%	0.904 0.921 -1.85%	1.135 1.159 -2.07%	1.039 1.069 -2.81%	1.389 1.373 1.17%	1.036 1.008 2.78%	1.409 1.371 2.77%	1.061 1.068 -0.66%	1.139 1.158 -1.64%	0.919 0.921 -0.22%	0.430 0.423 1.65%			D
			0.417 0.424 -1.65%	1.067 1.090 -2.11%	1.245 1.272 -2.12%	1.160 1.170 -0.85%	1.339 1.320 1.44%	1.187 1.169 1.54%	1.280 1.272 0.63%	1.075 1.090 -1.38%	0.425 0.423 0.47%				C
				0.377 0.388 -2.84%	0.781 0.797 -2.01%	1.050 1.052 -0.19%	0.800 0.793 0.88%	1.066 1.050 1.52%	0.820 0.796 3.02%	0.380 0.388 -2.06%					B
						0.256 0.261 -1.92%	0.290 0.285 1.75%	0.265 0.260 1.92%							A

INCORE	
ANC	
% DIFFERENCE	

Mean Absolute Difference = 0.009
Standard Deviation = 0.008

BURNUP = 10704 MWD/MTU POWER LEVEL = 100% D BANK AT 228 STEPS

FIGURE 4.3-19
TURKEY POINT UNIT 4 CYCLE 12
AXIAL POWER DISTRIBUTION COMPARISON
BETWEEN INCORE AND ANC

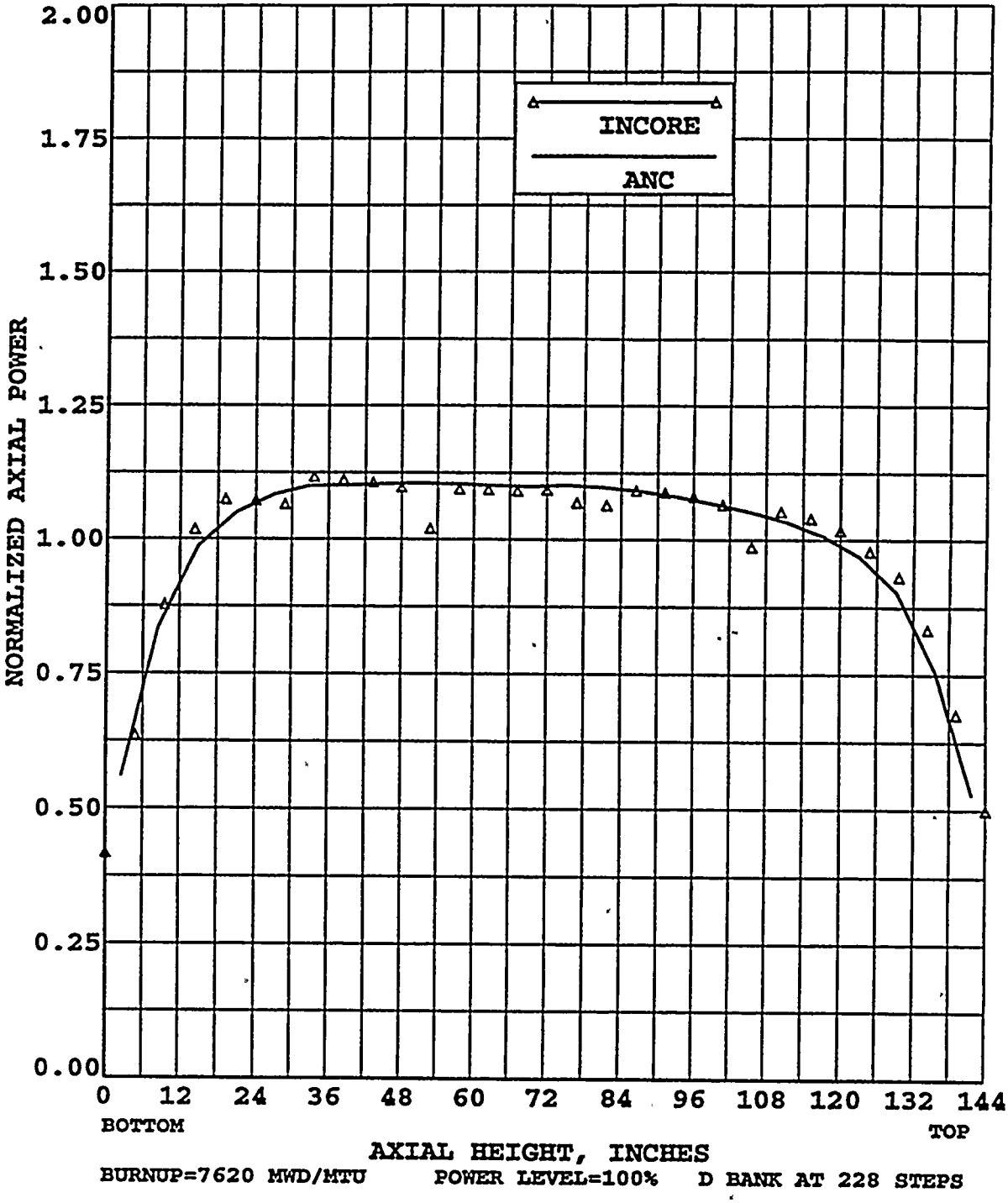

FIGURE 4.3-20
TURKEY POINT UNIT 4 CYCLE 12
AXIAL POWER DISTRIBUTION COMPARISON
BETWEEN INCORE AND ANC

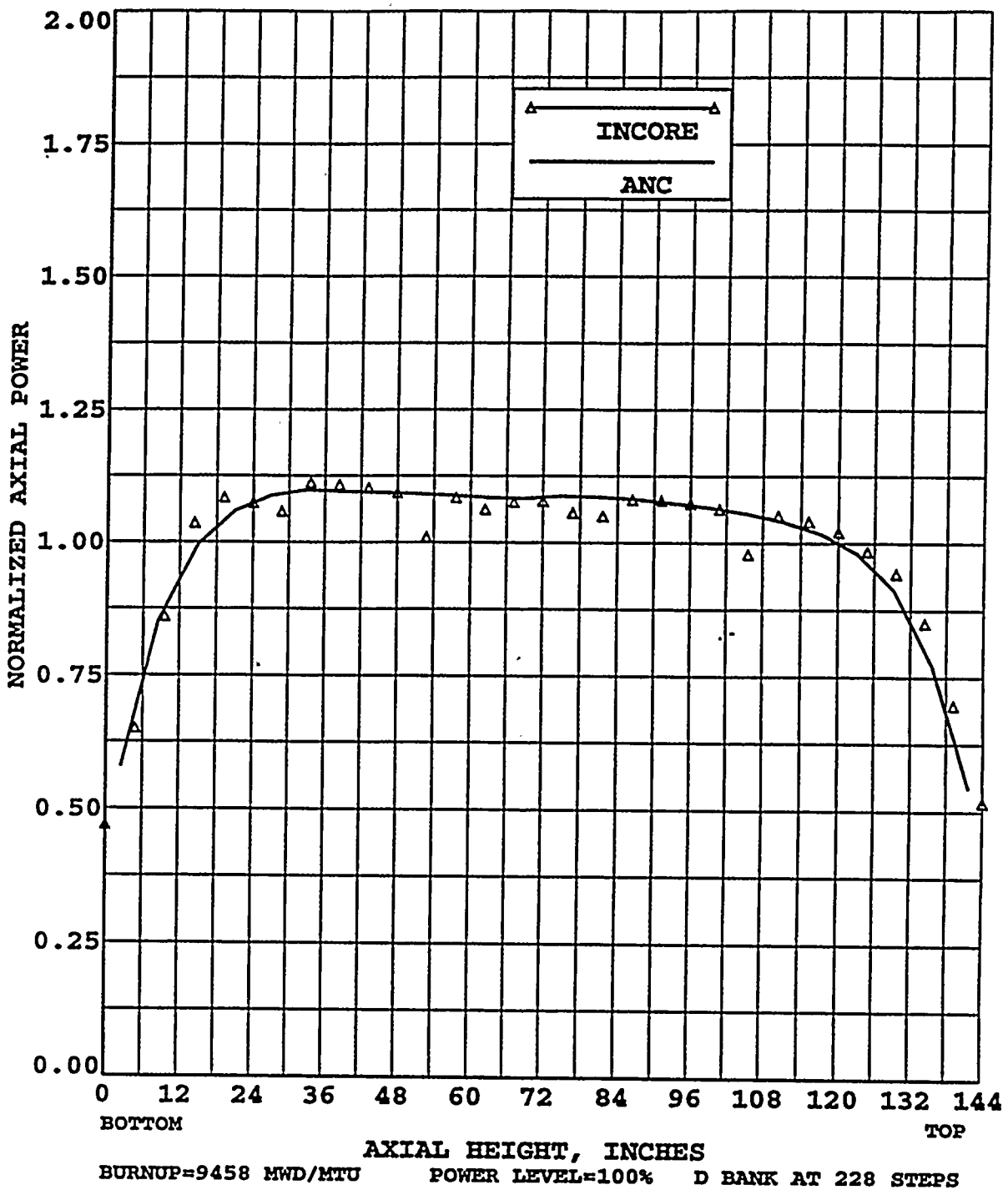

BURNUP=9458 MWD/MTU POWER LEVEL=100% D BANK AT 228 STEPS

FIGURE 4.3-21
TURKEY POINT UNIT 4 CYCLE 12
AXIAL POWER DISTRIBUTION COMPARISON
BETWEEN INCORE AND ANC

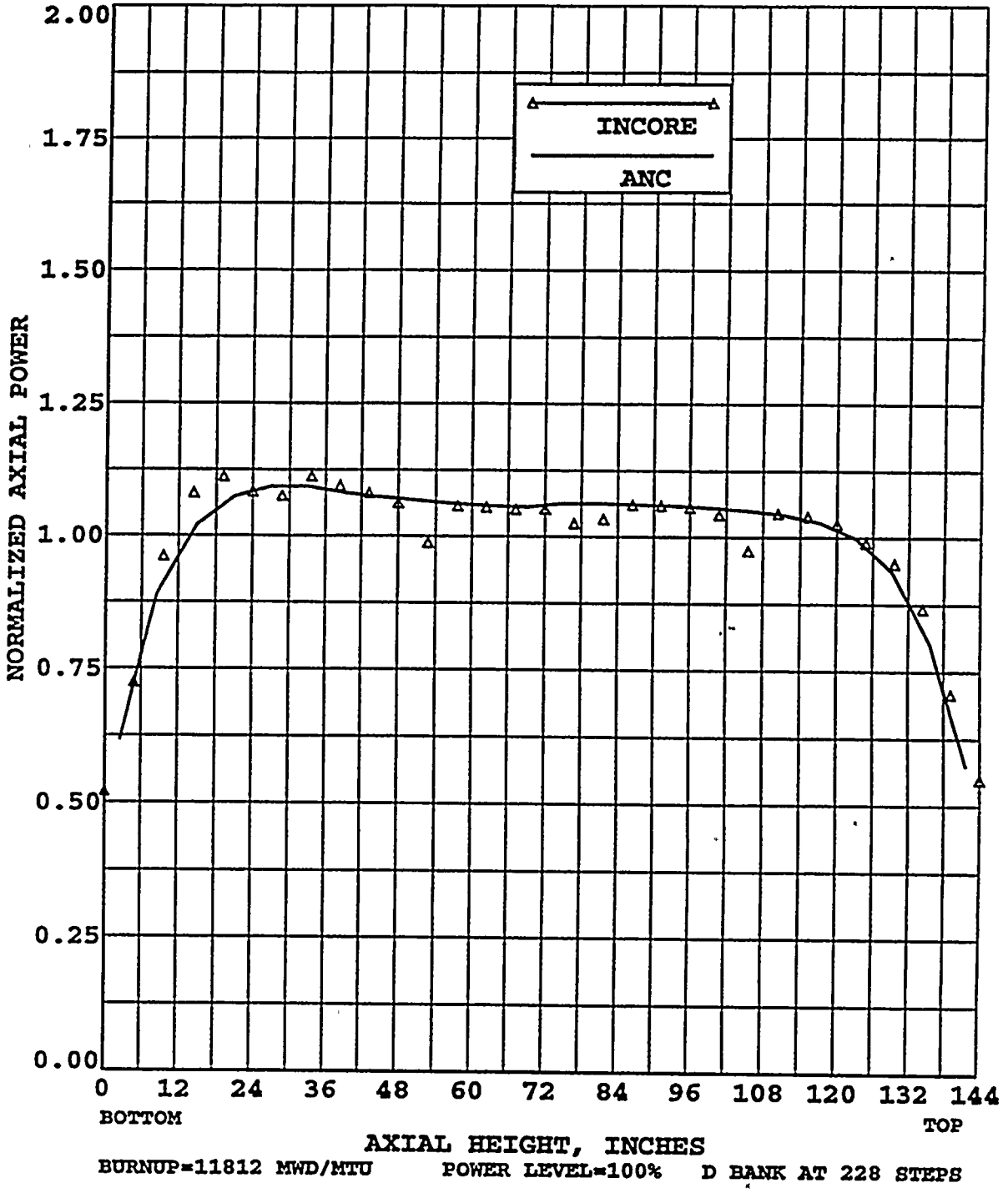

BURNUP=11812 MWD/MTU POWER LEVEL=100% D BANK AT 228 STEPS

FIGURE 4.3-22
TURKEY POINT UNIT 4 CYCLE 13
AXIAL POWER DISTRIBUTION COMPARISON
BETWEEN INCORE AND ANC

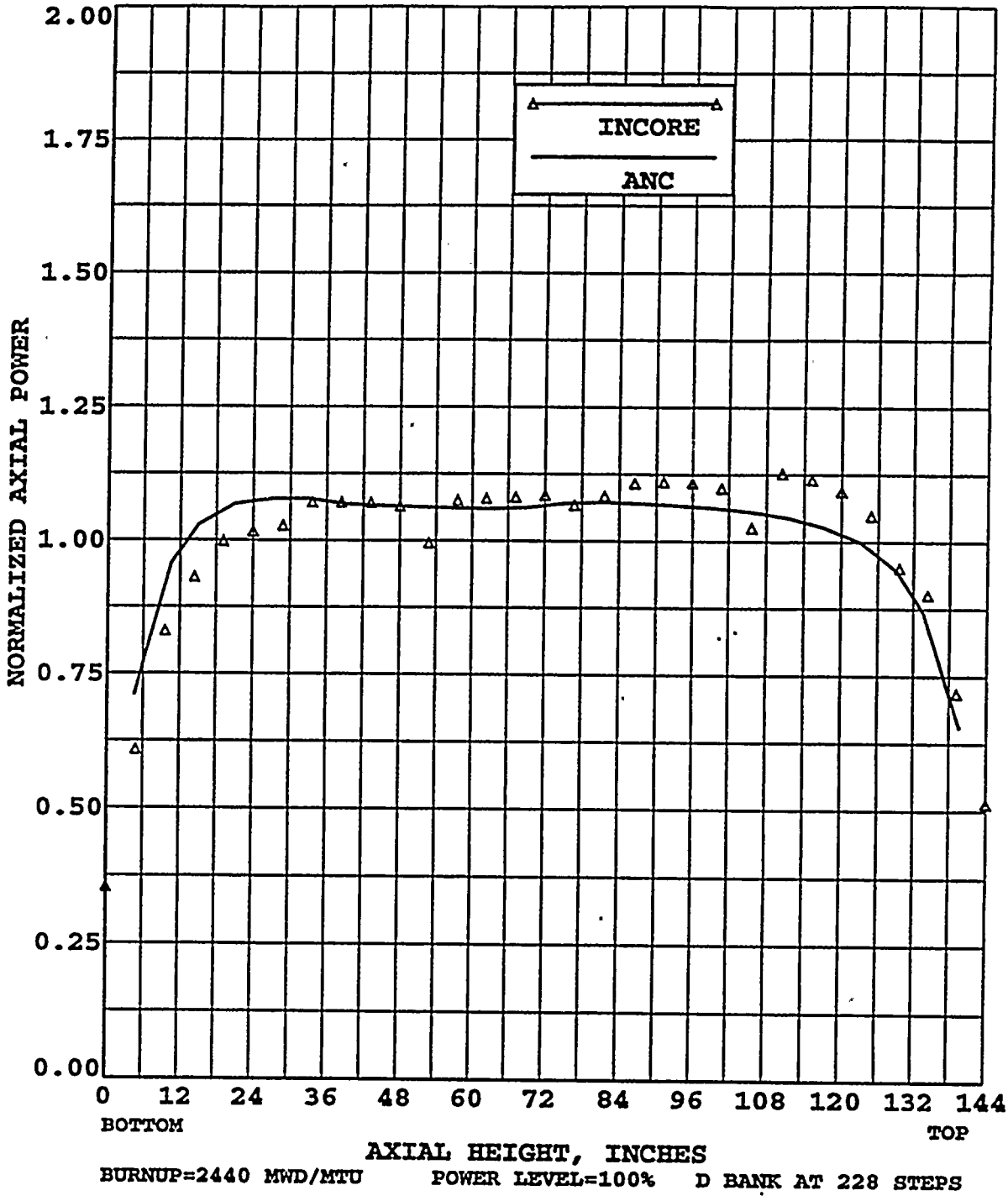

BURNUP=2440 MWD/MTU POWER LEVEL=100% D BANK AT 228 STEPS

FIGURE 4.3-23
TURKEY POINT UNIT 4 CYCLE 13
AXIAL POWER DISTRIBUTION COMPARISON
BETWEEN INCORE AND ANC

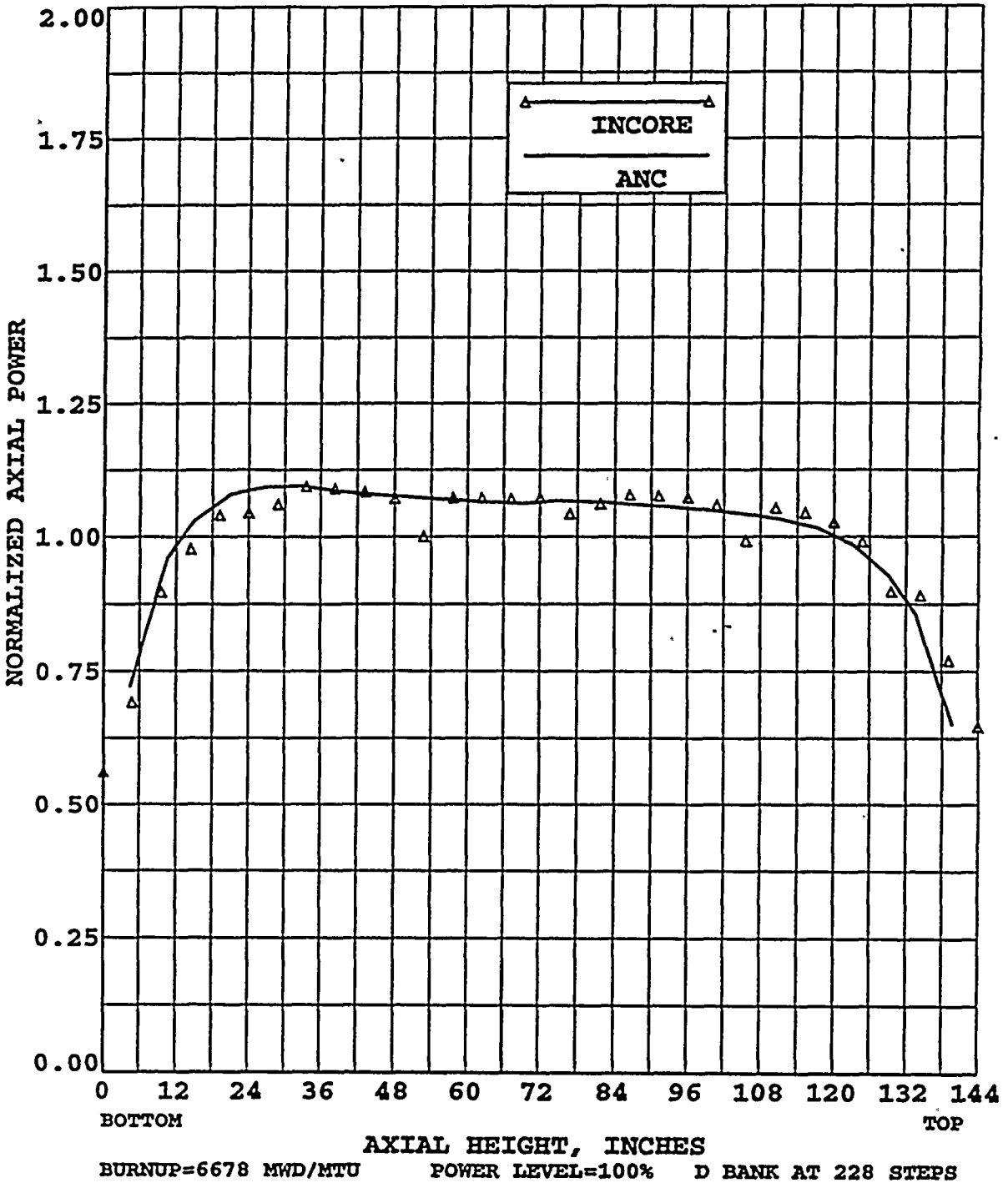

BURNUP=6678 MWD/MTU POWER LEVEL=100% D BANK AT 228 STEPS

FIGURE 4.3-24
TURKEY POINT UNIT 4 CYCLE 13
AXIAL POWER DISTRIBUTION COMPARISON
BETWEEN INCORE AND ANC

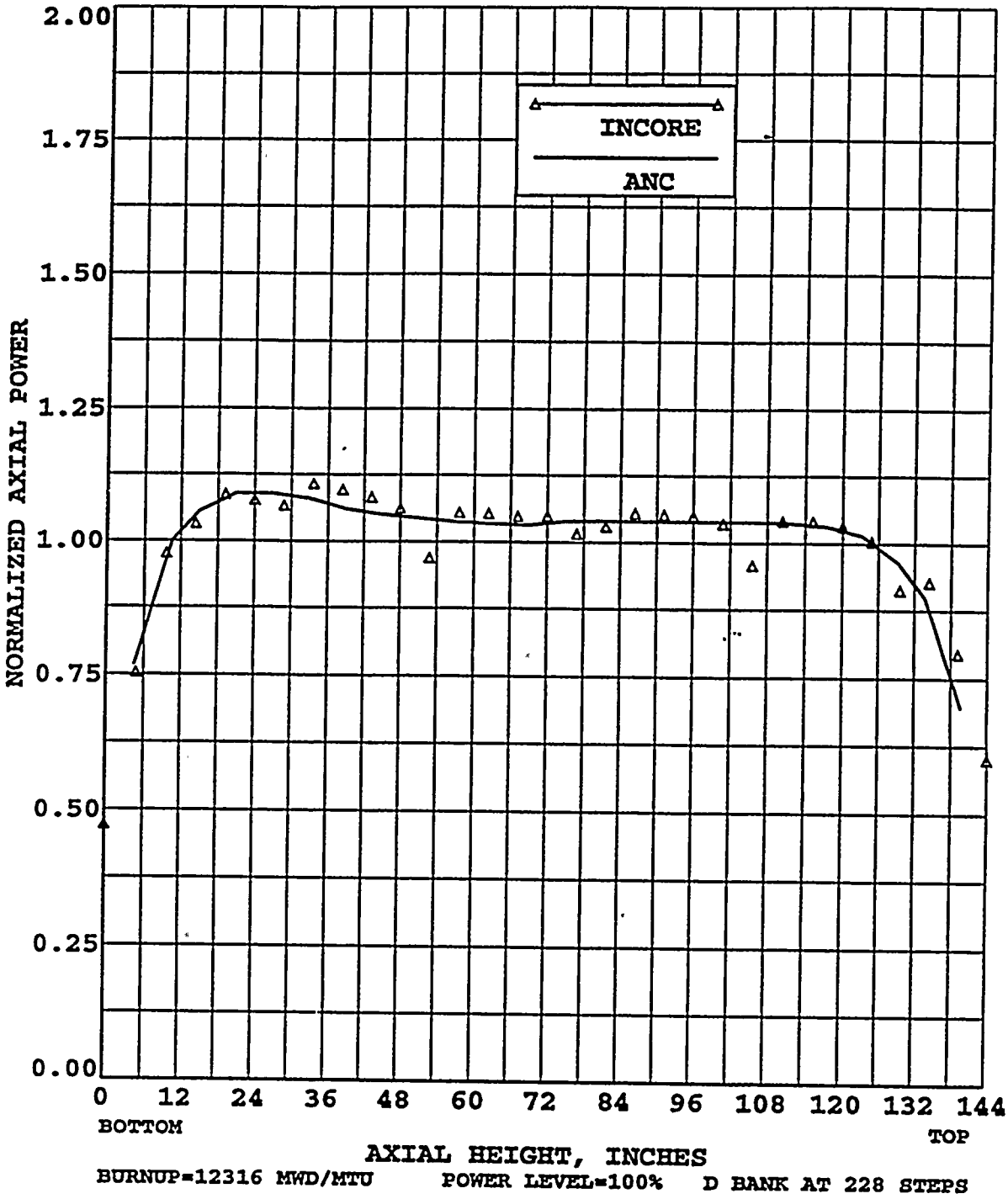

BURNUP=12316 MWD/MTU POWER LEVEL=100% D BANK AT 228 STEPS

FIGURE 4.3-25
TURKEY POINT UNIT 4 CYCLE 14
AXIAL POWER DISTRIBUTION COMPARISON
BETWEEN INCORE AND ANC

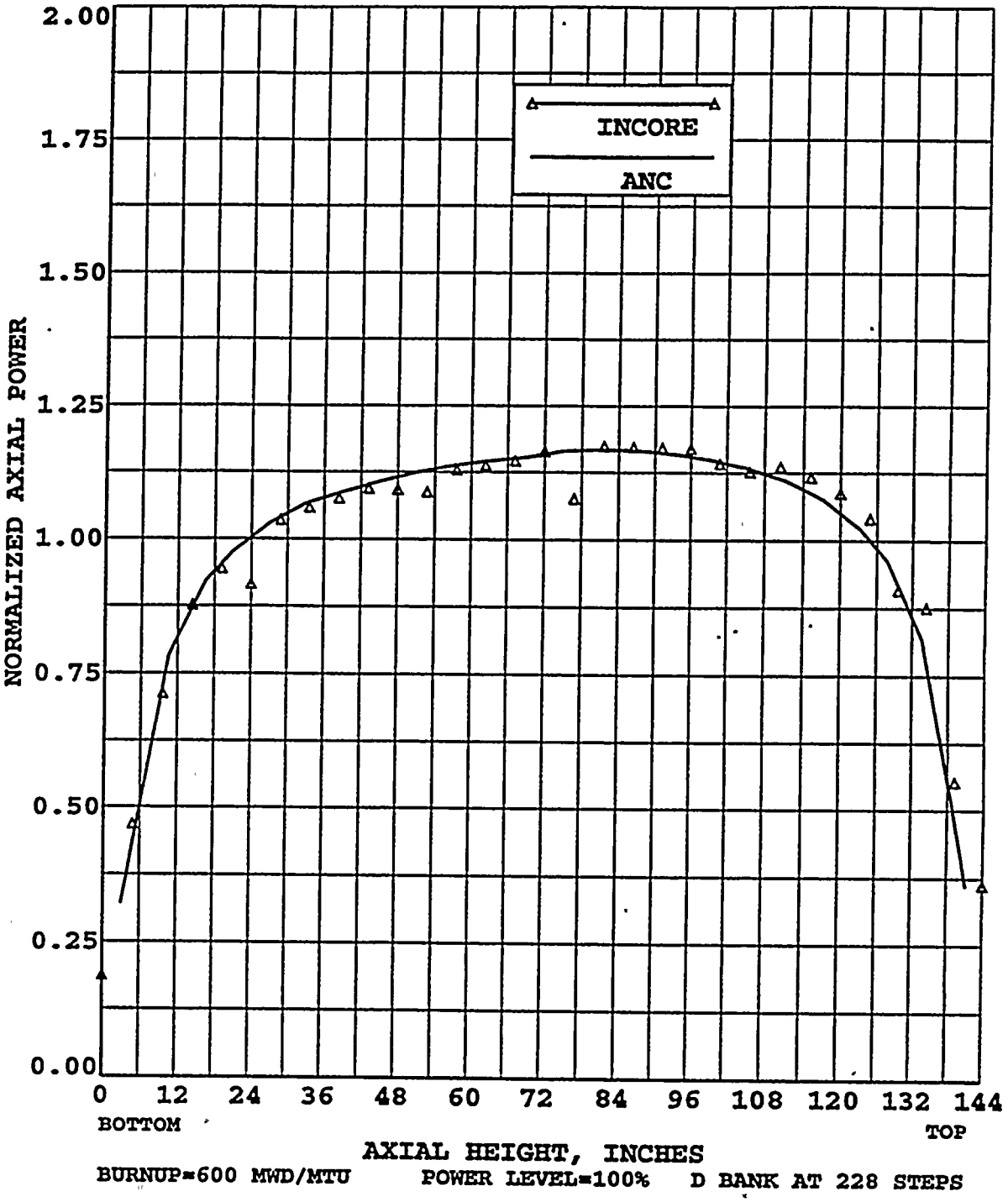

BURNUP=600 MWD/MTU POWER LEVEL=100% D BANK AT 228 STEPS

FIGURE 4.3-26
TURKEY POINT UNIT 4 CYCLE 14
AXIAL POWER DISTRIBUTION COMPARISON
BETWEEN INCORE AND ANC

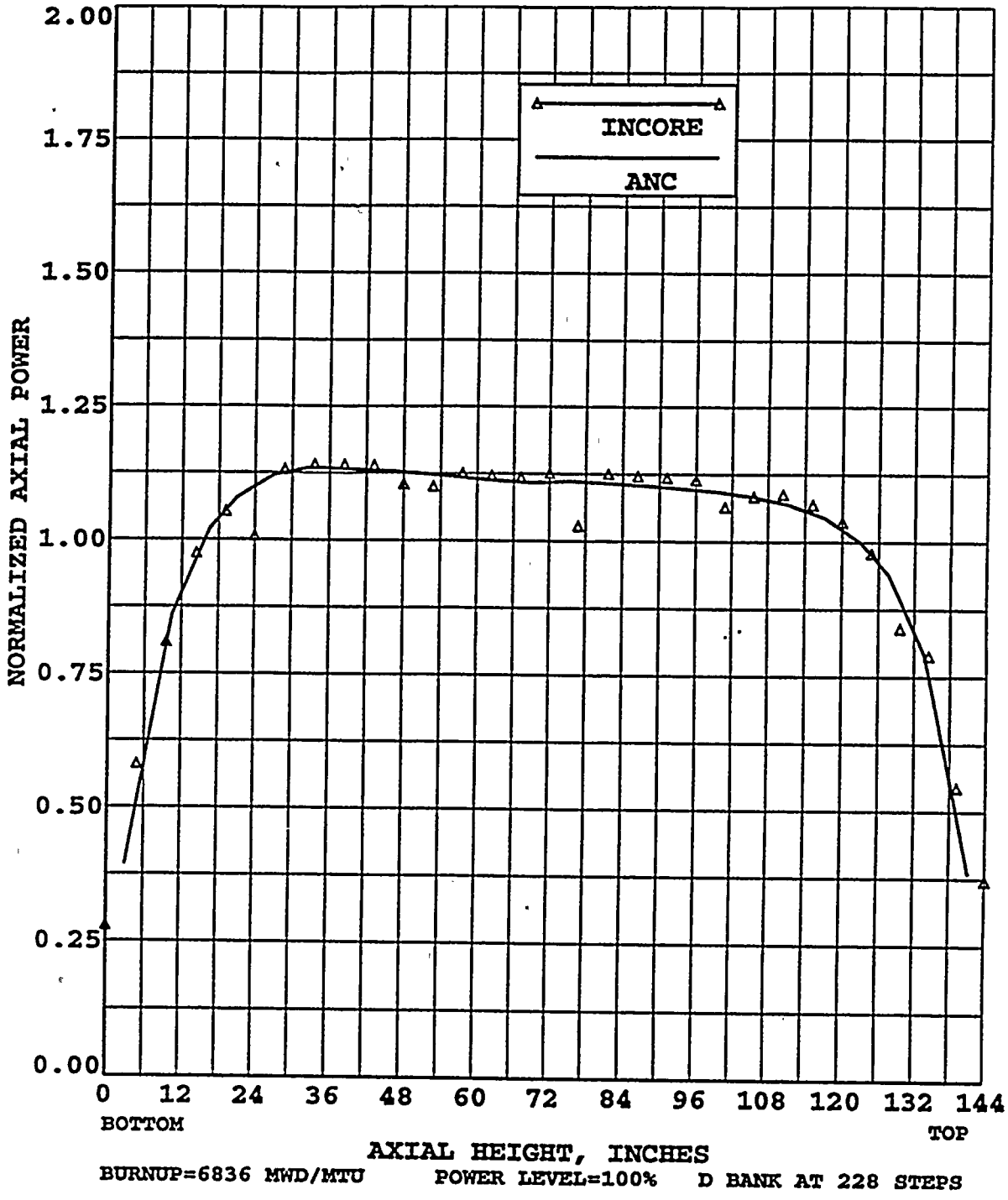

BURNUP=6836 MWD/MTU POWER LEVEL=100% D BANK AT 228 STEPS

FIGURE 4.3-27
TURKEY POINT UNIT 4 CYCLE 14
AXIAL POWER DISTRIBUTION COMPARISON
BETWEEN INCORE AND ANC

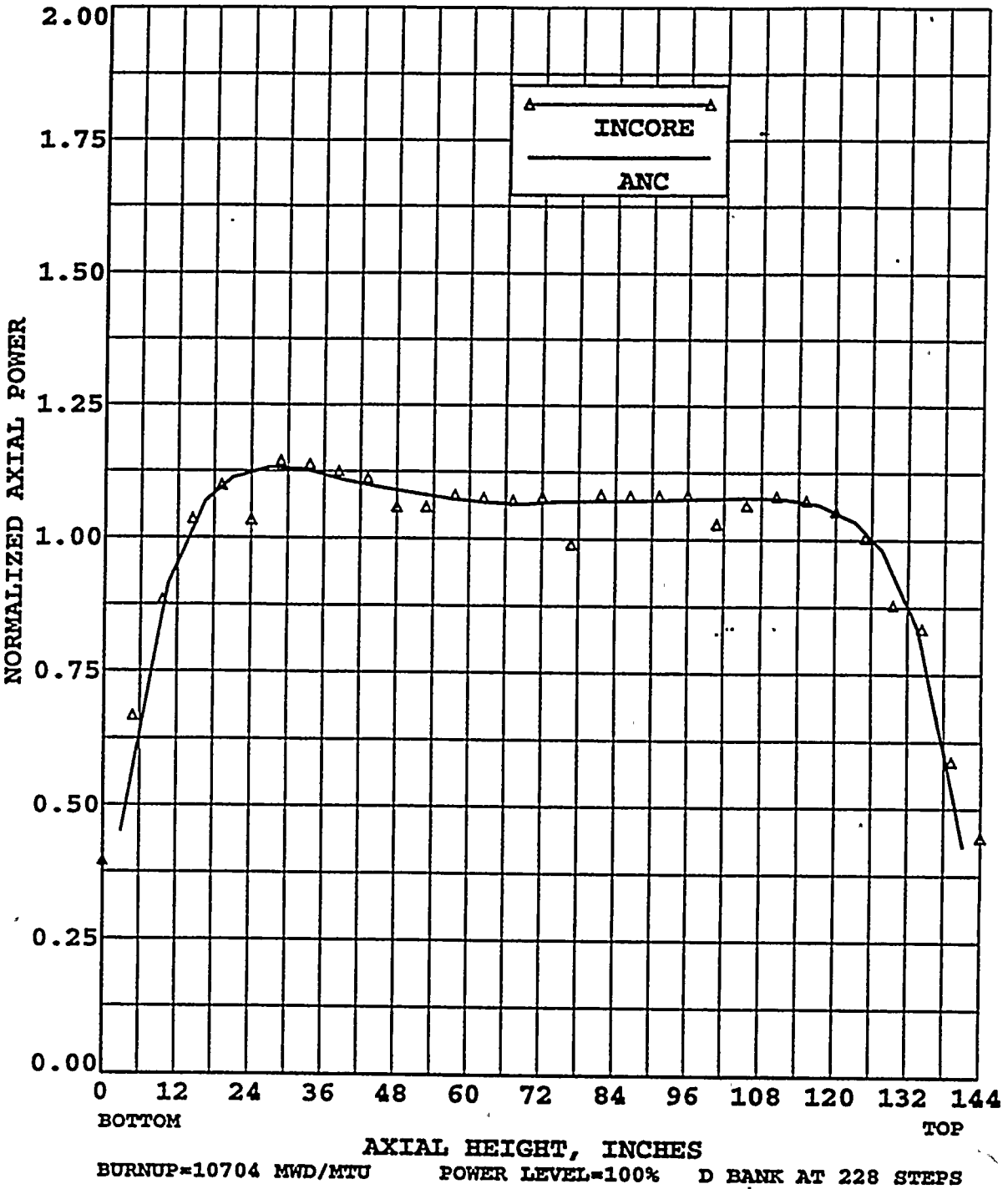

BURNUP=10704 MWD/MTU POWER LEVEL=100% D BANK AT 228 STEPS

5.0 PHYSICS MODEL VERIFICATION ST. LUCIE UNITS

Core physics model verification for St. Lucie will include comparisons between measurement and predictions for St. Lucie Unit 1. St. Lucie Unit 1 is currently in its thirteenth cycle of operation. In this section, predictions made using the physics methodology described in Section 2 are compared to zero power physics test measurements and at power operating data. As stated in Section 1, the methods employed to generate the predictions reported in this section are standard licensed methods used by Westinghouse's Commercial Nuclear Fuel Division. The purpose of these comparisons is to demonstrate FPL's competence to use these methods to analyze the core configurations found at the St. Lucie Units.

St. Lucie Units 1 & 2 are similar in design. St. Lucie Unit 1 is a Combustion Engineering (CE) reactor with a thermal rating of 2700 MW. The core consists of 217 assemblies of the CE 14x14 design. St. Lucie Unit 2 is also a CE reactor with a thermal rating of 2700 MW. The core for St. Lucie Unit 2 consists of 217 assemblies of the CE 16x16 design. The St. Lucie Unit 1 Cycles 10, 11, and 12 were selected for the core physics model verification due to the greater complexity in modelling the design features utilized in St. Lucie Unit 1. These design features include axial blankets, Gadolinium burnable absorbers, and Vessel Fluence Reduction Assemblies (initiated in Cycle 11) which contain uranium tails and Hafnium absorbers placed in the guide tubes.

5.1 CYCLE DESCRIPTIONS

St. Lucie Unit 1 Cycle 10 began operation in April 1990 and shutdown in October 1991 after a 477 Effective Full Power Days (EFPD) cycle. Cycle 10 consisted of debris resistant fuel (long end cap design) with an active fuel length of 134.06 inches. All fuel utilized axial blankets. The

core loading pattern for Cycle 10, including a description of the fresh fuel and the locations of control rods are shown in Figure 5.1-1. A quarter core representation is used since the core is symmetric.

St. Lucie Unit 1 Cycle 11 began operation in December 1991 and shutdown in March 1993 after a 442 EFPD cycle. Cycle 11 consisted of debris resistant fuel with an active fuel length of 136.7 inches. Vessel Fluence Reduction Assemblies (VFRA) on the core periphery were introduced in Cycle 11. The VFRA assemblies utilized uranium tails and Hafnium absorbers to reduce peripheral power. All fuel with the exception of VFRA utilized axial blankets. The core loading pattern for Cycle 11, including a description of the fresh fuel and the locations of control rods are shown in Figure 5.1-2.

St. Lucie Unit 1 Cycle 12 began operation in June 1993 and shutdown in October 1994 after a 463 EFPD cycle. Cycle 12 consisted of debris resistant fuel with an active fuel length of 136.7 inches. All fuel utilized axial blankets with the exception of the VFRA . The core loading pattern for Cycle 12, including a description of the fresh fuel and the locations of control rods are shown in Figure 5.1-3.

5.2 ZERO POWER PHYSICS TESTS

After each refueling at the St. Lucie Units, startup physics tests are conducted to verify that the nuclear characteristics of the core are consistent with design predictions. While the reactor is maintained at hot zero power (HZP) conditions, the following physics parameters are measured;

- Critical Boron Concentrations,
- Moderator Temperature Coefficient,
- Control Rod Worth, and
- Differential boron worth

5.2.1 CRITICAL BORON CONCENTRATION

Table 5.2-1 provides the comparisons between HZP critical boron concentrations measurements and predictions for Cycles 10, 11, and 12. The values represent all rods out (ARO) and reference bank in conditions. As shown, excellent agreement is demonstrated for each case with all differences well within the ±50 ppm review criteria.

5.2.2 MODERATOR TEMPERATURE COEFFICIENT

Table 5.2-2 provides the comparisons between HZP Moderator Temperature Coefficient measurements and predictions for Cycles 10, 11, and 12. Again, excellent agreement is demonstrated with all differences being well within the review criteria of ±2 pcm/°F.

5.2.3 CONTROL ROD WORTH

Table 5.2-3 provides the Control Rod Worth comparisons between measurement and prediction for Cycles 10, 11, and 12. In all cases, the agreement is within criteria with exceptional agreement being achieved for Cycles 11 and 12. Figures 5.2-1, 5.2-2 and 5.2-3 show the integral rod worth comparisons for the Reference Bank. The predicted rod worth and integral worth were calculated at the exact conditions which were present during the measurement. Excellent agreement is observed between measured and predicted integral worth.

5.2.4 DIFFERENTIAL BORON WORTH

Table 5.2-4 provides the Differential boron worth comparisons between measurement and predictions for Cycles 10, 11, and 12. Both the measured and predicted values are obtained using the worth of the Reference Bank in pcm divided by the change in boron concentration from ARO to Reference Bank inserted. All differences are well within the expected performance.

5.3 POWER OPERATION

5.3.1 BORON LETDOWN CURVES

Reactor coolant system boron concentrations are measured daily at the plant. Critical boron concentrations measured at or very close to hot full power all rods out equilibrium xenon and samarium conditions are compared to the predicted boron letdown curves for Cycles 10, 11, and 12 in Figures 5.3-1, 5.3-2 and 5.3-3. The predicted curves were obtained from design depletions with the three-dimensional ANC model. Table 5.3-1 shows the difference in ppm between measurement and ANC at various cycle exposures. The mean difference between measured and predicted critical boron concentration for all three cycles is 3 ppm with a standard deviation of 15 ppm.

5.3.2 AXIAL POWER DISTRIBUTIONS

Measured core average axial power distributions from Beginning-of-Cycle (BOC), Middle-of-Cycle (MOC) and End-of-Cycle (EOC) obtained with the incore monitoring code INPAX (Reference 13) using incore detector "snapshots" were compared to predicted axial distributions in Figures 5.3-4 through 5.3-12. The predicted distributions were obtained from three-dimensional ANC calculations performed for core conditions similar to those at the time of the "snapshots". Overall, the comparisons show excellent agreement between measured and predicted axial power distributions.

5.4 SUMMARY

In this section, predictions made using Westinghouse's reload core design methodology are compared to zero power physics test measurements and at power operating data from St. Lucie Unit 1, Cycles 10,11, and 12. In all cases, the predictions agree very well with the measurements. The excellent agreement between the predictions and

the measurements reported here demonstrates FPL's capability to apply the Westinghouse licensed methodology to perform reload core design for the St. Lucie Units.

TABLE 5.2-1

ST. LUCIE UNIT 1 CYCLE 10,11 AND 12
HZP CRITICAL BORON CONCENTRATION COMPARISON
BETWEEN MEASUREMENT AND PREDICTION

CYCLE	BANK CONFIGURATION	CRITICAL BORON CONCENTRATION (PPM)		
		MEASURED M	PREDICTED P	DIFFERENCE (M-P)
10	ARO	1598	1609	-11
10	BANK A in	1477	1496	-19
11	ARO	1393	1396	-3
11	BANK A in	1279	1281	-2
12	ARO	1419	1427	-8
12	BANK A in	1303	1307	-4

Acceptance Criteria is ±50 ppm

TABLE 5.2-2

ST. LUCIE UNIT 1 CYCLE 10,11 AND 12
HZP MODERATOR TEMPERATURE COEFFICIENT
COMPARISON BETWEEN MEASUREMENT AND PREDICTION

CYCLE	BANK CONFIGURATION	MODERATOR TEMPERATURE COEFFICIENT (PCM/°F)		
		MEASURED M	PREDICTED P	DIFFERENCE (M-P)
10	ARO	4.41	5.70	-1.29
11	ARO	2.56	2.57	-0.01
12	ARO	1.54	2.18	-0.64

Acceptance Criteria is ±2 pcm/°F

TABLE 5.2-3

ST. LUCIE UNIT 1 CYCLE 10,11 AND 12 CONTROL ROD WORTH COMPARISON BETWEEN MEASUREMENT AND PREDICTION

CYCLE	BANK CONFIGURATION	CONTROL ROD WORTH (PCM)		
		MEASURED M	PREDICTED P	DIFFERENCE(%) ((M-P)/P)*100
10	BANK 7	516	480	7.50
	BANK 6	367	404	-9.16
	BANK 5	374	430	-13.02
	BANK 4	584	631	-7.45
	BANK 3	368	420	-12.38
	BANK 2	789	848	-6.96
	BANK 1	746	822	-9.25
	BANK B	543	584	-7.02
	BANK A(1)	1015	1014	0.10
	TOTAL(2)	5302	5635	-5.91
11	BANK 7	590	522	13.03
	BANK 6 & B	715	774	-7.62
	BANK 5 & 3	850	882	-3.63
	BANK 4	738	699	5.58
	BANK 2	791	795	-0.50
	BANK 1	808	806	0.25
	BANK A(1)	1136	1106	2.71
	TOTAL(2)	5628	5583	0.81
12	BANK 7	654	573	14.14
	BANK 6 & 3	929	915	1.53
	BANK 5 & B	509	550	-7.45
	BANK 4	824	809	1.85
	BANK 2	699	740	-5.54
	BANK 1	759	771	-1.56
	BANK A(1)	1099	1136	-3.26
	TOTAL(2)	5473	5495	-0.40

Acceptance Criteria is ±15% or 100 pcm which ever is greater
(1) Reference Bank - Acceptance Criteria is ±10%
(2) Sum of all measured banks within ±10%

TABLE 5.2-4

ST. LUCIE UNIT 1 CYCLE 10,11 AND 12 HZP DIFFERENTIAL BORON WORTH COMPARISON BETWEEN MEASUREMENT AND PREDICTION

CYCLE	BANK CONFIGURATION	DIFFERENTIAL BORON WORTH (PCM/PPM)		
		MEASURED M	PREDICTED P	DIFFERENCE(%) ((M-P)/P)*100
10	Average Over Bank A insertion	8.39	8.97	-6.50
11	Average Over Bank A insertion	9.96	9.62	3.53
12	Average Over Bank A insertion	9.47	9.47	0.00

TABLE 5.3-1

ST. LUCIE UNIT 1 CYCLE 10,11 AND 12
BORON LETDOWN COMPARISON
BETWEEN MEASUREMENT AND PREDICTION

CYCLE	CYCLE BURNUP MWD/MTU	CRITICAL BORON CONCENTRATION (PPM)		
		MEASURED M	PREDICTED P	DIFFERENCE (M-P)
10	139	1160	1178	-18
	278	1130	1162	-32
	696	1090	1117	-27
	1392	1050	1074	-24
	2784	990	987	3
	4176	915	910	5
	5568	845	840	5
	6960	780	772	8
	8352	720	709	11
	9744	660	633	27
	11136	560	545	15
	12528	440	438	2
	13920	320	314	6
	15312	190	187	3
	15947	129	129	0
11	136	952	968	-12
	278	939	953	-14
	679	903	909	-6
	1359	857	862	-3
	2718	787	768	19
	4078	687	681	6
	5437	611	599	12
	6796	528	517	11
	8155	455	440	15
	19514	372	359	13
	10874	291	276	15
	12233	195	176	19
	13592	82	63	19
	14404	13	-7	20

Acceptance Criteria is ±50 ppm

TABLE 5.3-1 (CONTINUED)

ST. LUCIE UNIT 1 CYCLE 10,11 AND 12
BORON LETDOWN COMPARISON
BETWEEN MEASUREMENT AND PREDICTION

CYCLE	CYCLE BURNUP MWD/MTU	CRITICAL BORON CONCENTRATION (PPM)		
		MEASURED M	PREDICTED P	DIFFERENCE (M-P)
12	132	961	991	-30
	265	940	976	-36
	661	920	934	-14
	1324	892	892	0
	2648	805	807	2
	3972	743	729	14
	5296	672	658	14
	6614	596	589	7
	7944	537	525	12
	9268	443	453	10
	10592	390	369	21
	11916	287	273	14
	13240	175	164	11
	13723	131	122	9

Acceptance Criteria is ±50 ppm

FIGURE 5.1-1

ST LUCIE UNIT 1 CYCLE 10
LOADING PATTERN

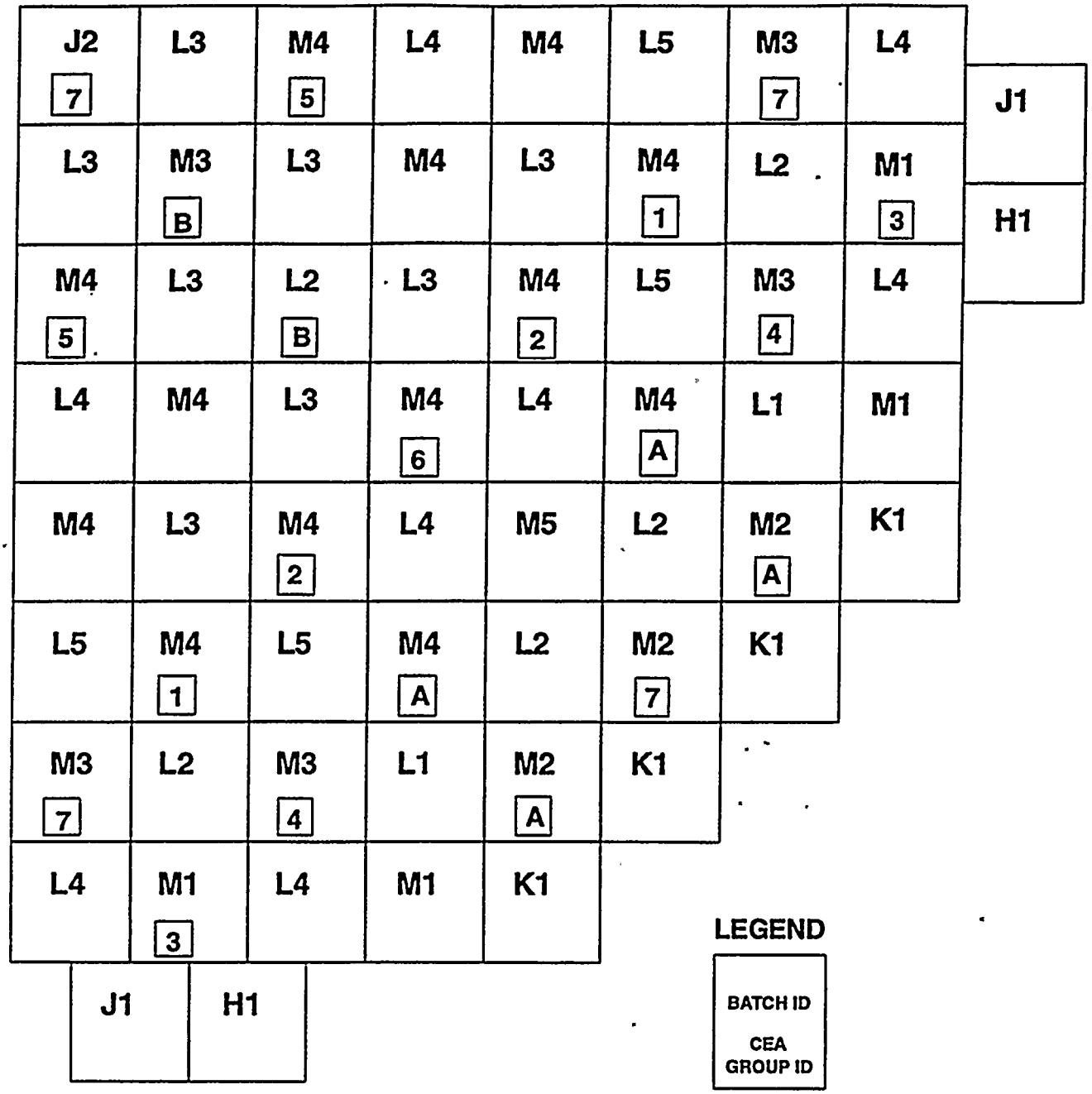

FRESH FUEL INVENTORY:
M1 - 4.0 W/O U-235
M2 - 4.0 W/O U-235, 4 RODS @ 4 W/O GD203
M3 - 4.0 W/O U-235, 12 RODS @ 6 W/O GD203
M4 - 4.0 W/O U-235, 12 RODS @ 8 W/O GD203
M4 - 4.0 W/O U-235, 12 RODS @ 6 W/O GD203 & 4 RODS @ 8 W/O GD2O3

FIGURE 5.1-2

ST LUCIE UNIT 1 CYCLE 11

LOADING PATTERN

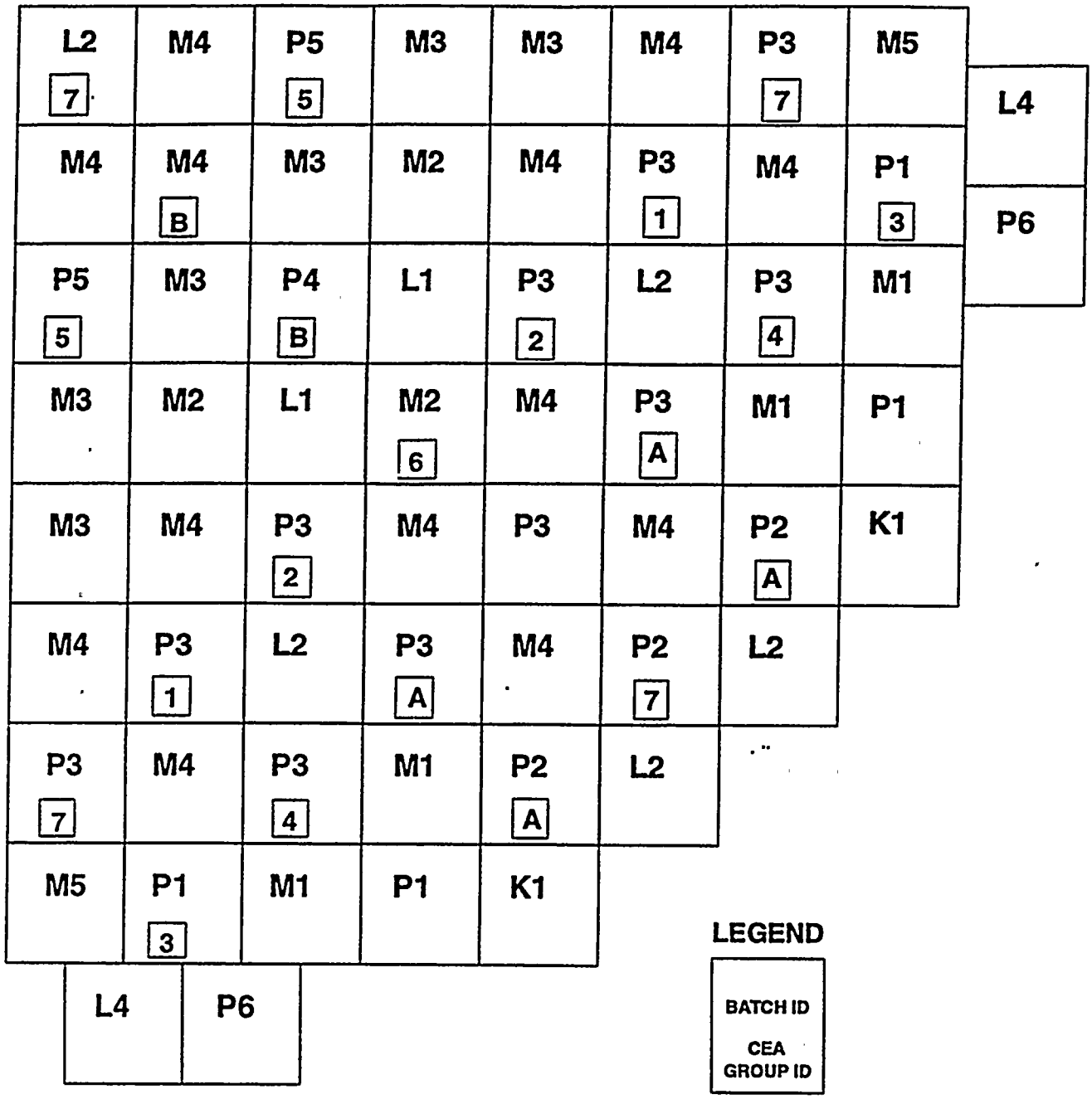

FRESH FUEL INVENTORY:

P1 - 3.75 W/O U-235

P2 - 3.75 W/O U-235, 4 RODS @ 4 W/O GD203

P3 - 3.75 W/O U-235, 12 RODS @ 8 W/O GD203

P4 - 3.75 W/O U-235, 16 RODS @ 6 W/O GD203

P5 - 3.75 W/O U-235, 12 RODS @ 8 W/O GD203 & 4 RODS @ 4 W/O GD2O3

P6 - 0.30 W/O U-235, 4 HAFNIUM FLUX REDUCTION INSERTS

FIGURE 5.1-3

ST LUCIE UNIT 1 CYCLE 12

LOADING PATTERN

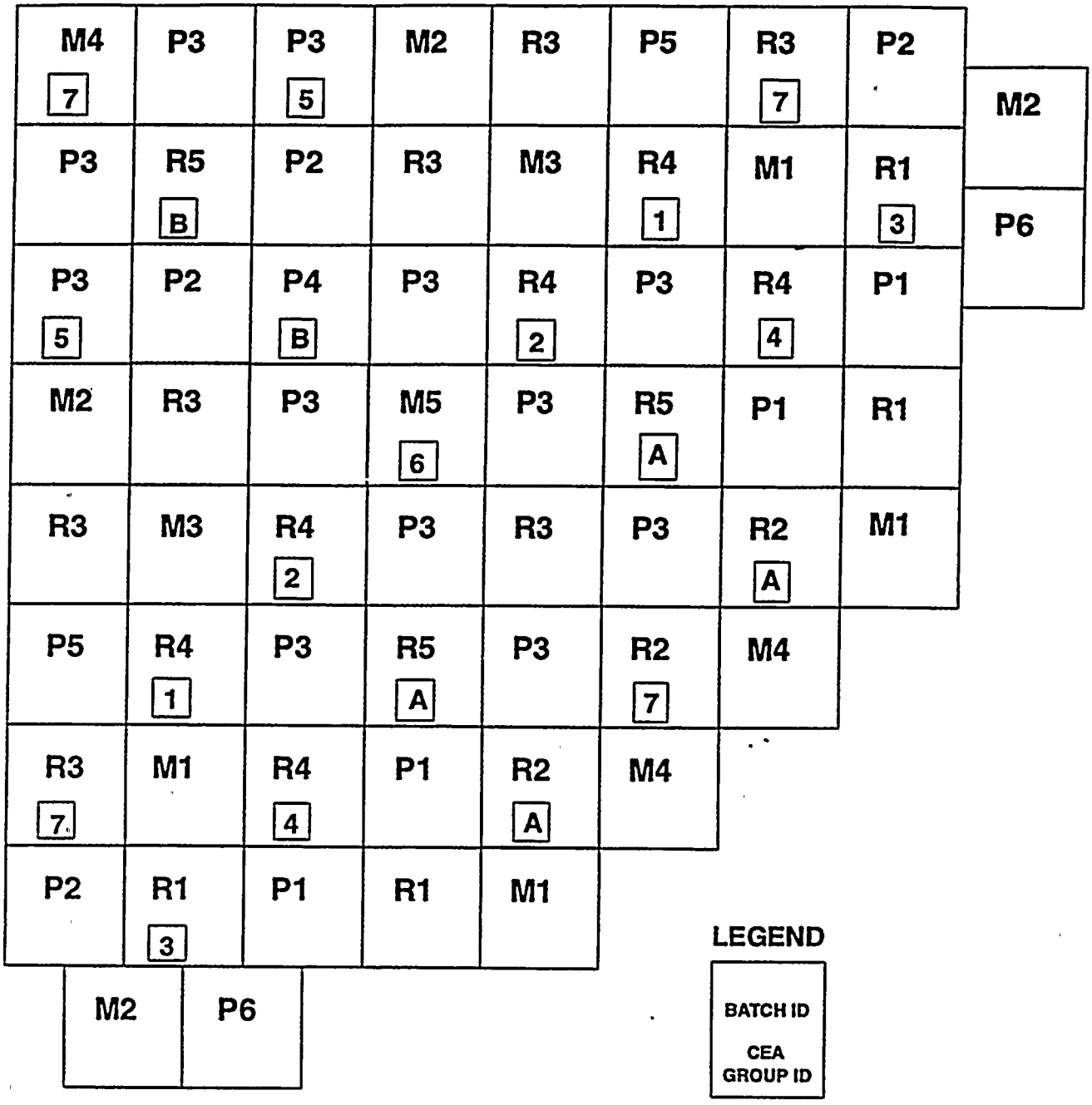

FRESH FUEL INVENTORY:

R1 - 3.90 W/O U-235

R2 - 3.90 W/O U-235, 4 RODS @ 4 W/O GD203

R3 - 3.90 W/O U-235, 12 RODS @ 6 W/O GD203

R4 - 3.90 W/O U-235, 12 RODS @ 8 W/O GD203

R5 - 3.90 W/O U-235, 16 RODS @ 8 W/O GD203

FIGURE 5.2-1
ST LUCIE UNIT 1 CYCLE 10
MEASURED VERSUS PREDICTED
REFERENCE BANK INTEGRAL ROD WORTH

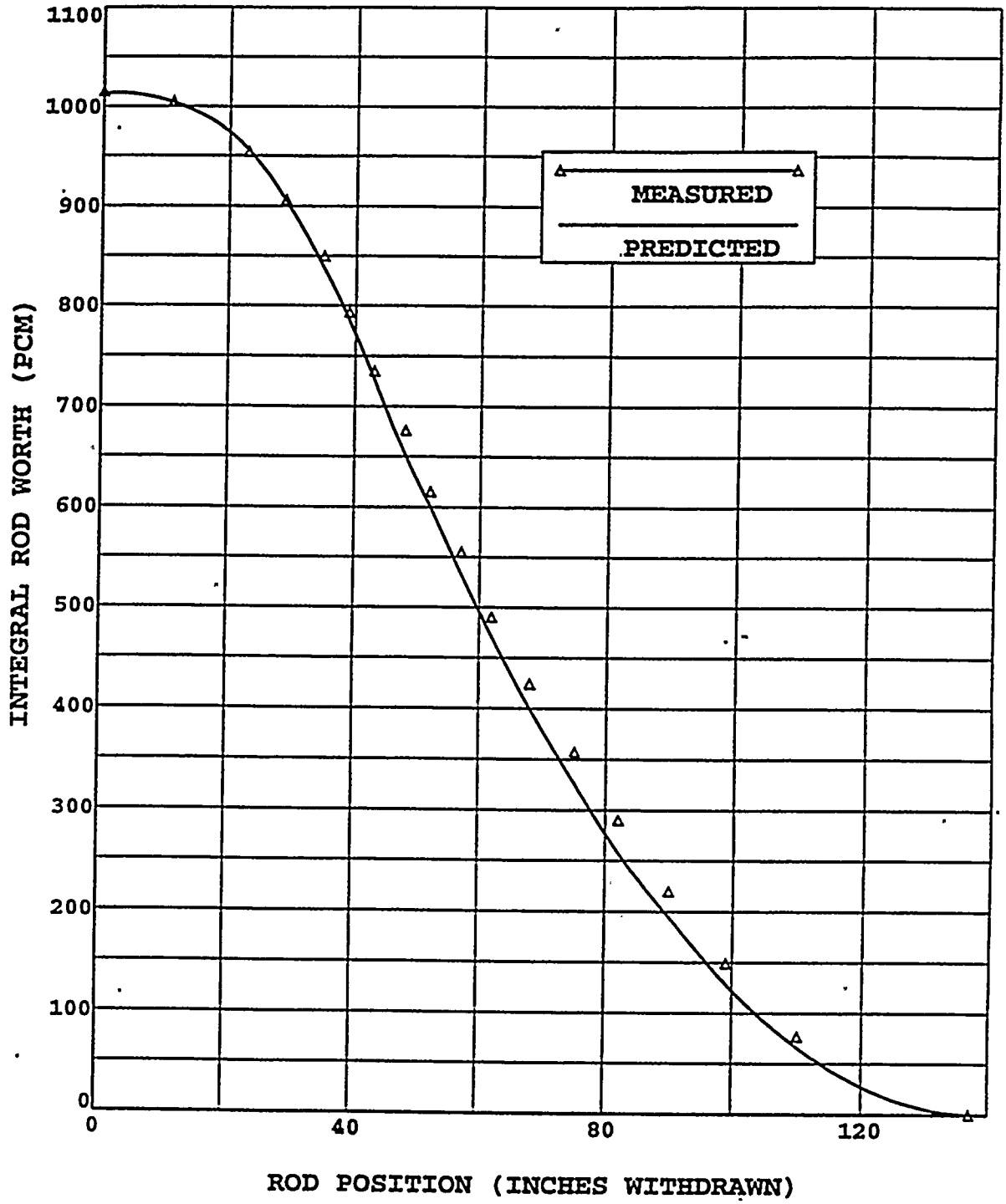

FIGURE 5.2-2
ST LUCIE UNIT 1 CYCLE 11
MEASURED VERSUS PREDICTED
REFERENCE BANK INTEGRAL ROD WORTH

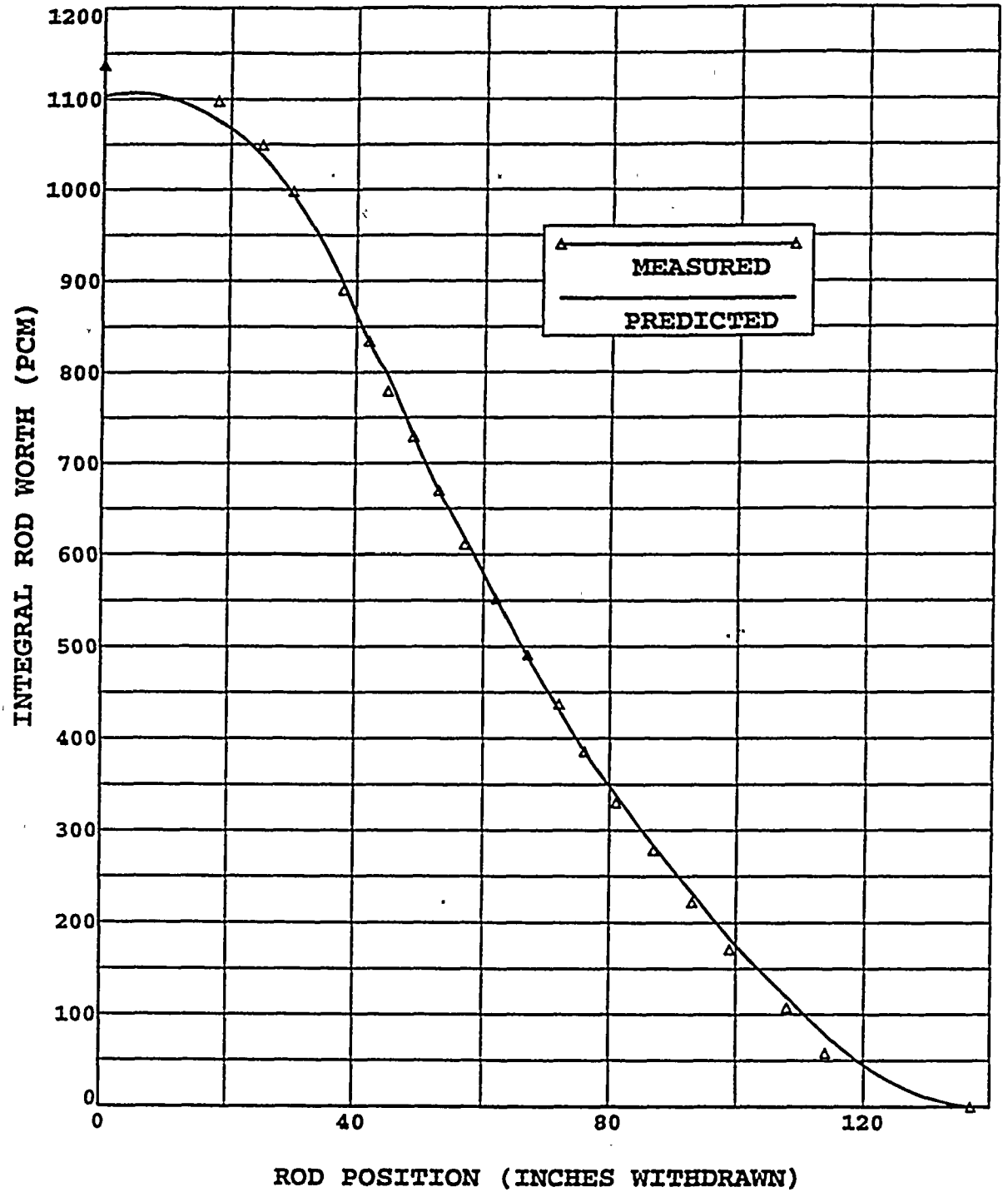

FIGURE 5.2-3
ST LUCIE UNIT 1 CYCLE 12
MEASURED VERSUS PREDICTED
REFERENCE BANK INTEGRAL ROD WORTH

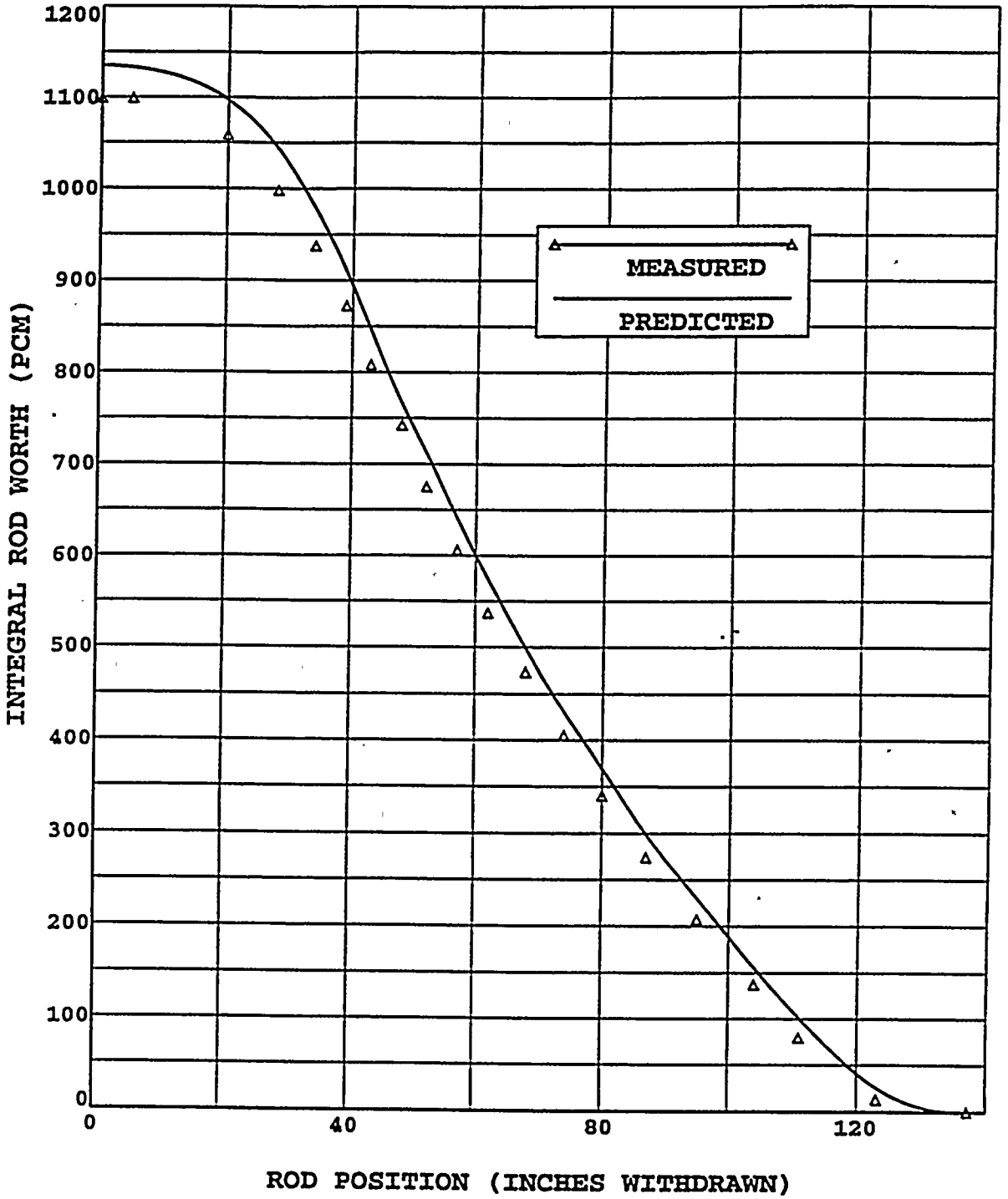

FIGURE 5.3-1
ST LUCIE UNIT 1 CYCLE 10
BORON LETDOWN COMPARISON
BETWEEN MEASUREMENT AND PREDICTION

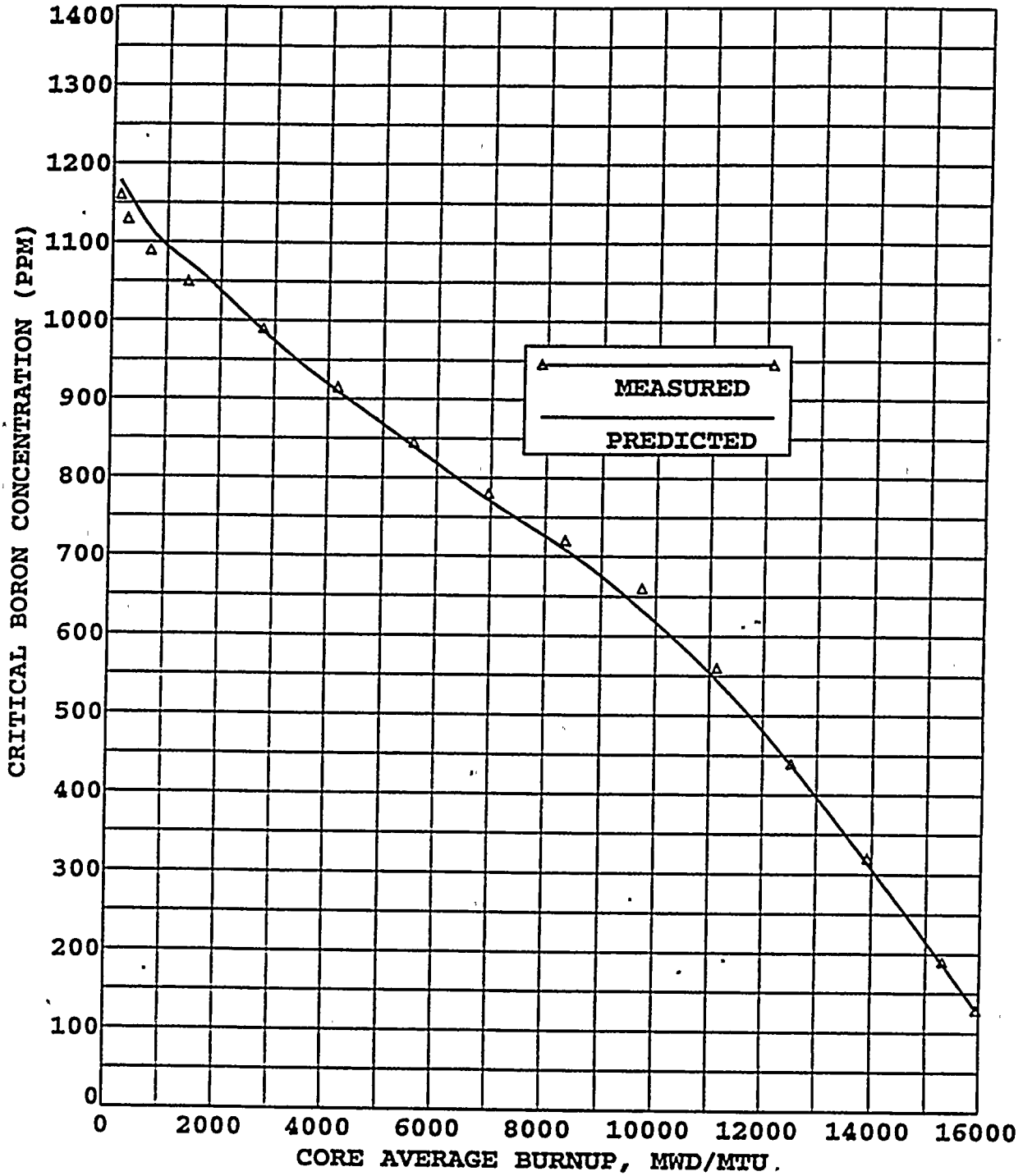

FIGURE 5.3-2
ST LUCIE UNIT 1 CYCLE 11
BORON LETDOWN COMPARISON
BETWEEN MEASUREMENT AND PREDICTION

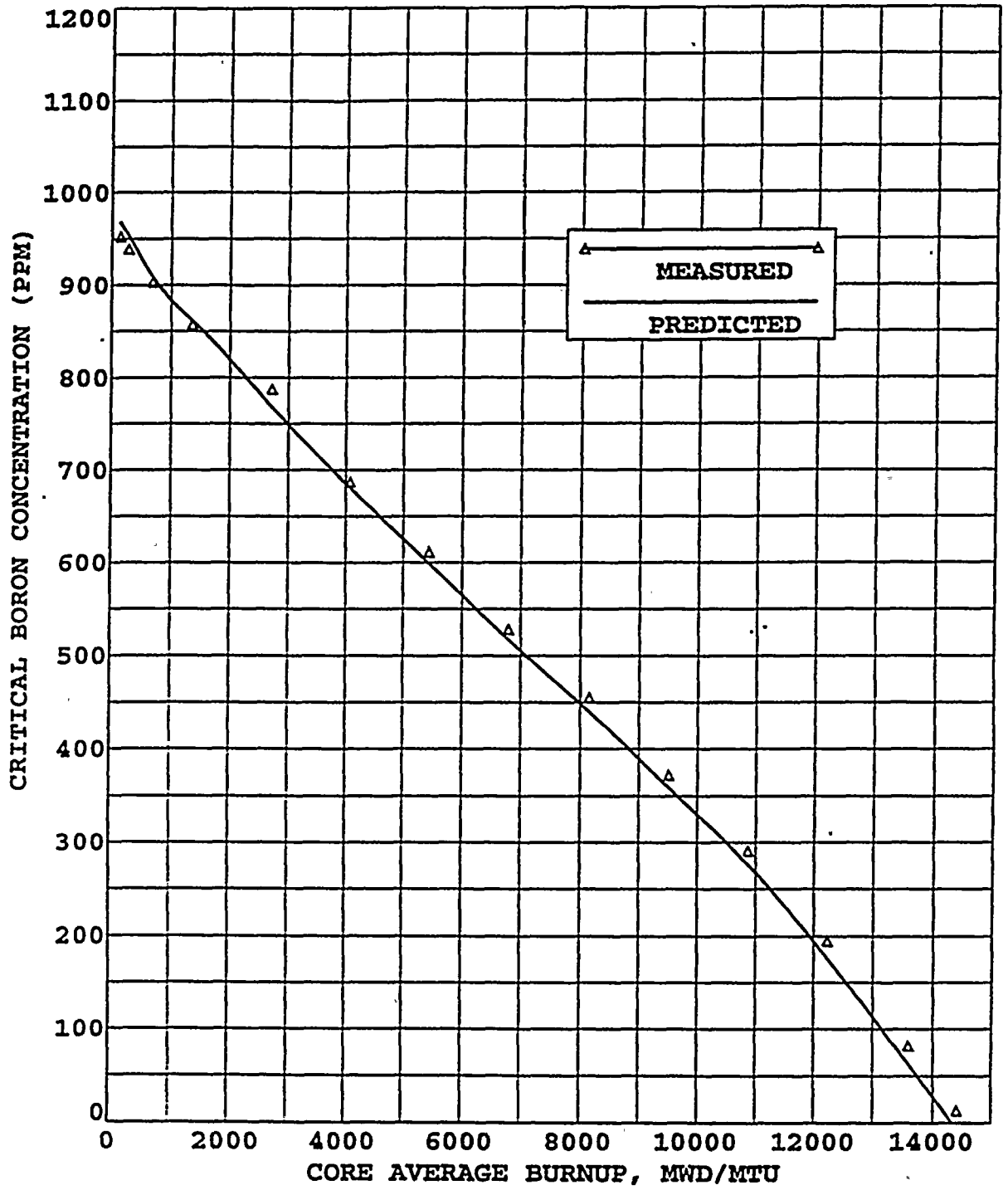

FIGURE 5.3-3
ST LUCIE UNIT 1 CYCLE 12
BORON LETDOWN COMPARISON
BETWEEN MEASUREMENT AND PREDICTION

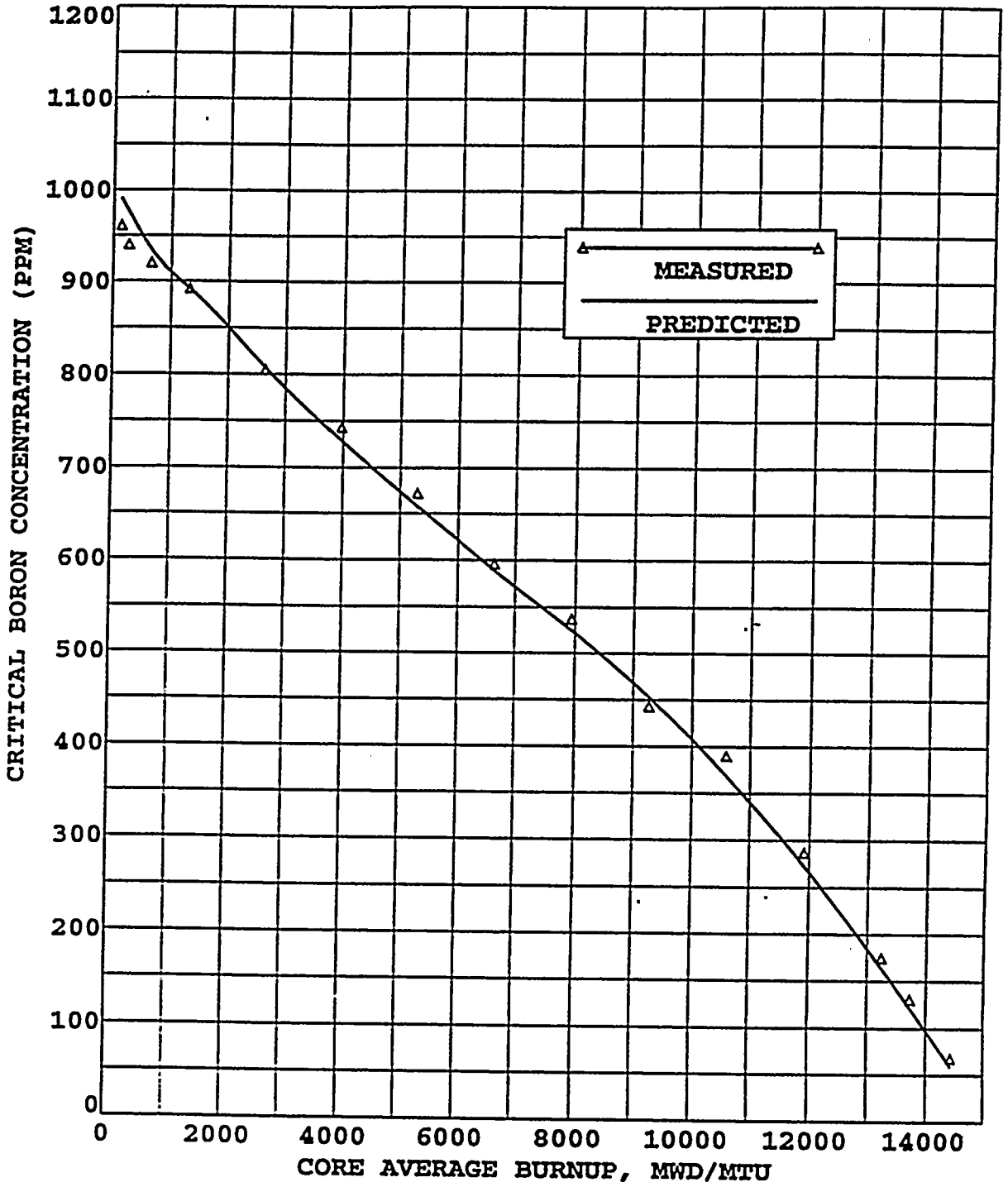

FIGURE 5.3-4
ST LUCIE UNIT 1 CYCLE 10
AXIAL POWER DISTRIBUTION COMPARISON
BETWEEN INPAX AND ANC

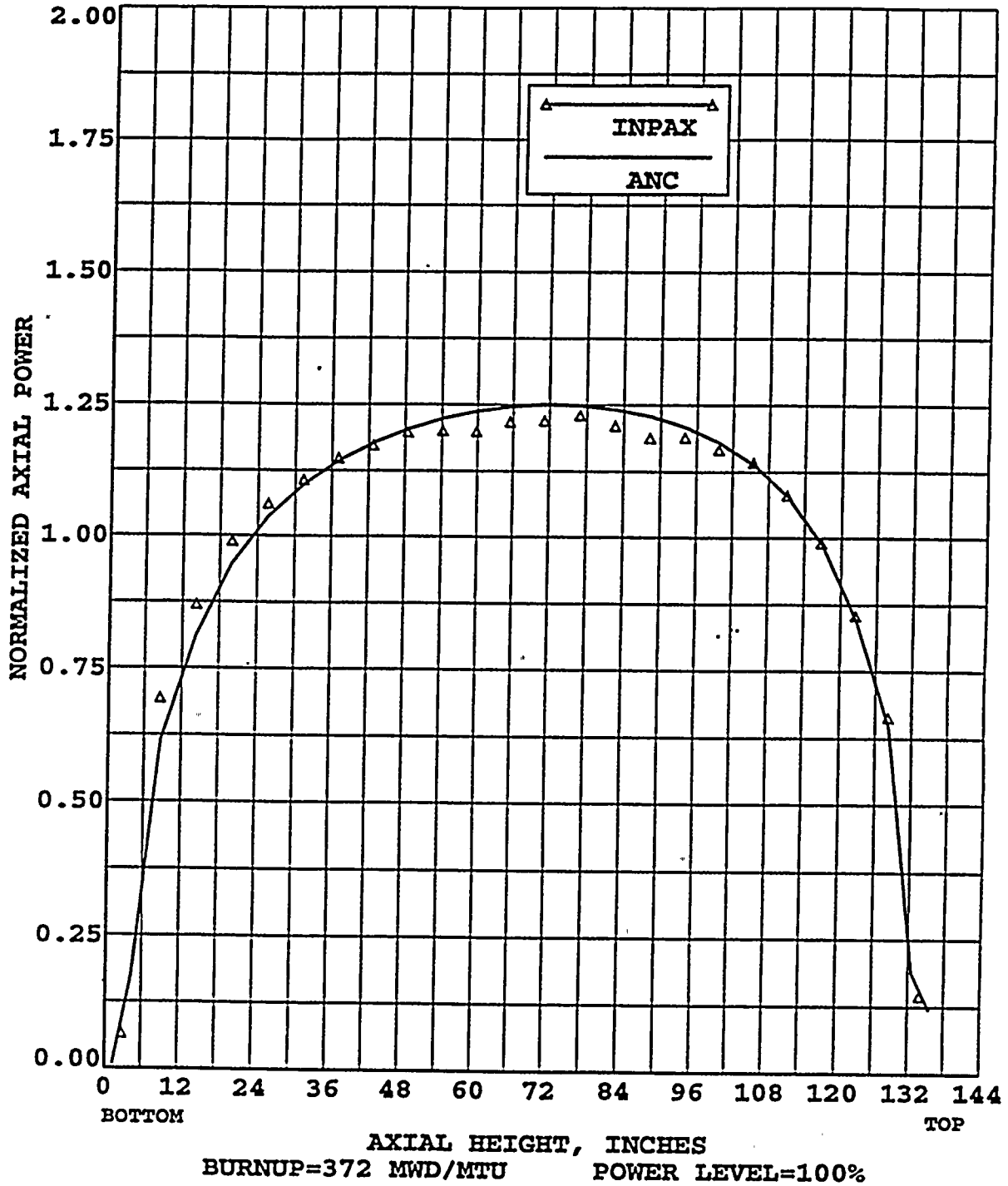

BURNUP=372 MWD/MTU POWER LEVEL=100%

FIGURE 5.3-5
ST LUCIE UNIT 1 CYCLE 10
AXIAL POWER DISTRIBUTION COMPARISON
BETWEEN INPAX AND ANC

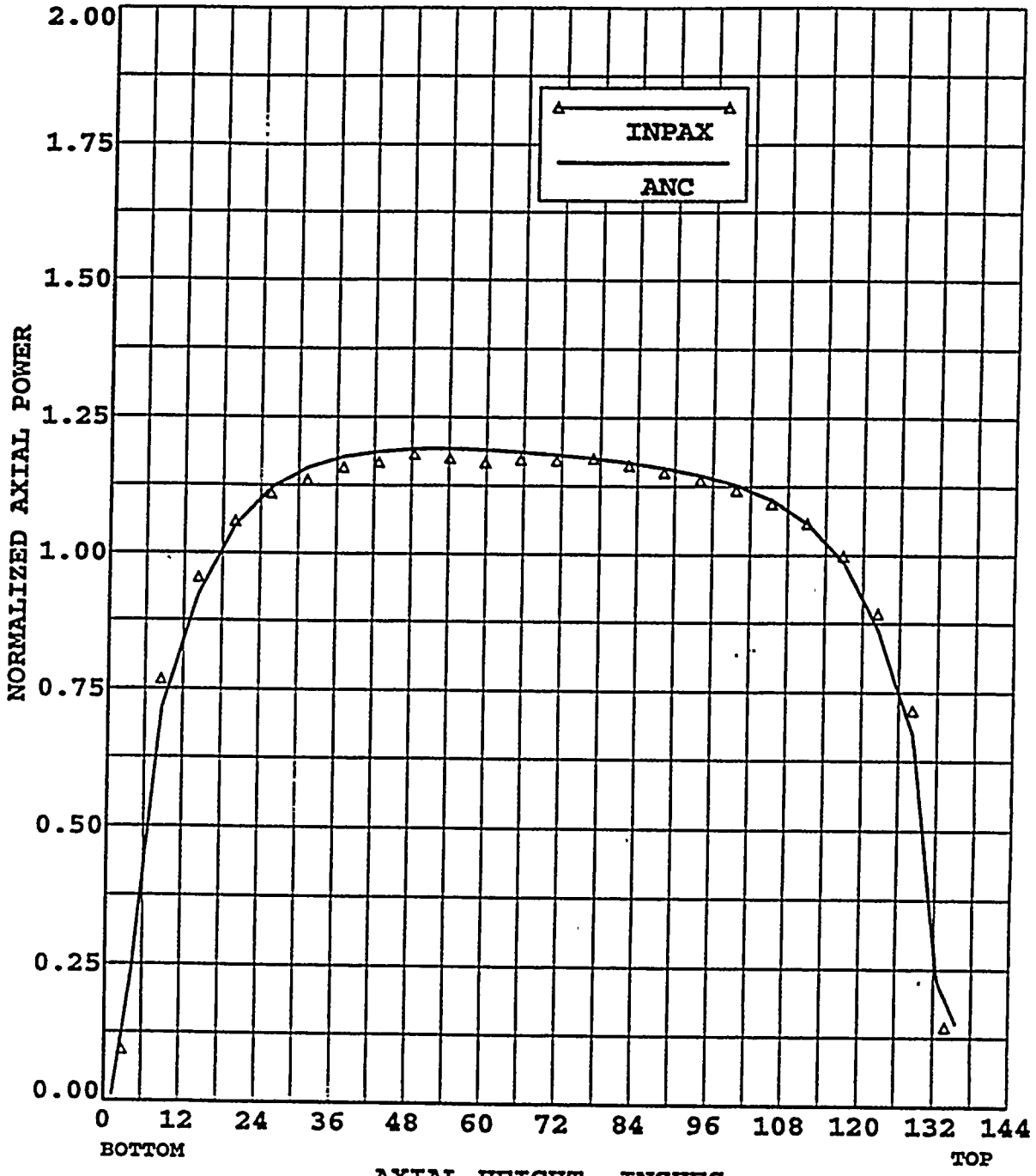

BURNUP=6,904 MWD/MTU POWER LEVEL=100%

FIGURE 5.3-6
ST LUCIE UNIT 1 CYCLE 10
AXIAL POWER DISTRIBUTION COMPARISON
BETWEEN INPAX AND ANC

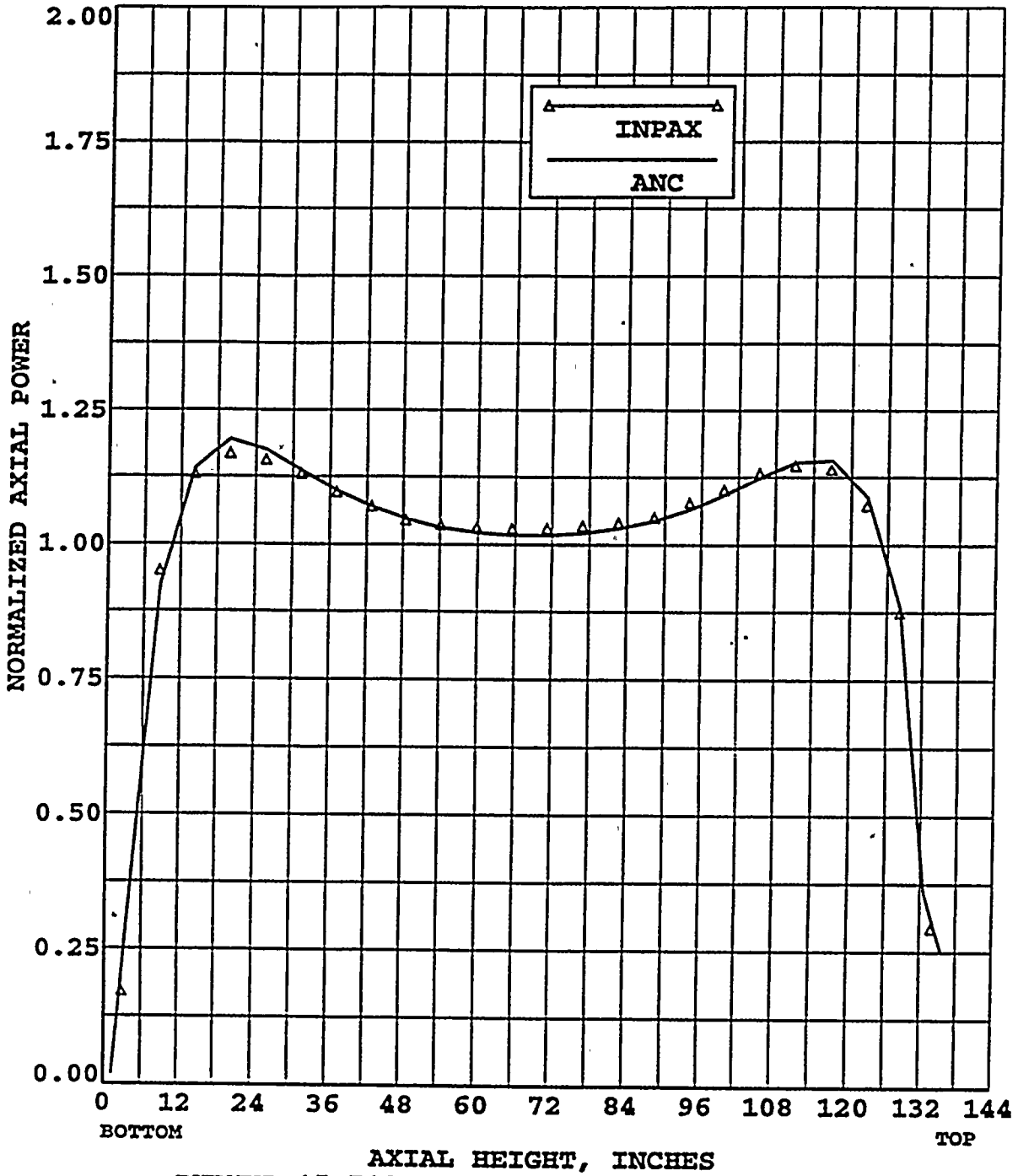

BURNUP=15,718 MWD/MTU POWER LEVEL=100%

FIGURE 5.3-7
ST LUCIE UNIT 1 CYCLE 11
AXIAL POWER DISTRIBUTION COMPARISON
BETWEEN INPAX AND ANC

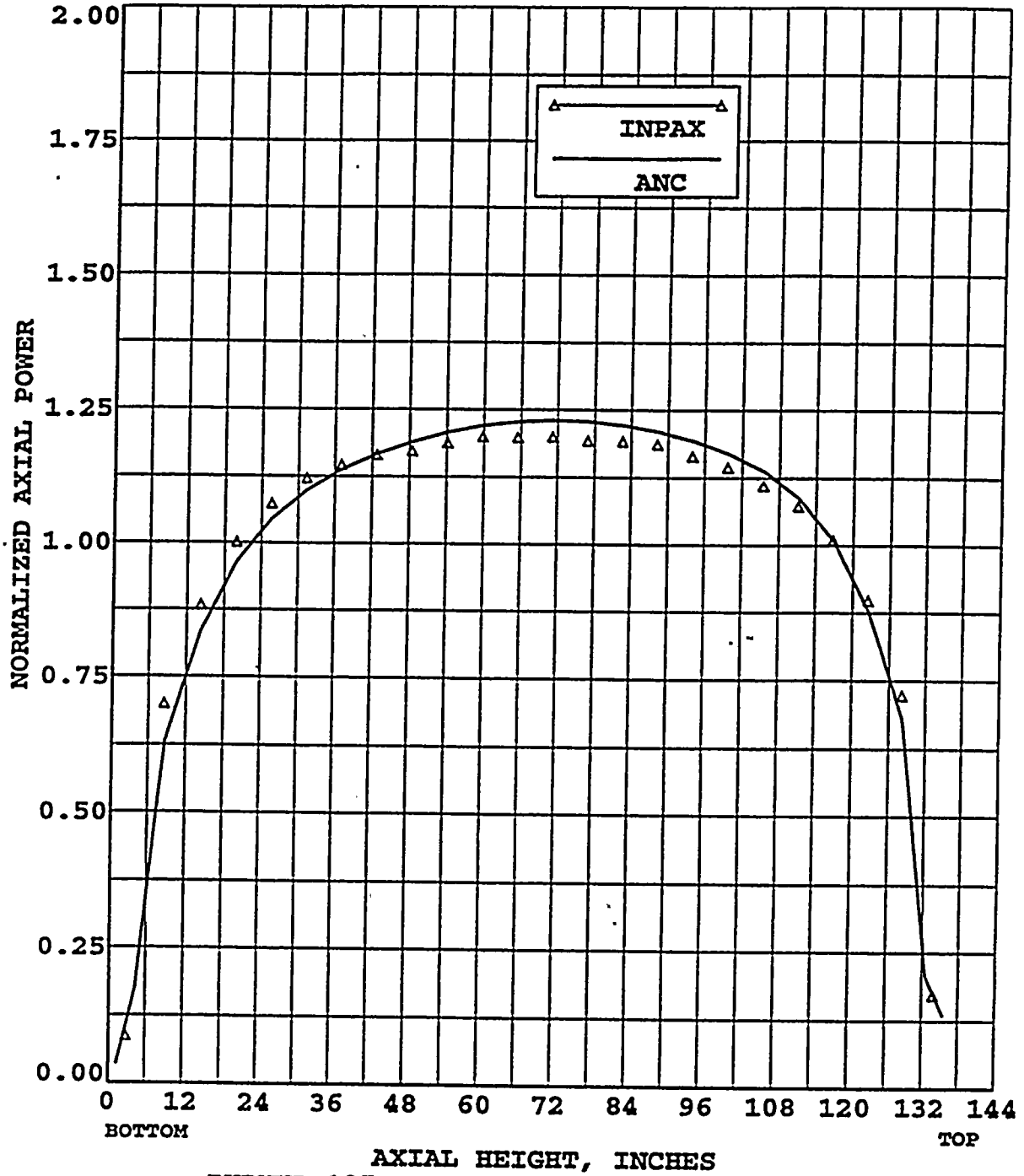

BURNUP=185 MWD/MTU POWER LEVEL=100%

FIGURE 5.3-8
ST LUCIE UNIT 1 CYCLE 11
AXIAL POWER DISTRIBUTION COMPARISON
BETWEEN INPAX AND ANC

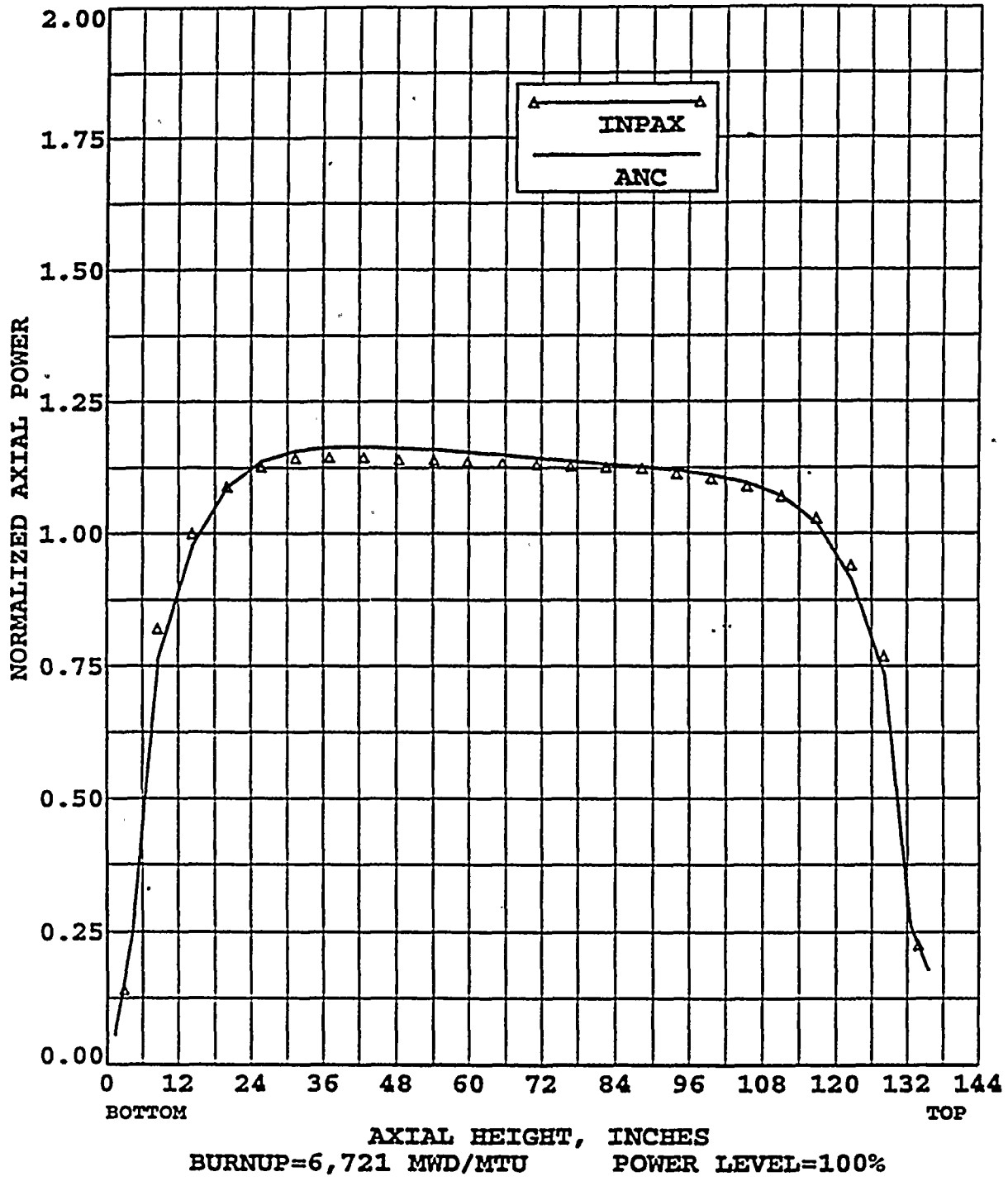

BURNUP=6,721 MWD/MTU POWER LEVEL=100%

FIGURE 5.3-9
ST LUCIE UNIT 1 CYCLE 11
AXIAL POWER DISTRIBUTION COMPARISON
BETWEEN INPAX AND ANC

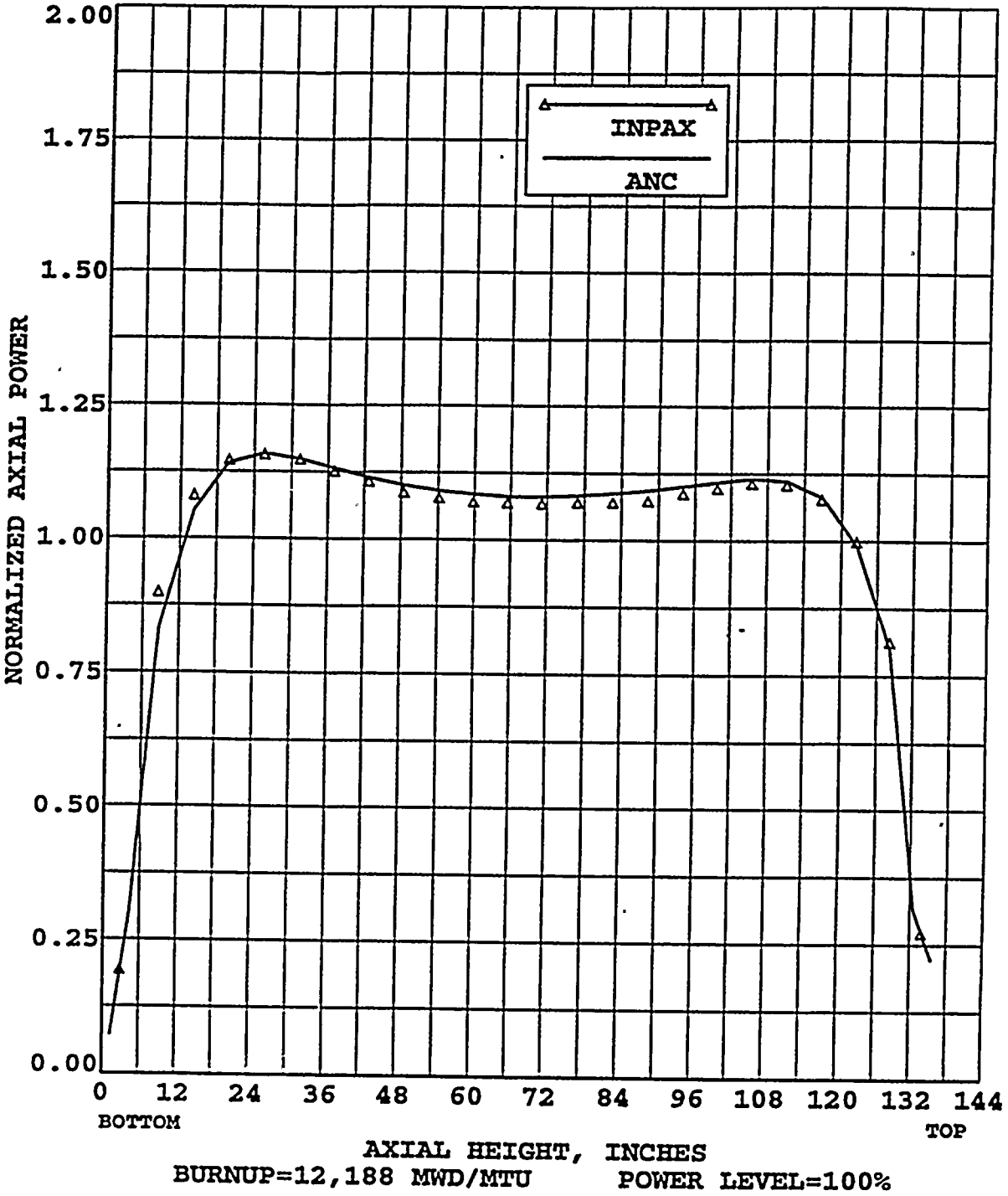

BURNUP=12,188 MWD/MTU POWER LEVEL=100%

FIGURE 5.3-10
ST LUCIE UNIT 1 CYCLE 12
AXIAL POWER DISTRIBUTION COMPARISON
BETWEEN INPAX AND ANC

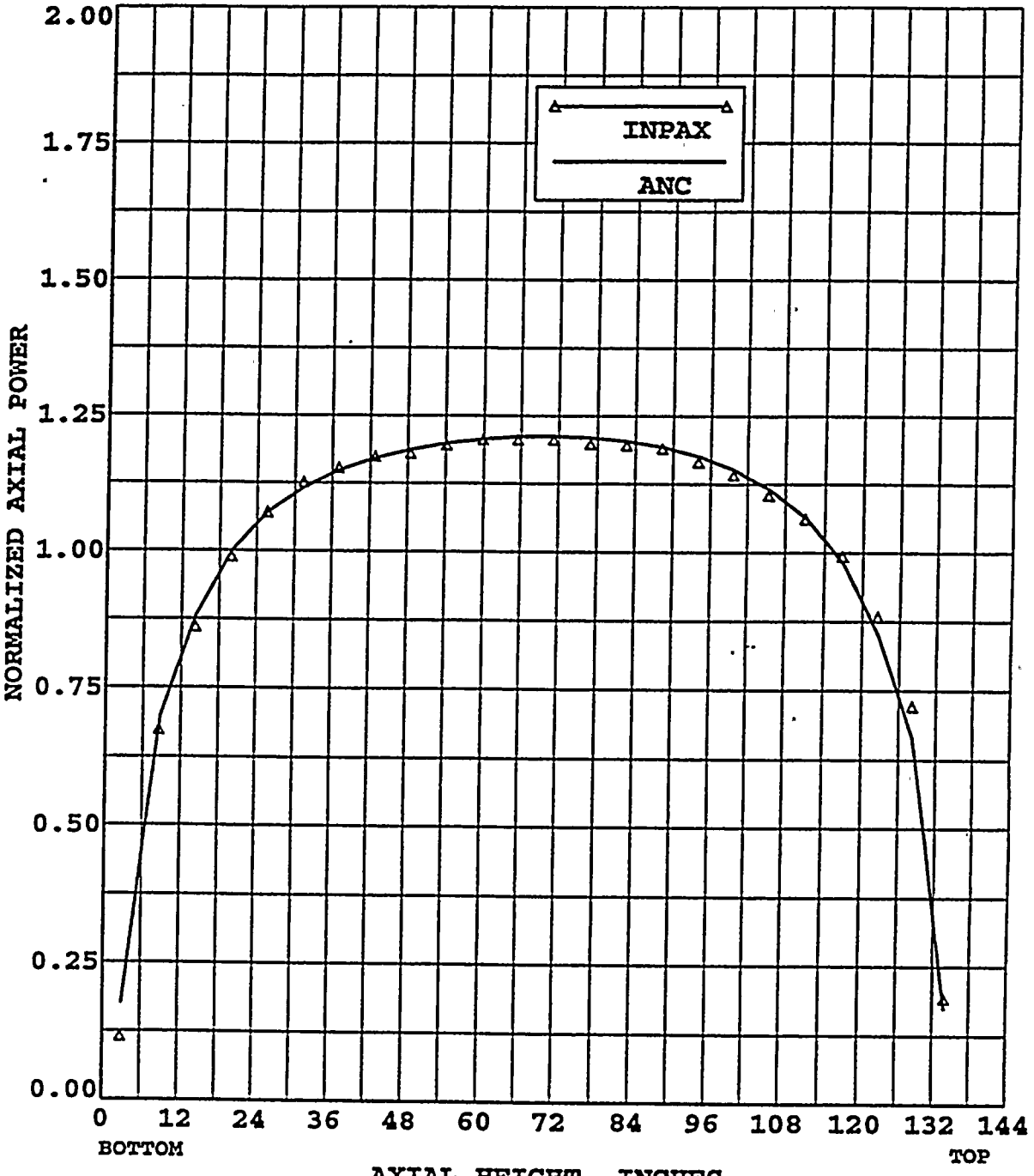

BURNUP=625 MWD/MTU POWER LEVEL=100%

FIGURE 5.3-11
ST LUCIE UNIT 1 CYCLE 12
AXIAL POWER DISTRIBUTION COMPARISON
BETWEEN INPAX AND ANC

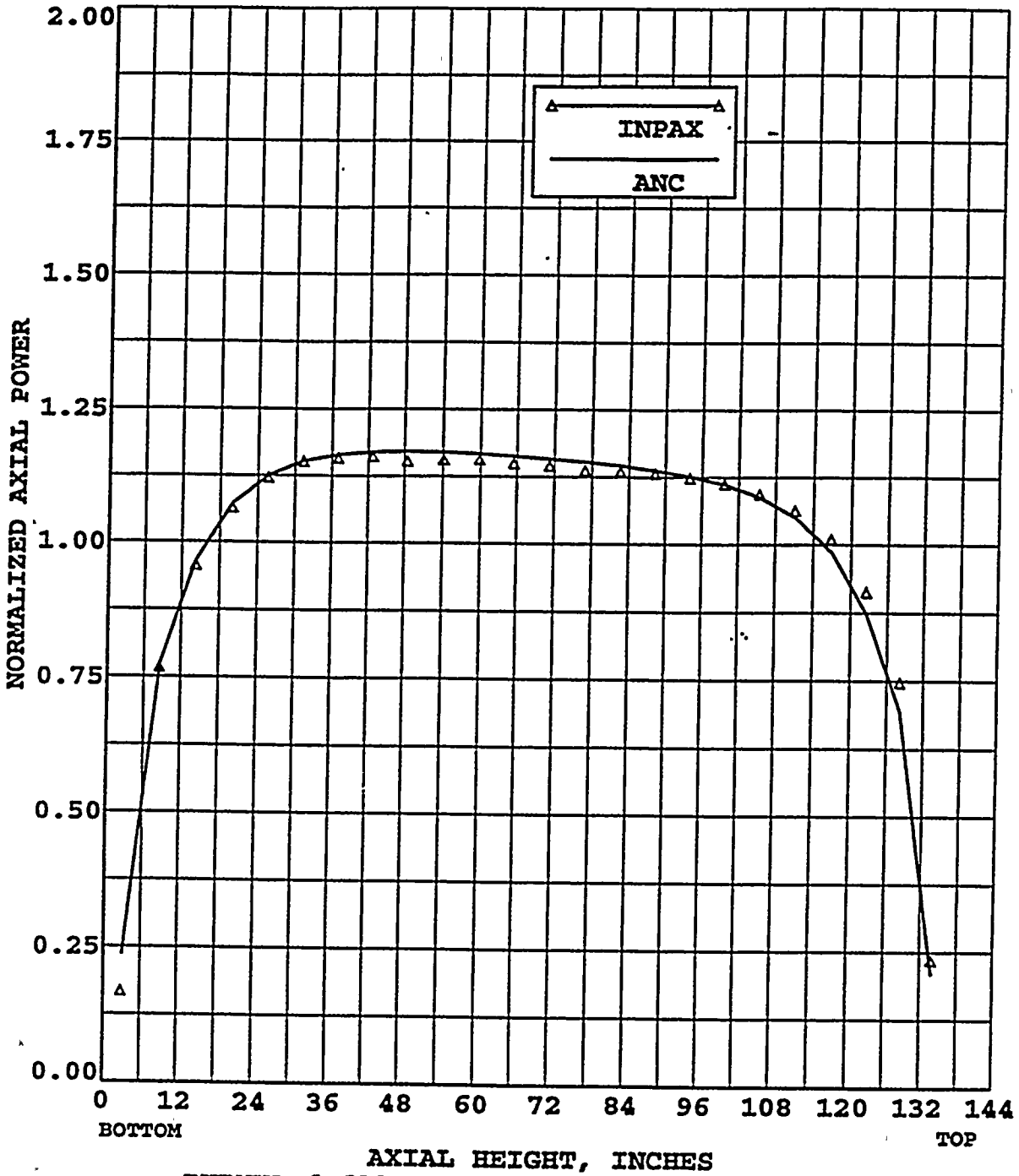

BURNUP=6,620 MWD/MTU POWER LEVEL=100%

FIGURE 5.3-12
ST LUCIE UNIT 1 CYCLE 12
AXIAL POWER DISTRIBUTION COMPARISON
BETWEEN INPAX AND ANC

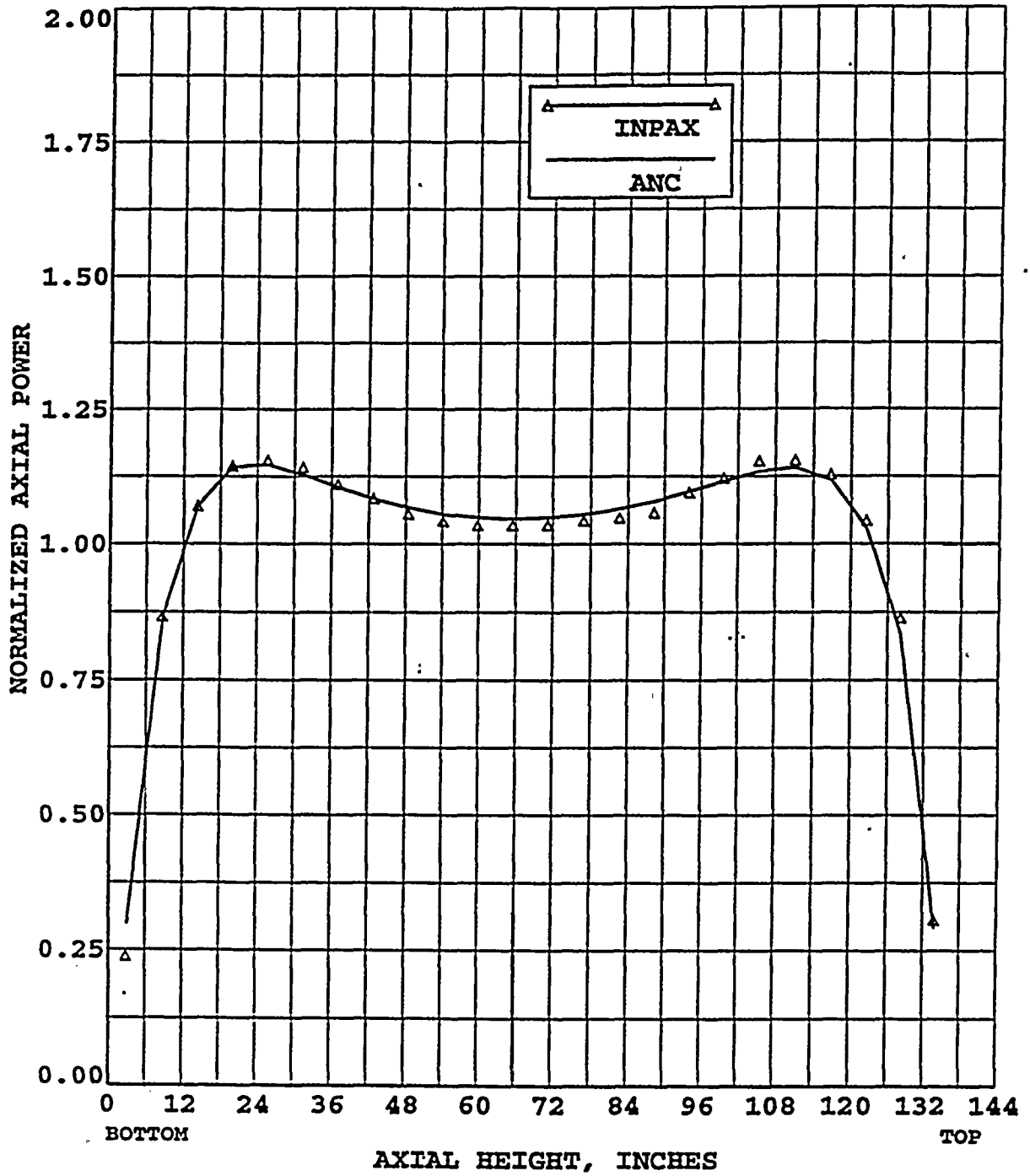

BURNUP=13,320 MWD/MTU POWER LEVEL=100%

6.0 REFERENCES

1. Langford, F.L. and Nath, R.J., "Evaluation of Nuclear Hot Channel Factor Uncertainties," WCAP-7308-L, April 1969, and Spier, E.M. and Nguyen, T.G., "Update to WCAP-7308-L-P-A (Proprietary), Evaluation of Nuclear Hot Channel Factor Uncertainties," June 1988.

2. Meyer, C.E. and Stover, R.L, "INCORE Power Distribution Determination in Westinghouse Pressurized Water Reactors," WCAP-8498, July 1975.

3. Nguyen, T.Q., et al, "Qualification of the PHOENIX-P/ANC Nuclear Design System for Pressurized Water Reactor Cores," WCAP-11596-P-A (Proprietary), June 1988.

4. Miller, R.W., et al, "Relaxation of Constant Axial Offset Control/FQ Surveillance Technical Specification," WCAP-10216-P-A (Proprietary), June 1983.

5. Bordelon, F.M., et al, "Westinghouse Reload Safety Evaluation Methodology," WCAP-9272-P-A (Proprietary), July 1985.

6. Camden, T.M., et al, "Rod Bank Worth Measurements Utilizing Bank Exchange," WCAP-9863-A (Proprietary), May 1982.

7. Camden, T.M., et al, "PALADON-Westinghouse Nodal Computer Program," WCAP-9485 (Proprietary) and WCAP 9486, December 1978 and Supplement 1, WCAP-9485-A (Proprietary) and WCAP-9486-A (Non-Proprietary), September 1981.

8. Liu, Y.S., et al, "ANC: A Westinghouse Advanced Nodal Computer Code," WCAP-10965-P-A (Proprietary), December 1985.

9. Poncelet, C.G., et al, "LASER - A Depletion Program for Lattice Calculations Based on MUFT and THERMOS," WCAP-6073, April 1966.

10. Olhoeft, J.E., "The Doppler Effect for a Non-Uniform Temperature Distribution in Reactor Fuel Elements," WCAP-2048, July 1962.

11. Harris, A.J., et al, "A Description of the Nuclear Design Analysis Programs for Boiling Water Reactors," WCAP-10106-P-A (Proprietary), June 1982.

12. Barry, R.F., et. al, "The PANDA Code," WCAP-7048-P-A (Proprietary) and WCAP-7757-A, January 1975.

13. Correll, G.R., et al, "INPAX-II: A Reactor Power Distribution Monitoring Code," Exxon Nuclear Company, XN-NF-83-09(p), March 1983.

14. Morita, T., et al, "Power Distribution Control and Load Following Procedures - Topical Report," WCAP-8385, September 1974.

APPENDIX A

This section describes the primary Westinghouse computer programs used by FPL to perform the required reload core design calculations for Turkey Point and St. Lucie. These codes are used in a manner similar to that outlined in Section 3 of Westinghouse's licensed reload methodology topical report (Reference 5). Although the codes described in this appendix are not specifically addressed in the topical, two of the codes, FIGHTH and APOLLO (Reference 12), contain the same basic methodology as the licensed versions. The updated code versions include engineering enhancements (e.g., editing improvements, minor modeling improvements, and larger problem size capabilities) relative to the original code versions. The updated code versions were described at a meeting between the NRC Core Performance Branch and Westinghouse's Nuclear Fuel Division at the October 1984, at which time the differences between the original and updated code versions were discussed. The NRC concurred that the updated code versions were essentially the same as the original versions, employing the same fundamental solution algorithms as the original versions.

The two major remaining codes, PHOENIX-P and ANC incorporate significant improvements to the methodologies discussed at the 1984 Westinghouse/NRC meeting. PHOENIX-P is a two-dimensional multigroup lattice code which does not rely on the spatial/spectral interaction assumptions inherent in the previous methodology. ANC is an advanced version of the PALADON code (Reference 7) incorporating nonlinear nodal expansion, equivalence theory (for cross section homogenization), and a pin power recovery model. The topical reports (References 3 and 8) qualifying PHOENIX-P and ANC for use in reload core design have been approved by the NRC.

A.1 FIGHTH

The FIGHTH code computes effective temperatures in low enriched, sintered UO_2 fuel rods for specified values of burnup, linear heat

generation rate, moderator temperature, and flow rate. Resulting fuel and clad temperatures are used as input for the PHOENIX-P code. FIGHTH accounts for the radial variation of the heat generation rate, thermal conductivity, and thermal expansion in the fuel pellet; elastic deflection in the cladding; and pellet-clad gap conductance. The pellet-gap conductance is dependent upon the type of initial fill gas, the hot open gap dimensions, and the fraction of the pellet circumference over which the gap is effectively closed due to pellet cracking. References 9 and 10 provide a description of the basis of the FIGHTH program.

A.2 PHOENIX-P

PHOENIX-P is a two-dimensional multigroup transport theory code used to calculate lattice physics parameters for PWR core modeling. In PHOENIX-P, the detailed spatial flux and energy distribution solution is divided into two major steps. In step one, a two-dimensional fine energy group nodal solution which couples individual subcell regions (pellet, clad, and moderator) as well as surrounding pins, is obtained. PHOENIX-P uses a Carlvik's collision probability approach and heterogeneous response fluxes to preserve the heterogeneity of the pin cells and their surroundings. The nodal solution provides a detailed and accurate local flux distribution. This distribution is then used to spatially homogenize the pin cells into fewer groups.

In the second step of the solution process, PHOENIX-P solves for the angular flux distribution using a standard S^4 discrete ordinates calculation. This technique utilizes group-collapsed and homogenized cross sections obtained from the first step of the solution. The S^4 fluxes are then utilized to normalize the detailed spatial and energy nodal fluxes. These normalized nodal fluxes are used to compute the reaction rates and power distributions used to deplete the fuel and burnable absorbers. A standard B1 calculation is used to evaluate the critical spectrum of the fundamental

mode and to provide an improved fast diffusion coefficient for the core spatial codes.

PHOENIX-P employs a 42 energy group library which has been derived primarily from ENDF/B-V files. The PHOENIX-P cross section library was designed to correctly capture integral properties of the multi-group data during the group collapse, in order to properly model significant resonance parameters. The library contains all the neutronic data necessary for modeling fuel, fission products, cladding and structural, coolant, and control/burnable absorber materials present in most PWRs.

A detailed discussion of the methodology and models incorporated in PHOENIX-P may be found in References 3 and 11.

A.3 ANC

ANC is an advanced multidimensional nodal methods program used to predict core reactivity parameters, power distributions, detector thimble fluxes, and other important core characteristics. ANC uses the nodal expansion method to solve the two-group diffusion equations. Partial currents and average neutron fluxes for the nodes are determined from continuous homogeneous neutron flux profiles by employing fourth order polynomial expansions for each of the x, y, and z directions across the node. Discontinuity factors are used to adjust the homogeneous cross-sections in order to preserve the nodal surface fluxes and currents that would be obtained from an equivalent heterogeneous model. In addition, ANC contains a pin-power recovery algorithm which couples the analytic solution of the two-group diffusion equations with the pin power information from PHOENIX-P. ANC is able to accurately reconstruct the results of fine mesh models using these methods. A detailed description of the methodology employed in ANC is contained in Reference 8.

ANC is capable of performing either two or three-dimensional calculations with a wide variety of options. The code can handle geometries ranging from octant to full core and supports various symmetries. Feedback mechanisms make adjustments to the macroscopic cross sections to account for any changes in fuel temperature or moderator density. Xenon and samarium buildup and decay are modeled in addition to fuel and burnable absorber depletion. Typical applications of ANC include:

- Differential and integral control rod worth,
- Axial and radial power distributions,
- Reactivity coefficients,
- Critical core configurations,
- Shutdown margins, and
- Fuel and burnable absorber loading patterns.

A.4 APOLLO

APOLLO is based on a one-dimensional two-group algorithm utilizing steady state diffusion theory solved via the finite difference method. Normally, an APOLLO model is generated by radially homogenizing a three-dimensional ANC model. APOLLO is an advanced version of the PANDA code, described in Reference 12. Cross sections are flux and volume weighted over each mesh interval and a burnup and elevation dependent radial buckling search is performed to normalize the APOLLO model to ANC. APOLLO is used for applications which require a finer mesh in the axial direction than ANC, as a relatively high number of mesh points are available. Applications typically include:

- Axial power distributions, including F_Q synthesis,
- Differential and integral control rod worth,
- Trip reactivity curves,
- Load follow evaluations, and
- Control rod insertion limits.

The algorithms used in APOLLO account for space dependent feedback effects due to xenon, samarium, rod position, boron, fuel temperature, and water density.